**Title**
Effects of Exhaust Gas Recirculation on Performance of a 49 cc Spark Ignited Engine



**Author**
KIM, SOUNG UK

**Publication Date**
2018

Peer reviewed|Thesis/dissertation

UNIVERSITY OF CALIFORNIA,
IRVINE

# Effects of Exhaust Gas Recirculation on Performance of a 49 cc Spark Ignited Engine

THESIS

submitted in partial satisfaction of the requirements
for the degree of

MASTER OF SCIENCE

in Mechanical and Aerospace Engineering

by

Soung Uk Kim

Thesis Committee:
Professor Derek Dunn-Rankin, Chair
Professor Jacob Brouwer
Associate Professor Manuel Gamero-Castaño

2018

# TABLE OF CONTENTS

# LIST OF FIGURES

# LIST OF TABLES

# ACKNOWLEDGMENTS

I would like to express the deepest gratitude to my advisor and committee chair, Professor Derek Dunn-Rankin, who has the enthusiastic attitude and the encouragement: he continually and convincingly conveyed a spirit of adventure and excitement in regard to my M.S research. Without his guidance, support, and persistent help for the experimental research, this M.S thesis would not have been possible. I feel very fortunate to have had the opportunity to investigate my research with his all valuable and considerate advice.

I thank Professor Jacob Brouwer and Associate Professor Manuel Gamero-Castaño for being on my M.S thesis committee and whose courses, such as 'Radiation Heat Transfer' and 'General Thermodynamics' conveyed me to thermal science and heat transfer and whose enthusiasm has been an academically lasting effect on my research.

I also thank the LFA members for sharing the experience of their own research, theoretical advice and instruction, and experimental techniques to apply to parts of the research for my M.S thesis.

# ABSTRACT OF THE THESIS

Effects of Exhaust Gas Recirculation on Performance of a 49 cc Spark Ignited Engine

By

Soung Uk Kim

Master of Science in Mechanical and Aerospace Engineering

University of California, Irvine, 2018

Professor Derek Dunn-Rankin, Chair

Exhaust gas recirculation (EGR) is a proven and effective strategy for reducing the nitrogen oxides ($NO_x$) emission of automotive-scale internal combustion engines. $NO_x$ formation is highly correlated with conditions when the flame temperature in the combustion chamber of the engine exceeds 1900K. The EGR method recirculates some of the exhaust gas back into the intake manifold where it mixes with the fresh intake air. The exhaust gases dilute the oxygen but provide some sensible heat, thereby reducing peak flame temperatures but helping to maintain combustion stability. This work is novel in its application of a customized EGR system to a 49 cc engine, where the single cylinder and small scale make its performance particularly susceptible to combustion upsets. The reduction of combustion and exhaust gas temperatures resulted in a 642ppm reduction of $NO_x$ (77.3%) at 6000 RPM with an EGR rate of 11.7%. Thus EGR was very effective for reduced $NO_x$ emission, but it resulted in typical penalties of EGR including a slight increase in fuel consumption at all RPM conditions (8.6mg/s (8.7%) at 2100 RPM to 2.6mg/s (9.8%) at 6000 RPM) and a slight decrease in engine torque and power at high RPM conditions (0.14N·m at 4000 RPM to 0.59N·m at 6000 RPM and 0.06 HP at 4000 RPM to 0.37 HP at

6000 RPM). Hence, there was the trade-off between gas emission and the pollutant emissions and performance penalties.

There is an optimal and applicable range of EGR rate, 7.5% - 12%, at these speeds when considering the ratio of exhaust gas temperature and engine coolant temperature (E/C Temperature Ratio) appropriate for extending the life of the engine with EGR. In addition, an EGR rate was found at the high RPM that maximized the advantages of the reduction of $NO_x$, CO, and HC and minimized the disadvantages of decreasing the engine torque, power, and fuel consumption. An experimental investigation on pollutant emissions and performance of a small (49 cc) single cylinder, four stroke, port fuel injection, spark ignited engine was conducted to observe and analyze the effects of EGR. EGR in such a small engine experimental testbed configuration has not been studied before, and through the research a customized EGR concept consisting of an EGR copper pipe system (Hot EGR system), which is necessary for effective small engine use of EGR, was developed.

# MOTIVATION

Internal combustion (IC) engines are the most common form of heat engines, converting the chemical energy of liquid fuel to mechanical energy. IC engines have been used for all manner of vehicles, including boats, ships, trains, and airplanes in different sizes and configurations, and each engine is dependent on its own work objectives. There alternative power technologies developing (notably electric and fuel cell vehicles) but vehicles powered by internal combustion engines will be conservatively comprise 75% - 85% of the fleet beyond 2025. Electric and fuel cell vehicles are progressing, and they are very promising technologies due to their reduced air pollution [46, 48], but they still have some problems to overcome, such as the expense of constructing infrastructures, cost, and lack of a sufficiently high-power density [46].

Large scale IC engines are used in a wide variety of applications. The spectrum ranges from the stationary generators to general automobiles. Compared to large engines, small scale IC engines (which generate torque in the range of 1 - 10 (Nm) and power in the range of 1 - 10 kW) are generally used for small personal transportation vehicles or portable devices such as power yard management equipment, unmanned aircraft, wearable or small robots of military applications, scooters, small size motorcycles, and portable power generators [45]. In contrast to the large IC engines, small scale IC engines have advantages of low expense, convenient maintenance, and portability. Their smaller size and lower cost, however, makes it more difficult to implement advanced performance and pollution control technologies on them. Hence, while the large scale IC engines will continue to dominate power sources for a wide variety of high power density applications for at least the next several decades [44, 47], small IC engines need substantial

improvements to maintain their power role as battery and motor technology continues to improve. In particular, if emission controls are tightened dramatically, the small IC engine will have difficulty maintaining viability without advanced efforts.

Governments around the world have begun enforcing stricter gas emission regulations for global air pollution, in contrast to the past when there was no burden of any expense of gasoline and environmental regulations. For example, recently India has enforced the policy of the required reduction 50% of CO, 75% of HC, 85% of $NO_x$ by 2020, and South Korea has enforced stricter regulation for the small scale engines. The U.S EPA has highway motorcycle exhaust emission standards [36]. With these challenges, the vehicles using internal combustion engines are still a promising mainstream design, potentially meeting 80% of the total need by 2030 if they can be improved towards environment-friendly and high technology concepts, while still investing less cost as compared to the electric and fuel cell vehicles [35].

Furthermore, small scale IC engines, with the advantages and the range of small scale combustion power, have great potential to be applied in hybrid electric or fuel cell designs [44]. The combination of standalone and hybrid applications will encourage their continued development and improvement. This thesis examines one such improvement, a passive exhaust gas recirculation method suitable for small engines.

## BACKGROUND

### Internal Combustion Reciprocating Engines

In order to describe the focus of this thesis on small scale, spark-ignited engines, a review of the basic classifications is useful. For small scale IC engines, there are three ignition types [48]:

SI engines refer to gasoline engines where the air/fuel mixture of the combustion process is ignited by a spark from a spark plug (See Figure 1). They are less costly, smaller in size and weight, and easier to operate and maintain compared to diesel engines with the same output. Therefore, they can be used for a wide range of applications in a wide range of sizes and configurations for aircraft, automobiles, motorcycles, motor boats, tillage machines, fire pumps, generators, etc. For these reasons, small scale engines with displacements less than 50cc are of this SI engine type.

SI engines are further categorized based on the number of cylinder cycles per combustion event. These are considered 4-stroke engines and two-stroke engines [51]. In a 4-stroke cycle engine, as compared to the 2-stroke cycle system, there is no uncertainty because each stroke is exactly divided, the thermal load of each part is small due to the cooling effect in the intake stroke, and the range of rotation speed from low speed to high speed is wide. Also, since the duration of the intake stroke is long, the volumetric efficiency can be high, blow-by gas loss is small, the combustion efficiency is high, and the fuel consumption rate is low. Four stroke engines are easy to start and rarely cause a misfire due to unstable combustion from poor mixing of the combustion charge. On the other hand, the disadvantages of the 4-stroke engines are considered to be a relatively larger size and lower power/weight ratio, a complicated valve mechanism, large vibration, and the

associated high mechanical noise. Also, when the number of ignition/power cycle events is small, the fluctuation of the rotational force is large, and particularly when the number of cylinders is small, operation is difficult, the price is high, and the weight per hp is large. In addition, while hydrocarbon emissions are low, nitrogen oxide emissions are high. For full scale engines, nitrogen oxide emissions can be reduced by after treatment, but for small scale engines, such post combustion processes are too bulky to meet the portability demands.

In summary, for 4-stroke engines, the advantages include: good fuel economy, improved gas emission, and long service life; the disadvantages include: the size of the engine, the complicated mechanical system, and the power/weight ratio is lower than for 2 -stroke designs.

For 2-stroke SI engines, two strokes of compression and power are repeated. The intake and exhaust occur as a natural scavenging as fresh intake air pushes burned exhaust gases out at the end of the power stroke and beginning of the compression stroke. Compared to 4-stroke engines, the instantaneous output is high, and the engine is light-weight and its simple structure makes it easy to repair. But, the disadvantage is that the combustion efficiency is poor so the fuel consumption is higher than that of the 4-stroke. In addition, the engine lubricating oil and fuel are burnt together, so there can be substantial smoke and gas emission, and it is necessary to replenish the engine oil periodically compared to the 4-stroke cycle system. Since the exhaust gas is not completely exhausted, the combustion occurs with a mixture of fresh intake and residual exhaust gas, and at the same time during the exhaust stroke some of the fresh intake gas will leave the chamber. This combination of events increases to exhausting of unburned fuel and reduces the

incoming charge capacity of the engine. Two stroke designs remain popular for very small and high-power demand engines. The advantages of the 2-stroke engine are that it is lightweight, small, and simple in structure (only ports rather than valves, for example). The disadvantages are poorer fuel economy and substantially increased emissions. Hence, next generation small scale engines are required to be designed in the 4-stroke cycle system rather than the 2-stroke cycle system since performance and gas emissions of the former are more in the line with the trends of the enforced environmental regulations.

Compression ignition (CI) engines are also referred to as diesel engines, where the high heat produced from high compression with the fuel injection ignites the charge without any spark plug in the combustion process (See Figure 1). For fixed maximum pressure, the thermal efficiency of a diesel engine is better than that of a gasoline engine, and therefore the fuel economy can be higher. Part of the high fuel economy includes the portion where the fuel density of diesel fuel is higher than that of gasoline, so that the energy density per liter is increased and the performance is then increased when converted to the fuel efficiency per liter. The price of CI engines is higher than for SI engines of the same displacement. Compared to SI engines, the CI approach is disadvantageous to suppress pollutant emissions. In the case of diesel engines, pollutants are generated mainly by two routes. First, in the case of soot, that is, fine carbonaceous species growing in the fuel rich region of the chamber, the size of fine fuel droplets ejected from the injector is too large to be rapidly and completely burned. The second is that, while operating in a supercharged atmosphere, the high CI temperatures needed and the excess nitrogen and oxygen supplied react with each other to form a relatively large amount of NOx. CI engines are rare for small scale except for the case of model airplane engines where

a glow plug assisted compression ignition is used. For the 49 cc scale engine, CI approaches would be to heavy and bulky to meet the key portability demand.

With the growing capability for advanced combustion control, there are new combustion approaches that combine features of both SI and CI engines. The most common of these is the homogeneous charge compression ignition (HCCI) or sometimes more generally the reaction controlled compression ignition (RCCI) engine. HCCI engines [48, 49] are regarded as compression ignition engines and a future promising engine type (See Figure 1). The engines explode the air/fuel mixture in the cylinder through either high compression or spark plug. Prior research found that the HCCI combustion engine had an important trade-off [49]. There were reduced $CO_2$ emissions due to the improved fuel efficiency [55] and low $NO_x$ and particulate emission [54]. So then, there was no pollutant after-treatment technique required. However, there were the main problems of the reduction of the power density with lean air/fuel mixture combustion [57] and high HC and CO emissions [56] from incomplete combustion. The reduction of power density was due to the air/fuel ratio becoming leaner as the RPM conditions increased. Particularly, high RPM conditions let the torque and power of the HCCI engines dramatically decrease. The studies to date have indicated that HCCI engines are not yet suitable to the applications which should require the cases of a certain extent of the torque and power at high RPM without regard to the improved fuel consumption. Specifically, HCCI engines operate well under low load conditions but these are the conditions where emissions are lowest anyway so the advantages of HCCI are not as clear. For higher load conditions, controlling the combustion initiation by compression is difficult so adding a spark plug can help.

Therefore, this thesis concentrates on the standard SI small scale combustion engine, with the specific goal of a cost-effective aftertreatment to be applied to overcome the main challenge of pollutants emissions.

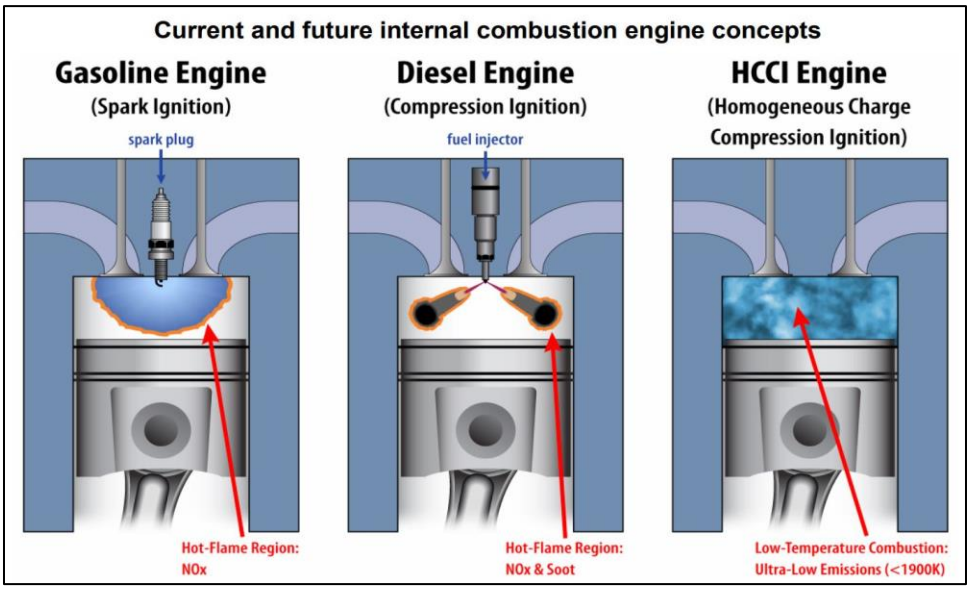


*Figure 1. The types of the internal combustion engines [48]*

**Cooling Systems** [52]:

The cooling of engines affects significantly their design and performance. The cooling system is to maintain the temperature properly so that the engine does not overheat, and there are air cooled types and water cooled types of engines. Air-cooled engines are equipped with cooling fins, and water-cooled engines include water pumps, radiators (heat radiators), fans, and temperature controllers.

The previous research in [49, 50] used the HCCI engine with an air-cooled system. In this type of cooling system, there is no cooling water flowing through the engine and no radiator is needed. The cooling fins are installed so that the air cools the cooling fins. The system is simple and inexpensive. Also, the need for maintenance is low. But, since the

cooling has an uneven effect, the operating temperature of each part of the engine varies greatly. Since the specific heat of air is low compared to that of water or any liquid coolant, the heat transfer ability from the cooling fin to air is poor. In addition, blower drive power is relatively high (about 3 to 4% of engine power).

In contrast to the air-cooled system, a water-cooled system was used for the current investigation for a small scale engine. A water jacket is installed on the cylinder and the cylinder head, and the cooling water is filled in the cylinder and the cylinder head to constitute a cooling water circulation circuit. In the water-cooled type, heat is released into the cooling water. The cooling water circulates through the engine and discharges the absorbed heat to the atmosphere as it passes through the radiator. Liquid cooling systems with aluminum alloy engine walls offer the stable temperature control of the engine wall. By controlling the cooling rate at the radiator, higher and more stable engine wall temperature is achievable. Cooling action is uniform and moreover its power consumed in driving the water pump and the cooling fan is relatively small compared to the air-cooled system.

The use of water cooling also permits the control of the engine temperature for evaluation of higher temperature operation such as would be needed for an RCCI method.

**Compression Ratio**

The compression ratio is the ratio between the maximum volume (the volume at the bottom dead center) and the minimum volume (the volume at the top dead center) of the internal volume of the cylinder in the reciprocating piston type engine. If the compression ratio is increased, the thermal efficiency is improved and the fuel

consumption rate is lowered [53]. The previous research relevant to this work [49, 50] had the compression ratios of 8:1 and 11.9:1 respectively. This current investigation has the higher compression ratio of 12:1 in an SI engine. Thus, the expectation from this investigation is improved performance, thermal efficiency, and fuel efficiency. But, there is a note that in a gasoline engine, when the compression ratio is set too high, there is a limit because it causes abnormal combustion called engine knock where the charge auto-ignites and disrupts the stable burn across the cylinder fuel/air charge.

## Future Promising Technology for SI engines

### Promising Technologies for SI engines

Additionally, besides of the higher compression ratio, there are still future promising technologies for better internal combustion spark ignition engine efficiency, as outlined by [36]:

| | |
|---|---|
| 1 | High compression ratio |
| 2 | Direct injection |
| 3 | Exhaust gas recirculation |
| 4 | Lean burn |
| 5 | High efficiency supercharging |
| 6 | Long stroke |
| 7 | Low friction |
| 8 | Tumble flow |
| 9 | Hydrogenation |
| 10 | Thermal barriers |

*Table 1. Promising technology for improved internal combustion SI engine efficiency*

Based on this table, an SI 4-stroke small scale combustion engine with water-cooling is a promising candidate for further improvement. Among the 10 methods, exhaust gas recirculation was chosen since it was easy to install and convenient to operate and maintain as the main after-treatment to overcome the challenge of gases emission. Specifically, this thesis examines exhaust gas recirculation as an effective emission control technology for small scale SI internal combustion engines.

# Introduction

While the technologies of the IC engines have been improving, the gas emission for global air pollution have been still one of the most interesting challenges, particularly from the perspective of greenhouse gases and climate change. Exhaust gas pollutants emitted to the atmosphere have long been known to affect health and environmental sustainability. In Europe, all of the latest developed motorcycles are or will be under Euro 6 emission control norms, depending on their cylinder capacity. In the USA, Tier I and Tier II programs also impose gas emission standards, and these regulations have driven scientific and commercial interest towards devising an effective method to reduce toxic gas emission. Thus, continued investigations on reducing exhaust emission without degrading performance of the internal combustion engine is inevitable in automotive combustion areas. It is less obviously a driver, however, for the small scale IC engines. It may be that the same technologies can apply to both, but there are some important differences that also suggest specific challenges and opportunities when working with smaller displacements.

In all spark ignition combustion engines, the formation of $NO_x$ depends on the flame temperature in the combustion chamber. High combustion temperatures lead to high $NO_x$ levels, but high combustion temperatures also correlate with high thermal efficiency and improved combustion creating the classic trade-off between performance and emission control. There is a small temperature window that can optimize this trade-off, and thus, controlling the combustion temperature is essential for the reduction of $NO_x$ levels at each driving condition. EGR has been proven as an effective technique for the reduction of $NO_x$ levels in diesel engines or spark ignition engines with high displacements. This thesis study is the first to investigate EGR as an emission control technique on a 49cc spark ignition

small scale engine. If it is successful with this single cylinder engine, EGR can be a promising solution for pollution control for the small engine applications described in the motivation.

# Chapter 1: Formation of Mechanism of Pollutants

The formation of pollutant species during combustion is a well-researched area with relatively high agreement on the most important chemical pathways. This chapter reviews these basics with a consistent nomenclature to provide a complete document but the information is standard and can be found in many combustion texts. In most combustion processes, oxidizer is provided in the form of fresh intake air rather than pure $O_2$. Complete or theoretical combustion of a normalized one mole of octane with the air is [4]:

$$CH_yO_z + n(O_2 + \xi N_2)$$
$$\rightarrow aCO_2 + bH_2O + cC_3H_{3y} + dNO + eH_2 + fO_2 + gCO + hN_2 \quad (1.1)$$

(Where $\xi$: nitrogen/oxygen molar ratio of air, n: moles)

(Note: combustion reaction equations have been normalized by the effective number of carbon atoms in the fuel molecule)

Typically, there is some inefficient or incomplete combustion, and then this generates byproducts such as carbon monoxide (CO) and hydrocarbons (HC). There are also minor pollutant species formed in the reaction process, most notably the nitrogen oxides ($NO_x = NO + NO_2$).

Nitric oxide (NO) can rapidly be oxidized by the oxygen of fresh intake air and form nitrogen dioxide ($NO_2$) inside the combustion chamber with high in-cylinder temperature (over 1900K) and pressure. Most $NO_x$ is NO which is the common output during the combustion process and that there can be some $NO_2$ which generally occurs in the

environment with sunlight and ozone. $NO_2$ is a relatively small fraction except with some diesel engines [67]. $NO_2$ is a toxic gas for human lungs and plays a critical role as a source of acid rain. The mechanism of $NO_x$ formation in the combustion chamber follows primarily the Zeldovich $NO_x$ formation mechanism [24], describing that under high pressure and temperature conditions in an engine, nitrogen ($N_2$) and oxygen ($O_2$) in the air react to form $NO_x$. Key reactions include $O_2+M = O+O+M$ which is the dissociation of an oxygen molecule where M is a stable molecule of high energy required to break down the bonds of $O_2$; and $N_2+O \rightarrow NO+N$ where N atoms quickly react with O atoms. At the same time, $N+OH \rightarrow NO+H$, where the direct oxidation of N by hydroxyl radicals occurs. And then, $NO+HO_2 \rightarrow NO_2+OH$ where the direct oxidation of NO by the peroxy radicals is in sequence. Finally, $NO_2+O \rightarrow NO+O_2$ where the $NO_x$ formation mechanism repeats. Note that if equilibrium were to prevail, the majority of NO would be decomposed at the low temperature of the exhaust back to stable nitrogen and oxygen. However, the low chemical reaction rate at the low gas temperatures keeps some of the NO formed in the exhaust [27]. The NOx formation is then the following (1.2) - (1.4):

$$N_2 + O \rightarrow NO + N \tag{1.2}$$

$$N+OH \rightarrow NO + H \tag{1.3}$$

$$NO + HO_2 \rightarrow NO_2 + OH \tag{1.4}$$

It is clear from these key reactions that the high flame temperature and availability of $O_2$ are the main sources for the formation of $NO_x$. Evidently, most of $NO_x$ are produced by the slightly lean combustion processes (higher air/fuel ratio than stoichiometric air/fuel ratio) in internal combustion engines in particular having the larger amount of $NO_x$ in moderate and heavy loads rather than in light loads. At extremely lean conditions the low combustion temperatures can lead to reduced $NO_x$ but there is also a potential trade-off with power and misfire tendency.

Carbon monoxide (CO) is generally formed as the air/fuel mixture is rich in the combustion process. In other words, the small amount of CO is formed as the mixture is a has insufficient oxygen to fully combust. CO is regarded as a product of incomplete combustion and occurs when carbons in the fuel are partially oxidized rather than fully oxidized to carbon dioxide in the environment of deficient $O_2$ concentration for the combustion. This results when the air/fuel mixture does not have $O_2$ enough for the combustion process, incompletely burns, and then carbon atoms preferably bond with only one O atom for CO. The following chemical reactions occur before the equilibrium is established.

General incomplete combustion [70]: $aC_xH_y + bO_2 \rightarrow cCO + dH_2O$ (1.5)

The direct oxidation of carbon [6]: $2C + O_2 \rightarrow 2CO$ (1.6)

The oxidation of HC: $HC + O_2 \rightarrow CO + CO_2 + H_2O$ (1.7)

High-temperature oxidation of $CO_2$ [69]: $2CO_2 \rightarrow 2CO + O_2$ (1.8)

CO is a colorless, odorless, and tasteless gas that pollutes the atmosphere and is a toxic gas when encountered in concentrations above about 35 ppm. It is harmful to people and animals who breathe it [66].

Carbon dioxide ($CO_2$) is produced by the oxidation of CO during hydrocarbon combustion in which there is a breakdown of hydrocarbon fuel to CO and then oxidation of CO to $CO_2$, depending on the amount of $H_2$ or $H_2O$. In addition, as the products cool down the temperature of the exhaust, the majority of CO has a tendency to chemically react with $O_2$ in order to form $CO_2$. The $CO_2$ formation with combustion follows (1.6) - (1.9):

$$CO + O_2 \rightarrow CO_2 + O \quad (1.9)$$

$$O + H_2O \rightarrow OH + OH \quad (1.10)$$

$$CO + OH \rightarrow CO_2 + H \quad (1.11)$$

$$H + O_2 \rightarrow OH + O \quad (1.12)$$

$CO_2$ does not directly impair human health, but it is a major greenhouse gas that traps the earth's heat and contributes to deteriorating global warming. It also dissolves in water and can be responsible for ocean acidification which can be harmful to seashells and corals. Note that carbon dioxide cannot be avoided with any carbon-based fuel combustion,

so the only long term mitigation of this gas is capture and sequestration, including the possibility of oxy-fuel combustion to minimize the exhaust stream being controlled.

Hydrocarbons (HC) represent any unburned fuel, and result from the condition when fuel molecules in the engine do not burn or burn only partially. HC emission also plays a part in the fouling of the engine and oil contamination. Large amounts of HC can be produced during the combustion process where local rich mixtures are at lower temperature. In addition, a small amount of HC is produced from wall quenching effects which occur as the flame front burns toward the relatively cooler areas, such as the metallic walls of the combustion chamber. The solution for burning the unburnt HC would be enough $O_2$ concentration and high exhaust temperature for chemically complete oxidation. In a full sized engine, the control of these three main pollutants (HC, CO, NO) is handled by a three-way catalyst that reduces the NO and oxidizes the HC and CO. To date, the cost of the rare materials in such catalysts has been prohibitive for small engines, including the cost of high fuel/air ratio control necessary for high performance of such after-treatment. Hence, small engine combustion provides a unique emission control challenge where non-catalyst methods can be exploited.

# CHAPTER 2: Exhaust Gas Recirculation (EGR)

## 2.1 Chemical Process and Effects of EGR

Although it can be counterintuitive, the hot products of combustion retain sufficient sensible heat to improve the oxidative reactivity of the products from a combustion process. The main components of EGR are $N_2$ and $O_2$ of the fresh intake air and hot $H_2O$, $N_2$, and $CO_2$ recirculated. The additive effect of the $H_2O$ and $CO_2$ recirculated to a combustion chamber, specifically the oxidizer stream, through an EGR system has three effects (dilution, chemical, thermal) for reducing the flame temperature and $NO_x$ without severely affecting the combustion efficiency.

Recall the equation (1.1), the chemical combustion process not including EGR for general hydrocarbon fuel that might contain oxygen is the following [6]:

$$CH_yO_z + n(O_2 + \xi N_2)$$
$$\rightarrow aCO_2 + bH_2O + cC_3H_{3y} + dNO + eH_2 + fO_2 + gCO + hN_2$$

And then, based on (1.1), the derived chemical combustion process including EGR for general hydrocarbon fuel that might contain oxygen is the following [4]:

$$CH_yO_z + n(O_2 + \xi N_2) + \frac{EGR}{100}(aCO_2 + bH_2O + cC_3H_{3y} + dNO + eH_2 + fO_2 + gCO + hN_2)$$
$$\rightarrow aCO_2 + bH_2O + cC_3H_{3y} + dNO + eH_2 + fO_2 + gCO + hN_2 \quad (2.1)$$

which originates from

$$C_{n\_carb}H_{yn\_carb}O_{zn\_carb} + n'(O_2 + \xi N_2) + \frac{EGR}{100}(a'CO_2 + b'H_2O + c'C_3H_{3y} + d'NO + e'H_2 + f'O_2$$

$$+ g'CO + h'N_2) \rightarrow (a'CO_2 + b'H_2O + c'C_3H_{3y} + d'NO + e'H_2 + f'O_2 + g'CO + h'N_2 \quad (2.2)$$

By normalizing with n_carb:

$$CH_yO_z + \frac{n'}{n\_carb}(O_2 + \xi N_2) + \frac{EGR}{100}\left(\frac{a'}{n\_carb}CO_2 + \frac{b'}{n\_carb}H_2O + \frac{c'}{n\_carb}C_3H_{3y} + \frac{d'}{n\_carb}NO\right.$$

$$\left. + \frac{e'}{n\_carb}H_2 + \frac{f'}{n\_carb}O_2 + \frac{g'}{n\_carb}CO + \frac{h'}{n\_carb}N_2\right)$$

$$\rightarrow \frac{a'}{n\_carb}CO_2 + \frac{b'}{n\_carb}H_2O + \frac{c'}{n\_carb}C_3H_{3y} + \frac{d'}{n\_carb}NO + \frac{e'}{n\_carb}H_2 + \frac{f'}{n\_carb}O_2 + \frac{g'}{n\_carb}CO$$

$$+ \frac{h'}{n\_carb}N_2 \left(\text{Where } n = \frac{n'}{n\_carb}, a = \frac{a'}{n\_carb}, b = \frac{b'}{n\_carb}, c = \frac{c'}{n\_carb}, d = \frac{d'}{n\_carb},\right.$$

$$\left. e = \frac{e'}{n\_carb}, f = \frac{f'}{n\_carb}, g = \frac{g'}{n\_carb}, h = \frac{h'}{n\_carb}\right) \quad (2.3)$$

Complete and theoretical combustion with EGR yields only $CO_2$, $H_20$, and $N_2$.

$$CH_yO_z + n(O_2 + \xi N_2) + \frac{EGR}{100}(aCO_2 + bH_2O + hN_2) \rightarrow aCO_2 + bH_2O + hN_2 \quad (2.4)$$

Hence, equation (2.1) was considered for the actual incomplete combustion of a 49cc spark ignition small scale engine with an EGR system.

**Effects of EGR**

(a) The dilution effect

Some portion of the recirculated and inert exhaust gases dilutes the fresh intake air charge which disturbs and decreases the inlet oxygen concentration in the main stream. This leads to displacement and reduction of reactive species during the combustion process. As a result, the dilution effect of EGR reduces the flame temperature and the formation of $NO_x$ (Pierpont *et al* 1995) [39].

(b) The chemical effect

The recirculated $H_2O$ and $CO_2$ are hot enough to be active sources, when being partially dissociated to chemically participate in the combustion process (the dissociation is an active endothermic reaction), resulting in reduced flame temperature and lowered $NO_x$ formation.

(c) The thermal effect

EGR also has a thermal effect since heat absorption from $CO_2$ (36kJ/kmol·K) and $H_2O$ vapor (33.5kJ/kmol·K) is higher than the same molar content over $O_2$ (30kJ/kmol·K) and $N_2$ (29kJ/kmol·K). In this way, the exhaust gases function as an EGR heat sink. This thermal effect of EGR reduces the flame temperature and $NO_x$ during the combustion process.

In addition, replacing $CO_2$ and $H_2O$ with their higher heat capacity, along with the lowered in-cylinder temperature increases the γ of equation (2.5) which results in the ideal gross Otto cycle thermal efficiency of the engine to be higher based on the following:

$$\eta_{Thermal} = 1 - \frac{1}{r_c^{(\gamma-1)}} \quad (2.5)$$

Efficiency is a function of the mechanical system (compression ratio, $r_c$)

Efficiency is a function of the working gas properties, $\gamma = \frac{c_p}{c_v}$

As general thermodynamics theory describes, the ideal Otto cycle efficiency is merely used to provide insight and analysis. Real engines are not completely governed by the Carnot cycle efficiency since the working fluid components are renewed every cycle and changed throughout the cycle. Nevertheless, the improved theoretical efficiency is realized to a small extent.

**$CO_2$**

There are three effects described, the thermal effect, chemical effect, and dilution effect, of $CO_2$ in EGR. As shown in Figure 2, in internal combustion engines, the reduction of the $NO_x$ formation is due to about 90% dilution effect with small contributions of chemical effects, accounting for about 10% and thermal effects a negligible contribution [5, 71]. So then, the three effects combined (the dilution, the chemical, and the thermal effects) have an influence on substantially reducing $NO_x$ emission in the particular conditions of moderate and heavy load.

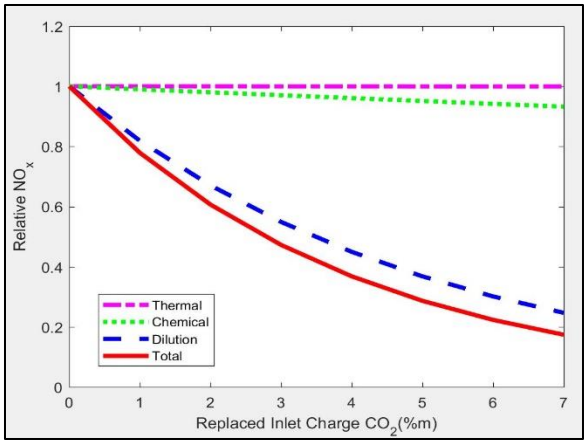


*Figure 2. Effects on relative $NO_x$ emission of $CO_2$ substituting $O_2$ in the inlet charge [5, 71]*

**$H_2O$**

$H_2O$ vapor is the second principal component of the EGR. For the case of the $H_2O$ vapor reduction of $NO_x$, the largest effect of the inlet charge is the dilution effect of the maximum at the 3% of the inlet charge with small contributions from the chemical effect and thermal effect. As the $H_2O$ effects combined (the dilution, the chemical, and the thermal effects) work, $NO_x$ is substantially reduced. The effects of $H_2O$ vapor have a similar tendency of that of $CO_2$ (Figure 3) [5, 71, 72]. And, generally, in internal combustion engines, at the inlet charge, $H_2O$ concentration is a half of the $CO_2$ concentration, which is the main component of the recirculated exhaust gas in EGR.

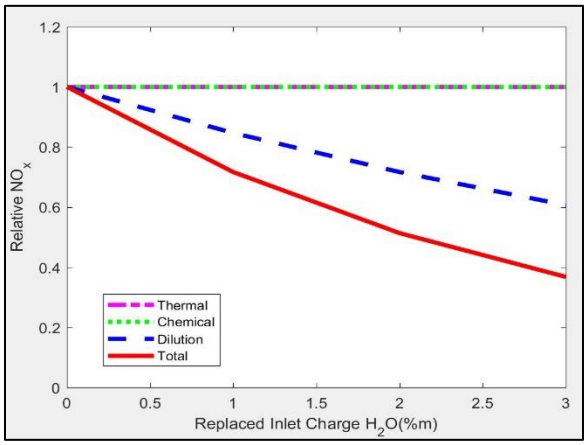


*Figure 3. Effects on relative $NO_x$ emission of $H_2O$ vapor substituting $O_2$ in the inlet charge [5, 72]*

**Blended $CO_2$ and $H_2O$**

Overall, substituting blended $CO_2$ and $H_2O$ vapor with $O_2$ as part of the inlet makes a synergistic effect on reducing NOx with the great contribution of the dilution effect of $CO_2$ and $H_2O$ vapor, and a smaller contribution of the thermal and chemical synergy effects. Moreover, the synergy is greater as the substitution of $CO_2$ and $H_2O$ with $O_2$ increases, with the most substantial reduction of $NO_x$ in the range of 20% - 40% (Figure 4) [5, 71, 72].

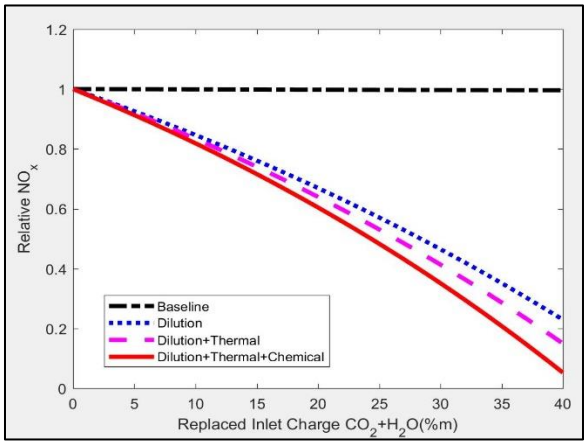


*Figure 4. Effects with blended $CO_2$ and $H_20$ vapor substituting $O_2$ in the inlet charge [5, 71, 72]*

## 2.2 EGR Equations

In order to define the extent of recirculation in EGR, it is important to agree on appropriate definitions. The following EGR definitions are used [4]:

$$Total\ EGR = \frac{Recycled\ mass}{Total\ gases\ mass\ of\ cyliner} \times 100 \tag{2.6}$$

$$Internal\ (Residual)\ EGR = \frac{Recycled\ residual\ mass}{Total\ gases\ mass\ of\ cyliner} \times 100 \tag{2.7}$$

$$External\ EGR = \frac{Recycled\ external\ mass}{Total\ gases\ mass\ of\ cyliner} \times 100 \quad (2.8)$$

$$Intake\ EGR = \frac{Recycled\ external\ mass}{Total\ intake\ gases\ mass} \times 100 \quad (2.9)$$

Among all of the EGR definitions, the most commonly used in experimental emission bench measurement is the external EGR.

The external *EGR rate (%)* (regarded as *EGR rate in percent)* is derived from the ratio of the volume of EGR and the total intake charge into the cylinder, see Equation 2.10. But, there is another practical approach, which uses an experimental technique and is based on the ratio derived from the atmospheric $CO_2$, intake $CO_2$, and exhaust $CO_2$, see Equation 2.11 (Baert *et al* 1999) [14]). The EGR technique depends on how much $CO_2$ is recirculated and tracks primarily the $CO_2$ addition effect in the inlet manifold.

$$EGR\ rate\ (\%) = \frac{Volume\ of\ EGR}{Total\ intake\ charge\ into\ the\ cylinder} \times 100 \quad (2.10)$$

$$EGR\ rate\ (\%) = \frac{[CO_2]_{Intake} - [CO_2]_{Atmosphere}}{[CO_2]_{Exhaust} - [CO_2]_{Atmosphere}} \times 100 \quad (2.11)$$

## 2.3 EGR Classification

Various EGR systems have been classified on the basis of the EGR configuration, the temperature, the and pressure [1].

2.3.1 Classification based on configuration

(a) Short route system (Lundquist *et al* 2000) [37])

The short route EGR system is a method to use a variable nozzle turbine with only a single entrance, which decreases the pulsation of the recirculated exhaust gases. Lundquist used this system where the EGR injector was allowed to move axially.

(b) Long route system

The long route EGR system allows pressure drop across the incoming fresh air and the stagnation pressure in the recirculated exhaust gases, and then its velocity results in a pressure difference for EGR across the entire engine system.

2.3.2 Classification based on temperature

(a) Partly cooled EGR

In a system to avoid the corrosion of water condensation, the temperature of the exhaust gas is kept above the dew temperature of the water.

(b) Fully cooled EGR

The recirculated exhaust gases are cooled down through a water-cooled heat exchanger system before mixing with incoming fresh air.

(c) Hot EGR

Exhaust gases are recirculated without being cooled down, resulting in intake air temperature increase. This EGR system was the version applied to the scooter engine in this thesis since it was easy to set up and investigate effects of EGR without considering the complications of an EGR cooler system. For such low cost engine applications, it is likely that the simplest possible EGR system would be preferred.

2.3.3 Classification based on pressure (Kohketsu *et al* 1997) [38]

(a) Low pressure route system

The low pressure routing EGR system is to use the route for EGR from downstream of a turbine system to upstream of a compressor, giving rise to a low pressure of the recirculated exhaust gases through the passage.

(b) High pressure route system

The high pressure routing EGR system uses the passage for EGR from upstream of a compressor to downstream of a turbine, in contrast to the low pressure routed EGR system. However, this technique makes the air/fuel richer and increases fuel consumption as a disadvantage.

## 2.4 EGR for 49 cc Scooter Engine

To summarize, the EGR system employed in this thesis research will be the simple low pressure, long route, hot EGR. While there are some disadvantages for each of these classification choices, the overall demand for simple and effective EGR for single cylinder use is more important.

# CHAPTER 3: Experimental Testbed Setup

The experimental facility includes an engine, a chassis dynamometer, a custom EGR system, and emissions instrumentation. In-cylinder pressure measurements will be a future addition but the current work focuses on emission outcome from passive EGR in a single cylinder scooter engine.

## 3.1 Specification of Engine

Compared to the earlier small-scale studies focusing on alternative combustion processes like the 25cc HCCI engine with an air-cooled system and compression ratio 8.7:1 of the 2002 Honda GX25 [49] and the 49.4cc HCCI engine with a liquid-cooled system and compression ratio 11.9:1 of the 2009 Honda Ruckus scooter [50], the current thesis uses a single cylinder of 2013 Yamaha Vino 49cc as the advanced engine and set for the investigation of EGR. This is the smallest fuel injected, water-cooled, 4-stroke system available commercially. It has forced radiator water-cooling, port injection, 12:1 compression ratio, 4-stroke/cycles, and spark ignition. Specifications of the engine are as given in Table 2.

| Test Engine (2013 Yamaha Vino 50) | 4-Stroke |
|---|---|
| Displacement | 49 cc |
| No. of Cylinder | 1 (Single) |
| Compression Ratio | 12 : 1 |
| Bore | 38 mm |
| Stroke | 43.6 mm |
| Ignition Timing (B.T.D.C) | 5.0° / 2100 r/min |
| Fuel Supply System | Port Injection |
| Cooling System | Water Cooling |
| Air Intake | Naturally Aspirated |
| Fuel | Unleaded Gasoline (Octane 87) |

*Table 2. Specification of the 2013 Yamaha vino 50 engine*

### 3.2 Specification of an EGR Copper Pipe

An EGR copper pipe was customized for the engine and connected between the exhaust port and the intake port on the engine. Some portion of the exhaust gases were recirculated through the EGR copper pipe and put back into the combustion chamber along with the fresh intake air. The copper EGR pipe has a thermal conductivity of 400 (W/m·K) at 25°C - 230°C for the recirculation and heat reduction of the gases. That is, the copper pipe acts as both the exhaust gas conduit and as a passive convective gas partial cooler. The spark ignition 49cc small scale combustion chamber allowed an EGR valve opening position from 0° to 40°. Each EGR valve opening position was converted from the opening valve position to a corresponding EGR rate 0% - 15%. At each RPM condition of the engine,

any setting over the EGR opening valve 40°, which corresponded to EGR rate 15%, the engine died because the dilution was excessive so there was insufficient inlet $O_2$ concentration in the main stream to permit a complete combustion process.

**Designing, Modeling the pipe of EGR, and Applying it to the Small Scale Engine**

There was a designed and modeled EGR copper pipe to be linked between the ports of intake air and exhaust gas (see Figure 5). A port was created and used for the gas analyzer close to the port of intake air with an EGR valve in order to control its opening position and rate.

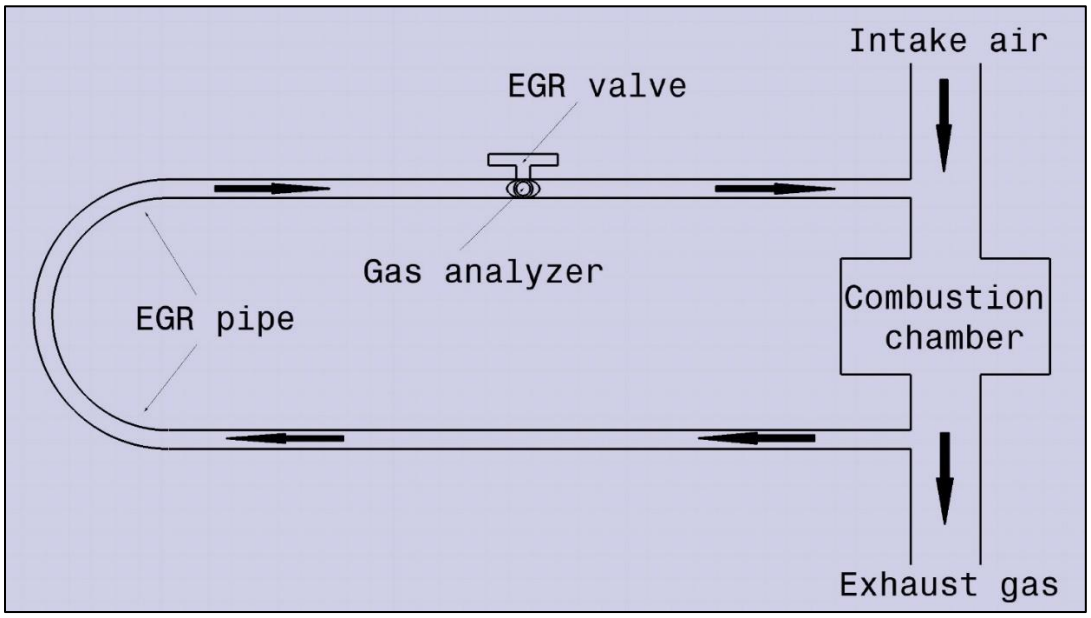


*Figure 5. Exhaust gas recirculation schematic*

The EGR copper pipe was indicated in detail by CATIA V5 showing the real view, isometric view, front view, and side view (see Figures 7-10). The parameters of the pipe are described in the unit of mm. All of the ports for the flow of the recirculated gases and the

gas analyzer had the exterior diameter of 8mm, and the interior diameter of 6mm, with a 1mm pipe thickness. The length of the pipe was 810mm which was sufficient for the temperature of the recirculated gases to be lowered by the heat transfer lost during their recirculating flow through the copper pipe with its high thermal conductivity, 400 (W/m·K) at 20℃ - 230℃.

Naturally, for a practical EGR system design, more thermal analysis will be needed to be certain that ambient temperatures and engine operating temperatures do not adversely affect the EGR heat transfer relied on for this thesis study by passive thermal control.

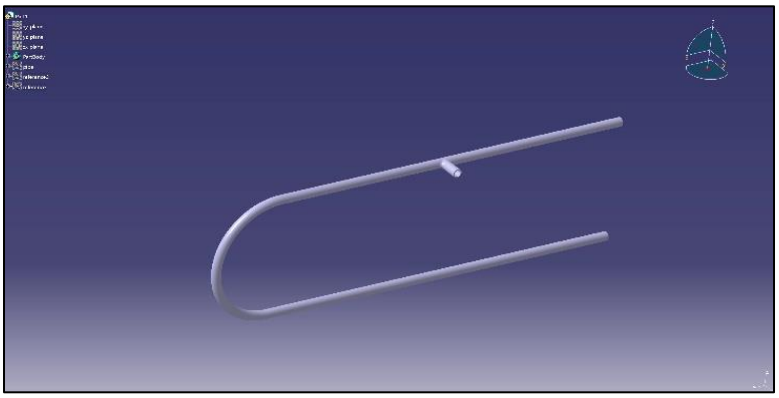

*Figure 6. EGR copper pipe by CATIA V5*

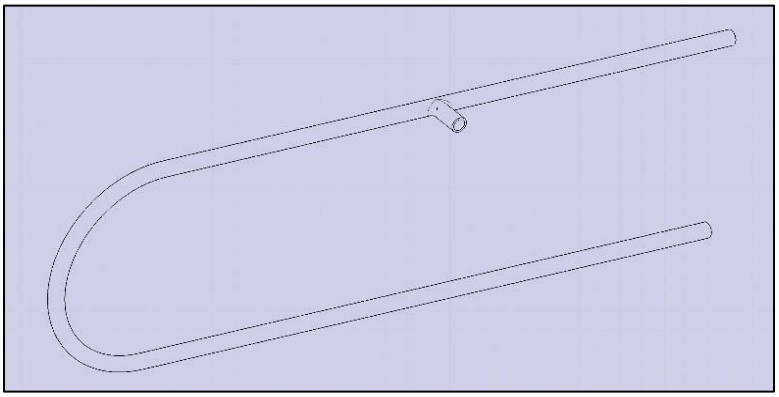

*Figure 7. Isometric view of the EGR copper*

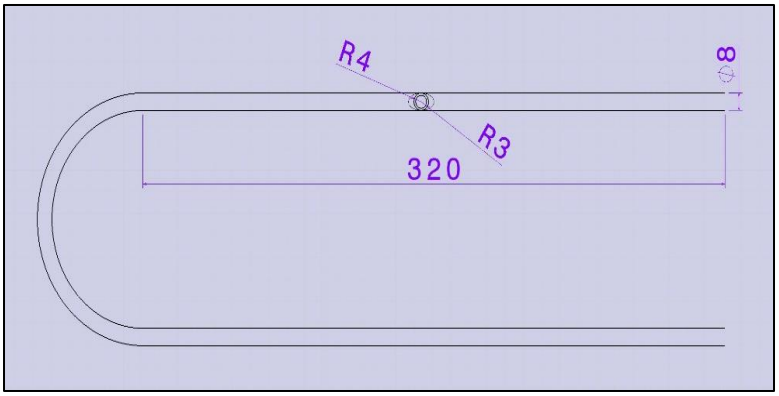


*Figure 8. Front view of the EGR copper*

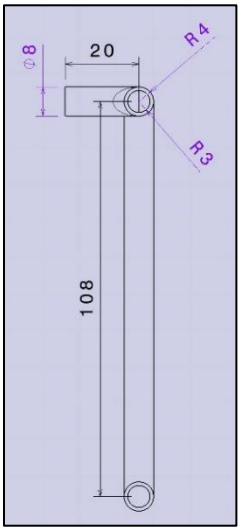


*Figure 9. Side view of the EGR copper pipe*

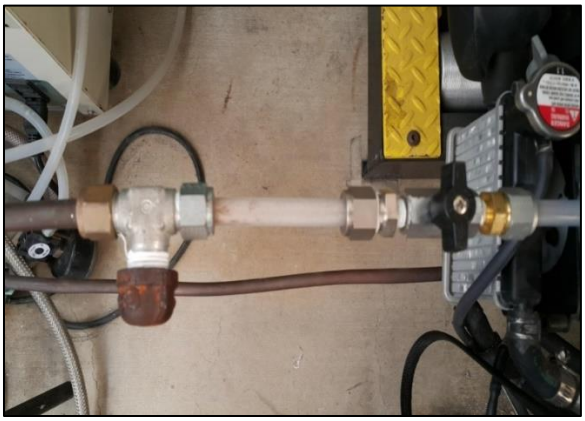

*Figure 10. Part for the gas analyzer and EGR opening valve*

Again, the objective of this system was to reduce the amount of $NO_x$ produced by the combustion process. The system was expected to reduce the peak flame temperature during the combustion process thereby preventing the high rate of $NO_x$ (NO and $NO_2$). Since changing the combustion would affect not only the variation of the $NO_x$, the EGR system was expected to affect other gas emission (CO, HC, and $CO_2$), and the torque and power of the engine affiliated with the EGR opening valve position and EGR rate. Hence, the study followed these engine response parameters over a range of conditions.

### 3.3 Experimental Testbed Setup

The spark ignition 49cc scooter was mounted on a testbed and uncovered for installing sensors and controlling driving conditions (See Figure 11).

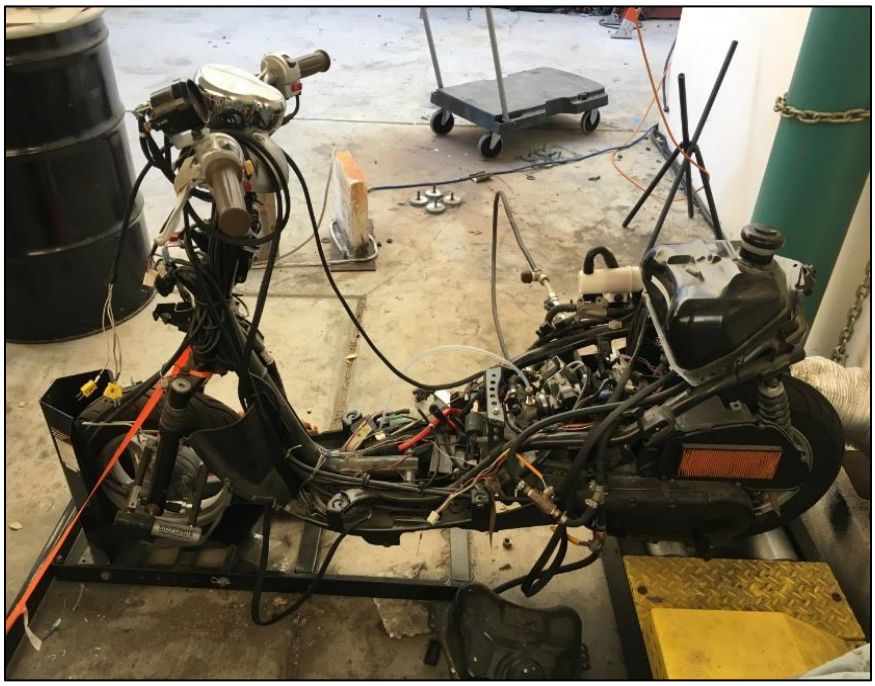

*Figure 11. 49cc scooter affiliated with the EGR copper pipe mounted on a testbed*

For measuring air/fuel ratio (AFR), a Bosch oxygen sensor with AEM air/fuel ratio gauge (AEM 35-8460 digital UEGO wideband AFR gauge) was set up (See Figure 12). This system used an $O_2$ sensor plugged into the exhaust port to calculate the AFR ratio. As a narrow band $O_2$ sensor could only tell if the air/fuel mixture was rich or lean, the wide band sensor used with this gauge was more accurate and could indicate the value of the AFR ratio with a precision of 0.1.


*Figure 12. Air/fuel ratio (AFR) gauge (AEM 35-8460 digital UEGO wideband AFR gauge)*

An Enerac 700 gas emission analyzer was utilized to detect and measure the $NO_x$ (NO and $NO_2$), CO, $CO_2$, $O_2$, and HC. This device is composed of a probe linked to a setting box that could be connected to a computer system (See Figure 13 and Figure 14). It indicated $O_2$, CO, and $CO_2$ rates as well as $NO_x$ and HC ppm. The filter block and condenser for soot products from the combustion process retained water. During running EGR tests, the probe was linked into a port of the EGR copper pipe for the gas analyzer after the device calibrated itself with ambient air. In this investigation, the indicated emissions were calculated as the mass flow rate of pollutants per unit of power output, and the indicated specific exhaust emission for the concentration of component gas $ISE_{Exhaust}$ was given as [9]:

$$ISE_{Exhaust} = \frac{n \times \dot{m}_{Exhaust}}{IMEP \times V_d \times Z} \quad (3.1)$$

(Where $\dot{m}$ = the mass flow of emissions, $n$ = the speed of the engine, $IMEP$ = the indicated mean effective pressure, $V_d$ = the displacement, and $Z$ = the number of cylinders).

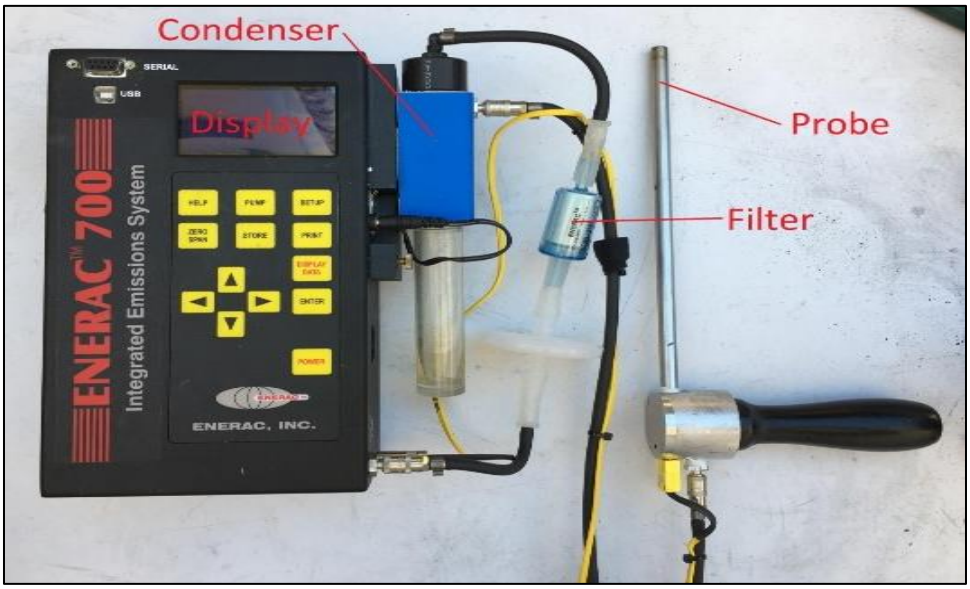


*Figure 13. Enerac 700 gas emission analyzer*

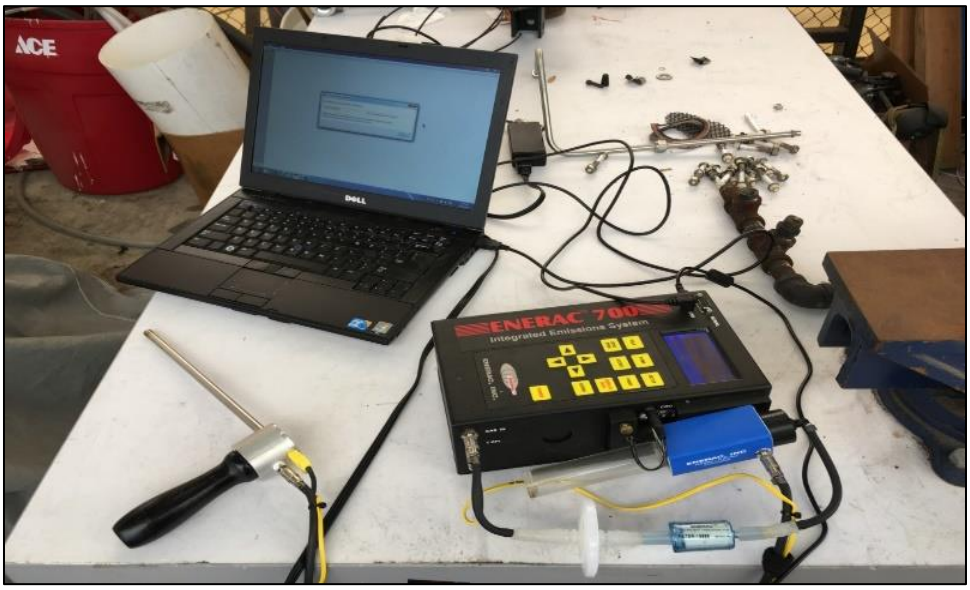


*Figure 14. Connection the Enerac 700 gas analyzer with a computer*

A Mustang dynamometer control box and its chassis dynamometer bench were set up for measuring the dynamometer chassis torque and the rear wheel speed of the scooter (See the Figure 15 and Figure 16). The rear wheel of the scooter was placed on the dynamometer bench linked to the control box. The control box indicated the dynamometer chassis torque and the rear wheel speed.


*Figure 15. Mustang dynamometer control box*


*Figure 16. Mustang chassis dynamometer bench*

An Adam GFK 165aH electronic scale was utilized to measure fuel consumption with respect to each EGR opening valve, EGR rate, and RPM condition. As the fuel tank of the scooter was detachable, it was placed on the scale to measure the variation of its weight over the test time. Based on this, the fuel consumption in mg/s was derived.

There were two fuel tanks set up, using the main tank and alternative fuel tank from the previous project [28] and to be used in further research (See Figure 17). For the EGR research, the main tank was only used for unleaded gasoline with octane 87 which meets the needs of most vehicles and has been most popular.

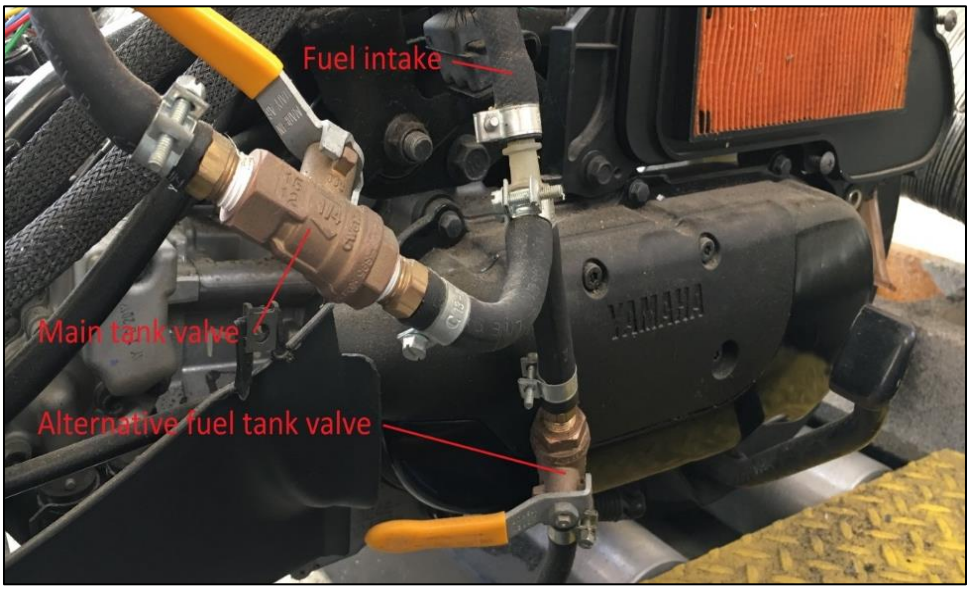


*Figure 17. Valve system to switch fuel tank*

For measuring the intake $CO_2$ into the combustion chamber for deriving the external EGR rate, based on the EGR equation (See Equation 2.12) with regard to each EGR opening valve position, a small opening hole for measuring the intake $CO_2$ was created to fit the size of the probe of the gas analyzer between the throttle body and the fuel injection port (See Figure 18).

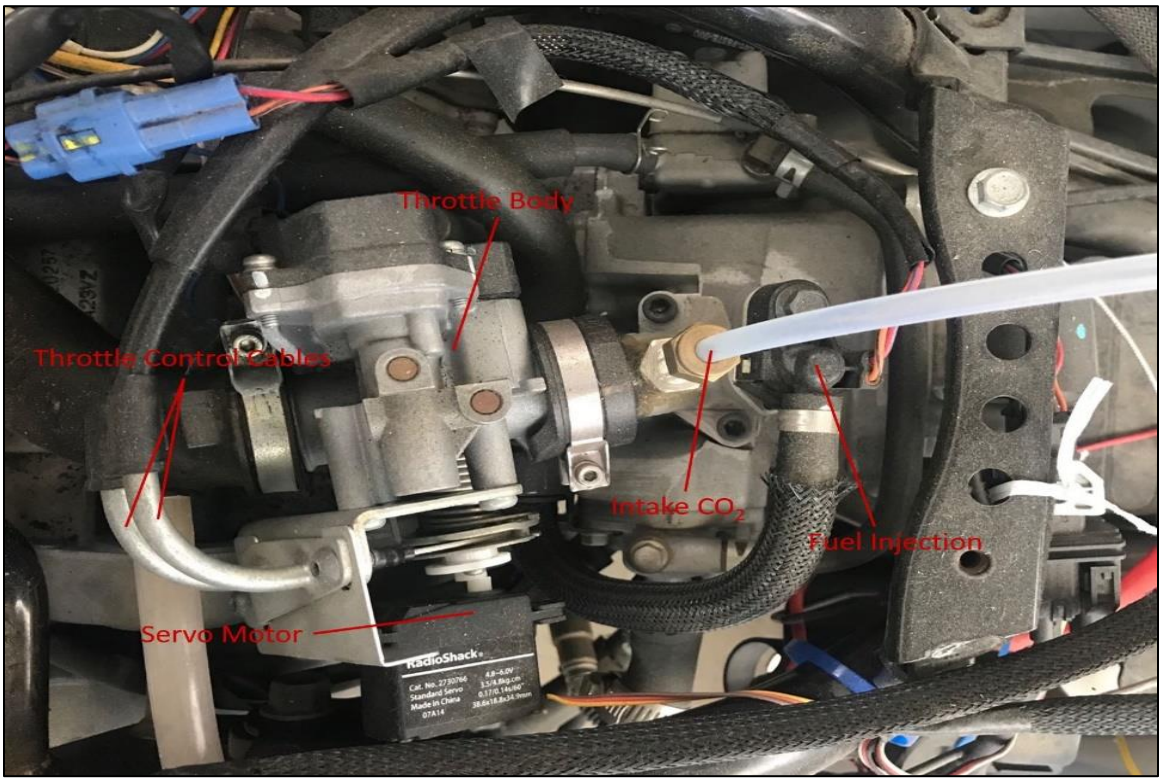


*Figure 18. Throttle body parts*

K-type thermocouples for the temperature sensors of intake air, engine coolant, and exhaust gas were used to specifically measure the temperature of the intake air charge into the cylinder, the coolant leaving the cylinder, and the exhaust gases before entering the muffler. The thermocouples were connected to a module that allowed the reading of the

temperature on a LabVIEW program in a computer data acquisition system and with a multi-meter (See Figure 19 and Figure 20).


*Figure 19. Temperatures sensors of intake air, engine coolant, exhaust gas*


*Figure 20. Multi-meter for the temperatures*

K-type thermocouples are inexpensive, and they operate in oxidizing atmospheres for the range of temperatures between 0°C and 1100°C. They were mounted on the exhaust port, the intake port, and the coolant circuit right around the cylinder. They were linked to

the National Instruments modules (NI cDAQ 9174 and NI 9211 for temperatures and DAQ 9205 for air/fuel ratio AFR) to allow data reading on a computer through a LabVIEW interface that displayed temperatures and air/fuel ratio in real time at once (See Figure 21 and Figure 22). For a double check, a simple multi-meter was used to read the data from the thermocouples (See Figure 19).

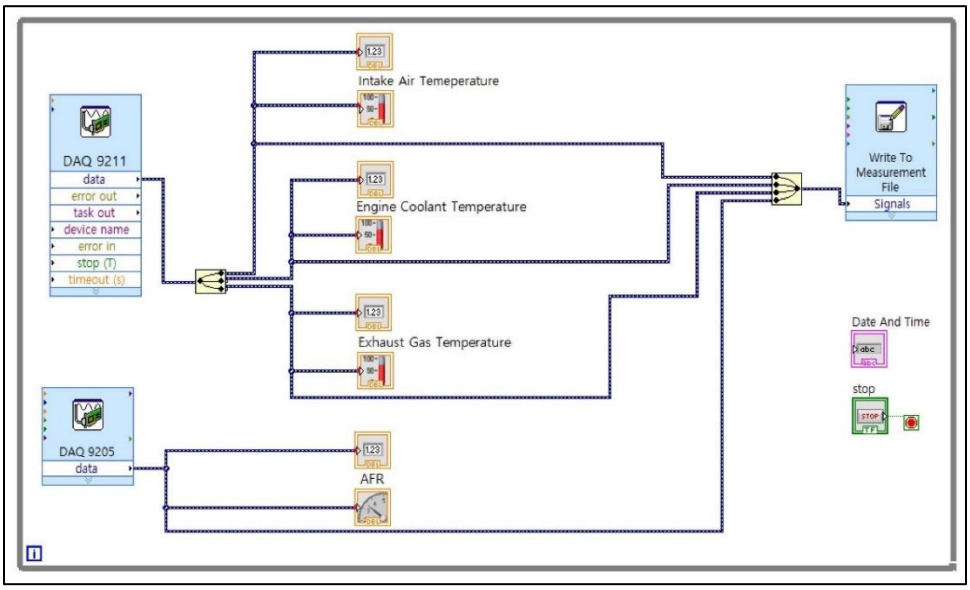


*Figure 21. LabVIEW codes for temperatures and air/fuel ratio (AFR)*

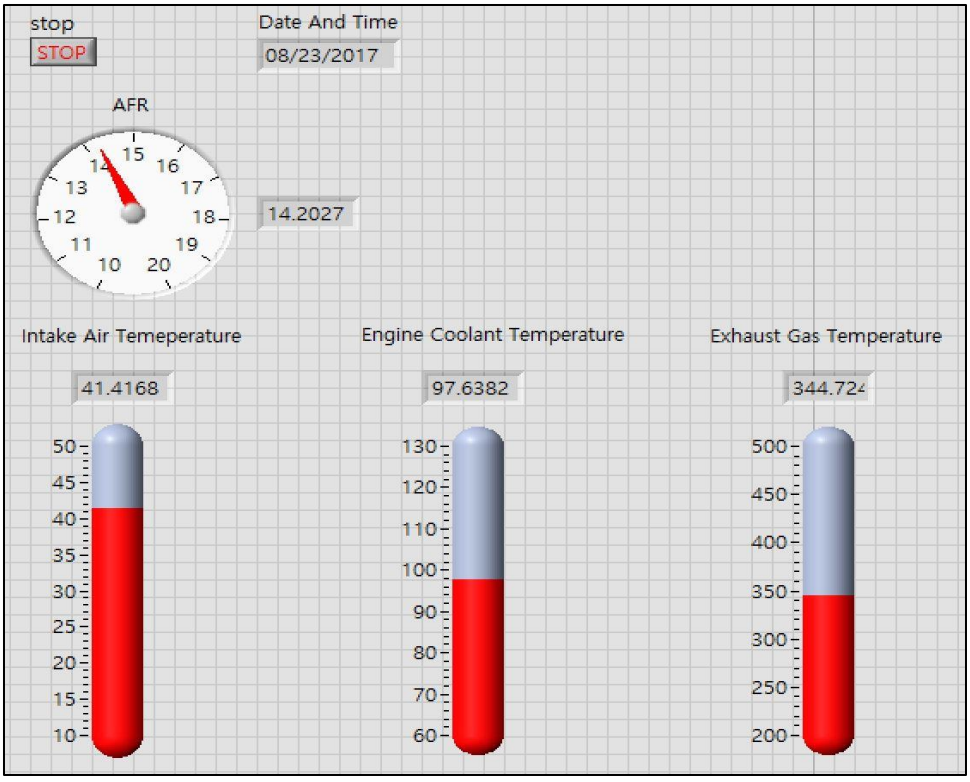


*Figure 22. Front panel of the temperatures and air/fuel ratio (AFR) on LabVIEW*

The rotating speed of the engine was measured through a small piece of reflecting tape attached on the radiator fan which rotates at exactly the same speed as the crankshaft of the engine for a laser tachometer to measure revolution per minute (RPM) (See Figure 23). It turned out that the scooter manual claims an idle speed of RPM 2100, which was just as the tachometer indicated.


*Figure 23. Tachometer and reflective tapes on the rotating radiative fan*

### 3.4 Experimental Procedures

In order to investigate the EGR effects, several repeated tests were carried out and results were collected at each RPM condition of the engine affiliated with the EGR copper pipe system.

The results were collected as the following:

- Exhaust gases (rate of CO, $CO_2$ and $O_2$ and ppm of $NO_x$ and HC)
- Temperatures of the intake air, the engine coolant, and the exhaust gases
- RPM of the engine and speed of the rear wheel of the scooter
- Air/fuel ratio
- Fuel consumption
- The torque of the dynamometer chassis, the torque and power of the engine

The 0° of the EGR opening valve position was completely the closed state and the 90° position was the fully open state. For experiments, the EGR opening valve position was

controlled and set as 0°, 10°, 20°, 30°, and 40° at an interval of 10°. The EGR opening valve positions could be correspondingly converted to EGR rate from 0% to around 15% based on the driving conditions. Interestingly, over the EGR opening valve position of 40° (around EGR rate 15%), the amount of exhaust gases recirculated into the intake port was too high and would not allow the engine to operate. After setting the EGR opening valve position, the RPM was set from the idle RPM2100 to RPM6000 at intervals of RPM1000.

The procedure for measurements at each EGR valve position and EGR rate was the following:

(1) The EGR opening valve position was set 0° (assumed as without EGR)

(2) The engine was turned on and warmed up at the idle RPM2100

(3) Once the temperature sensors displayed a stabilized value as a steady state, after 7 - 10 minutes, measurements from every sensor were written down (temperatures, exhaust gas components, speed of the wheel, AFR ratio, fuel consumption, dynamometer chassis torque).

(4) The EGR opening valve position was then set to the next EGR opening valve position at the interval of 10°

(5) The procedure of (4) was repeated for each EGR opening valve position until 40° at the constant RPM condition

(6) Each measurement was written down again

(7) The engine speed was then set to the next RPM condition at the interval with following all procedures of (1) - (6) at the each constant EGR opening valve position

(8) All procedures of (1) - (7) were repeated 3 times on the other days and all results in the steady state after 7 - 10 minutes were analyzed for their average value

(9) The engine was turned off to cool it down

(10) The results were all analyzed, deriving all possible and meaningful values for analyzing the effect of EGR on combustion of spark ignition 49cc small scale engine

# CHAPTER 4: Results and Discussion

This chapter provides a comprehensive set of results for all of the key measurables relative to the EGR rate for the 49 cc scooter engine. The results comprise: exhaust temperature, NOx, air/fuel ratio, engine coolant temperature, intake air temperature, fuel consumption, CO and HC emission, $CO_2$ concentration, engine torque, engine power, and thermal efficiency.

## Exhaust Temperature

The temperature of the exhaust gas decreased as the EGR opening valve and EGR rate increased, as would be expected (See Figure 24 and Figure 25). In particular, at high RPM (RPM4000 - RPM6000), the slopes of the temperature drop were steeper as compared to the change at the low RPM (RPM2100 - RPM3000). Once again, each RPM condition allowed its own maximum EGR rate as the electronic control unit (ECU) of the scooter optimally controlled for running the engine. The decrease of exhaust gas temperature should correlate with the in-cylinder temperature during combustion, assuming no change in extracted heat or work. Thus, this decrease in combustion temperature with the higher EGR rate was expected to give rise to a significant reduction of soot formation in the engine rather than soot oxidation in the cylinder, since the oxygen concentration was reduced due to the higher amount of exhaust gases recirculated [9].

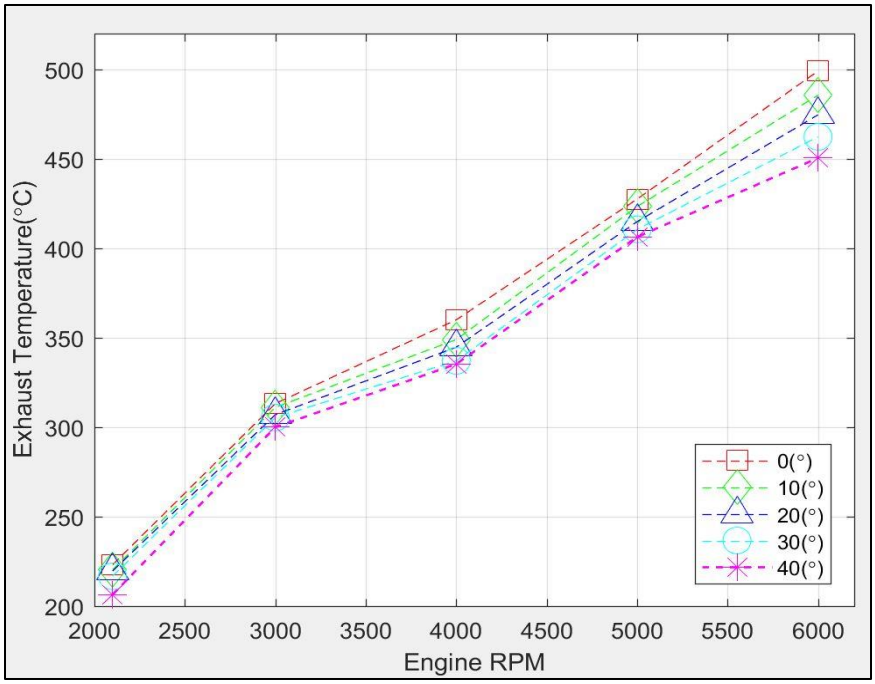


*Figure 24. Exhaust Temperature(℃) vs EGR opening valve(°)*

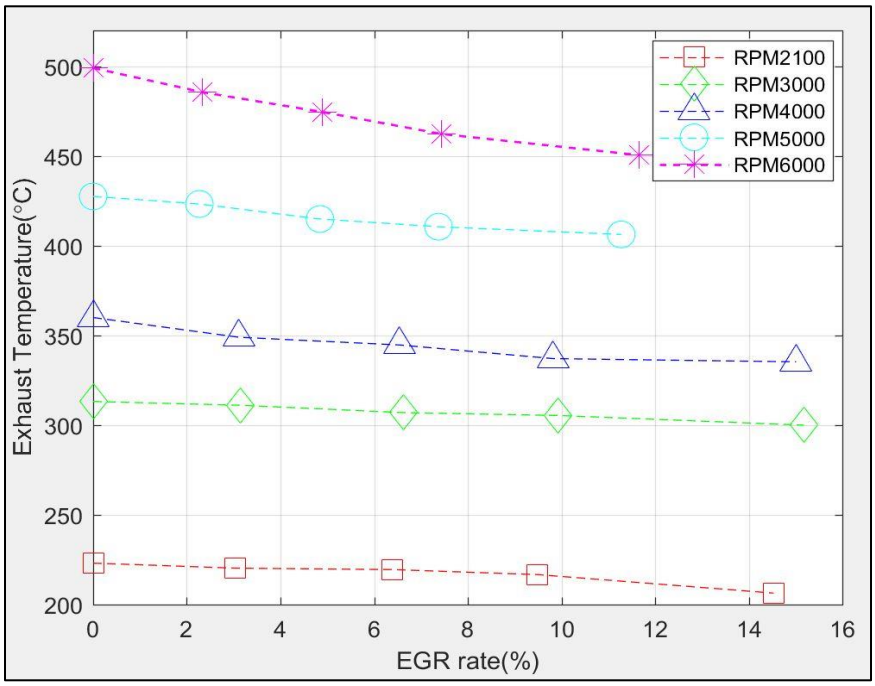


*Figure 25. Exhaust Temperature(℃) vs EGR rate(%)*

The reductions in exhaust gas temperature were -16.7℃ between the EGR rate 0% and 14.5% at the idle RPM2100, -13.2℃ between the EGR rate 0% and 15.2% at RPM3000,

-24.7℃ between the EGR rate 0% and 15.0% at RPM4000, -21.2℃ between the EGR rate 0% and 11.3% at the RPM5000, and -48.6℃ between the EGR rate 0% and 11.7% at RPM6000.

**Nitrogen Oxides ($NO_x$)**

The amount of $NO_x$ decreased as the EGR opening valve and EGR rate increased. Based on the real combustion with the EGR governing equation of (2.2), the fresh intake oxygen levels of n as a reactant were lowered due to the dilution effect of the recirculated gases (A.3).

Recall the equation (2.2) related to the oxygen levels for the reduction of $NO_x$,

$$CH_yO_z + n(O_2 + \xi N_2) + \frac{EGR}{100}(aCO_2 + bH_2O + cC_3H_{3y} + dNO + eH_2 + fO_2 + gCO + hN_2)$$

$$\rightarrow aCO_2 + bH_2O + cC_3H_{3y} + dNO + eH_2 + fO_2 + gCO + hN_2$$

As the fresh intake oxygen levels decreased and as the EGR value increased affiliated with $aCO_2$ and $bH_2O$ influenced the definite reduction of dNO which was the source for generating the $NO_x$ ($NO+NO_2$).

Low $NO_x$ was produced for a light load, and so the change in this pollutant with EGR rate was not substantial. However, high levels of $NO_x$ were produced for moderate and heavy loads, and at these conditions, EGR. In particular, at high RPM (RPM4000 - RPM6000), the drop in the amount of $NO_x$ was sharper compared to the cases of low RPM (RPM2100 - RPM3000). The results show that at RPM6000, there is a maximum 77.3 % reduction of $NO_x$ (See the Figure 26 and Figure 27). The cooling effect of EGR for the

combustion process increased the differential term of the heat absorption of the non-reacting gases and the heat absorbing capacity for the reduction of the exhaust gases temperature and $NO_x$ (See (4.1)).

$$\Delta Q = \Delta m_0 \times C_p \times \Delta T \tag{4.1}$$

$\Delta Q$ = Differential in heat absorption of the non-reacting gases

$\Delta m_0$ = Differential in mass in the cylinder

$C_p$ = Specific heat capacity at constant pressure

$\Delta T$ = Differential between EGR temperature and combustion temperature

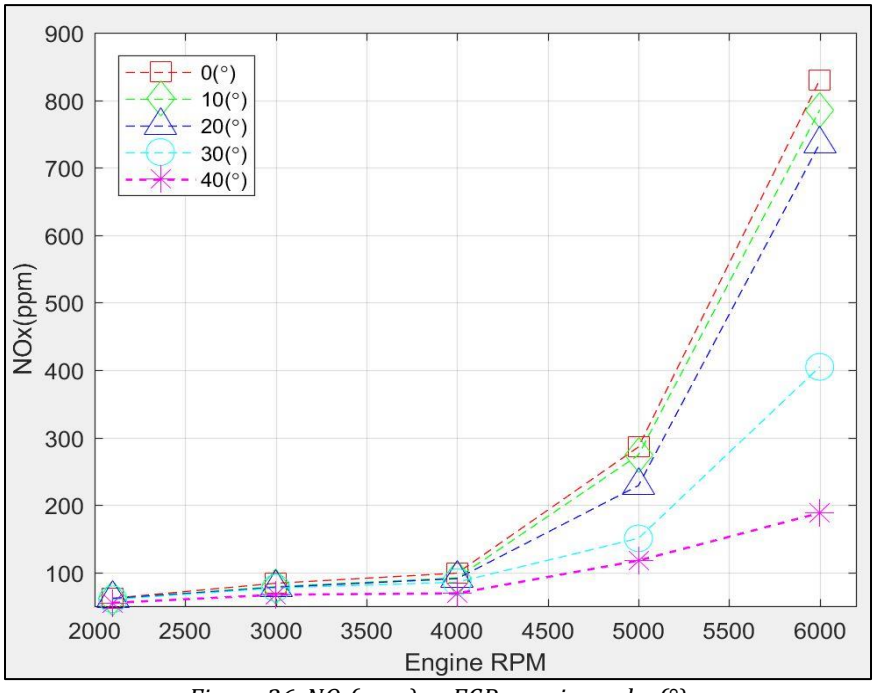


*Figure 26. $NO_x$(ppm) vs EGR opening valve(°)*

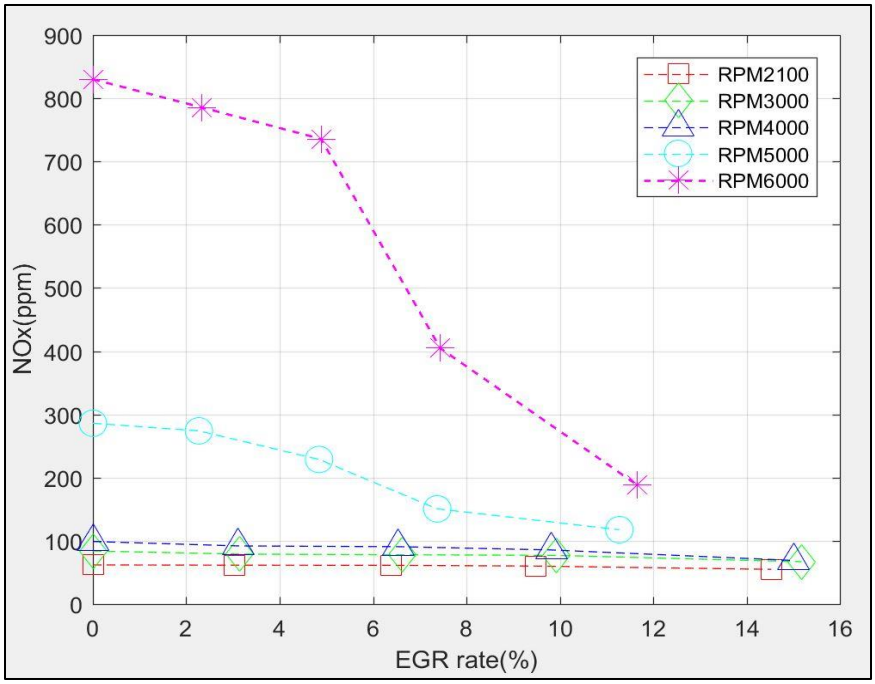


*Figure 27. $NO_x$(ppm) vs EGR rate(%)*

The results showed very clear advantages in using EGR for the reduction of the $NO_x$. They were -7ppm (-11.3%) between the EGR rate 0% and 14.5% at the idle RPM2100, -17ppm (-20.2%) between the EGR rate 0% and 15.2% at RPM3000, -30ppm (-33.3%) between the EGR rate 0% and 15.0% at RPM4000, -168.4ppm (-59%) between the EGR rate 0% and 11.3% at the idle RPM5000, and -642ppm (-77.3%) between the EGR rate 0% and 11.7% at RPM6000.

**Oxygen ($O_2$)**

Exhaust manifold $O_2$ concentration decreased as the EGR opening valve and EGR rate increased (See the Figure 28 and Figure 29). This is the direct measure of the dilution from the exhaust gas mixing into the intake. At high RPM (RPM4000 - RPM6000), the intake manifold $O_2$ drops were not linear due to the dilution effect of EGR with the

disturbance of the $CO_2$ recirculated to the $O_2$ (A.3). In fact, the oxygen concentration varies in a very nonlinear fashion with EGR rate. This indicates that the EGR is not simply a dilution phenomenon but one that affects the combustion in the engine cylinder as well.

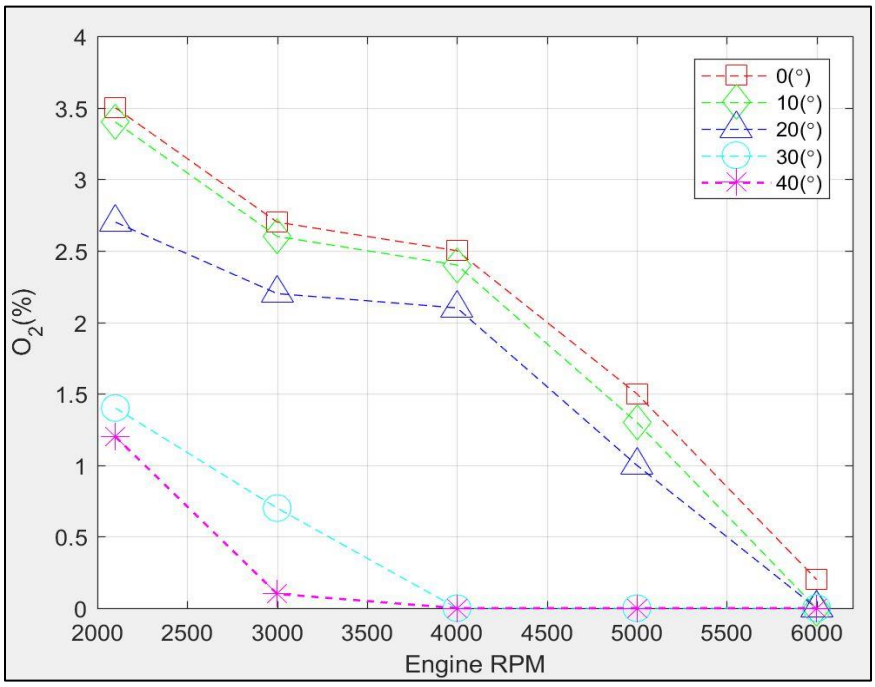


*Figure 28. $O_2$(%) vs EGR opening valve(°)*

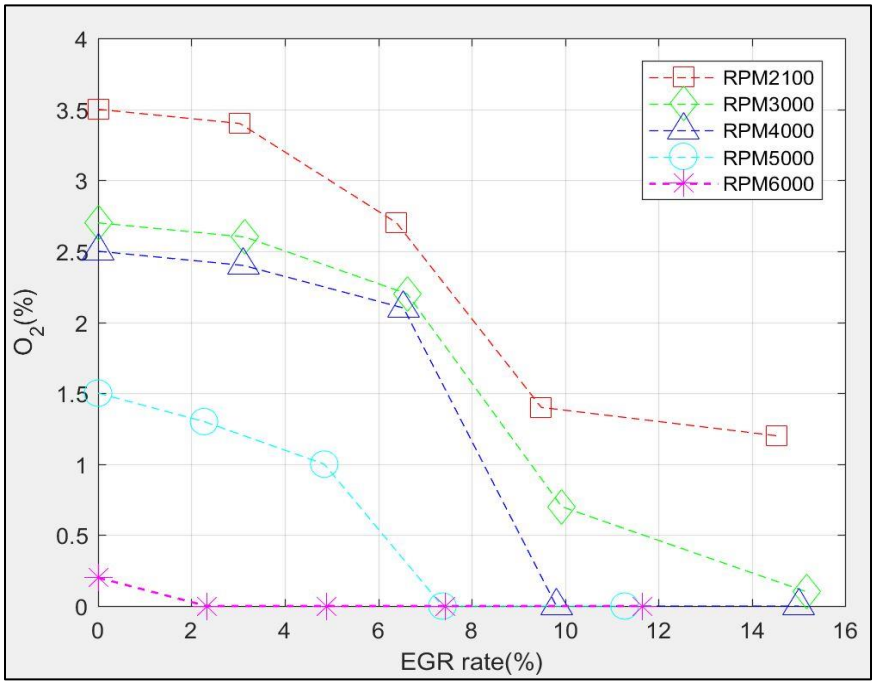


*Figure 29. $O_2$(%) vs EGR rate(%)*

**Air/Fuel Ratio (AFR)**

The air/fuel ratio (AFR) is the reference for internal combustion engines and is the ratio between the mass of intake manifold air and the mass of the fuel mixture (See (4.2)).

$$AFR = \frac{m_{Air}}{m_{Fuel}} \tag{4.2}$$

Furthermore, air/fuel equivalence ratio $\lambda$ is the ratio between the actual AFR and the stoichiometric AFR (which is 14.7 for typical octane fuel), with rich mixtures $\lambda$ <1 and lean mixtures $\lambda$>1 (See (4.3)). Note that this equivalence ratio is the inverse of typical combustion equivalence ratio where fuel is in the numerator so that values greater than 1 represent rich mixtures. The stoichiometric AFR has the exact amount and ratio of air and fuel in order to produce a chemically complete combustion.

$$\lambda = \frac{AFR}{AFR_{Stoichiometry}} \tag{4.3}$$

The ECU of the scooter was controlled to set up rich air/fuel mixtures (AFR14.2) in order to improve engine operation. This value then acted as a default AFR of the ECU of the scooter to allow the single cylinder of the 49cc engine to maximize the torque and power of the engine regardless of gas emission and fuel consumption. That is, the AFR for a single cylinder engine is not optimized for minimizing emissions nor for maximum fuel economy but instead to maximize power and torque, since this is the metric most affecting the scooter's perceived performance.

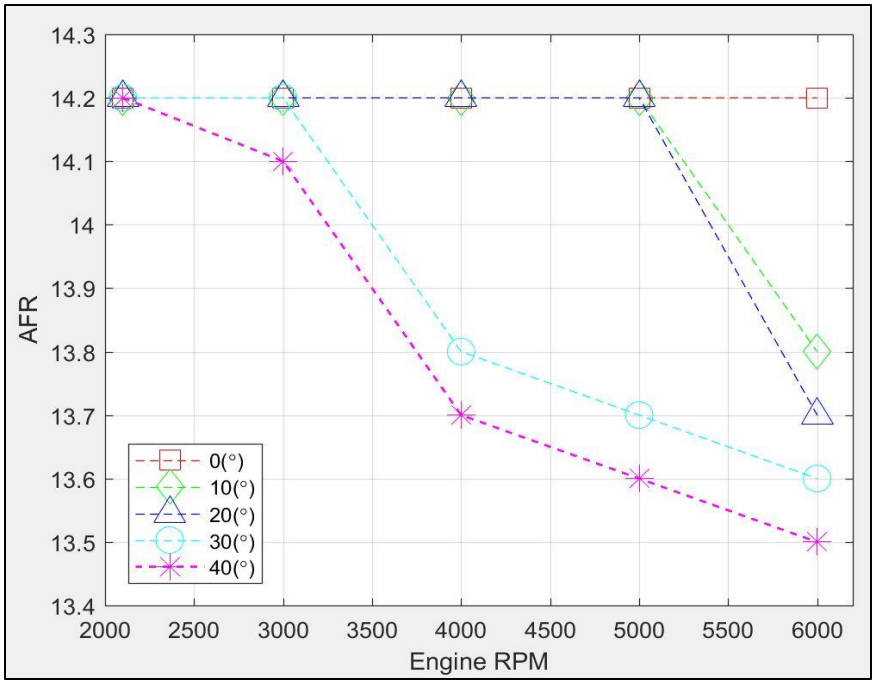


*Figure 30. AFR vs EGR opening valve(°)*

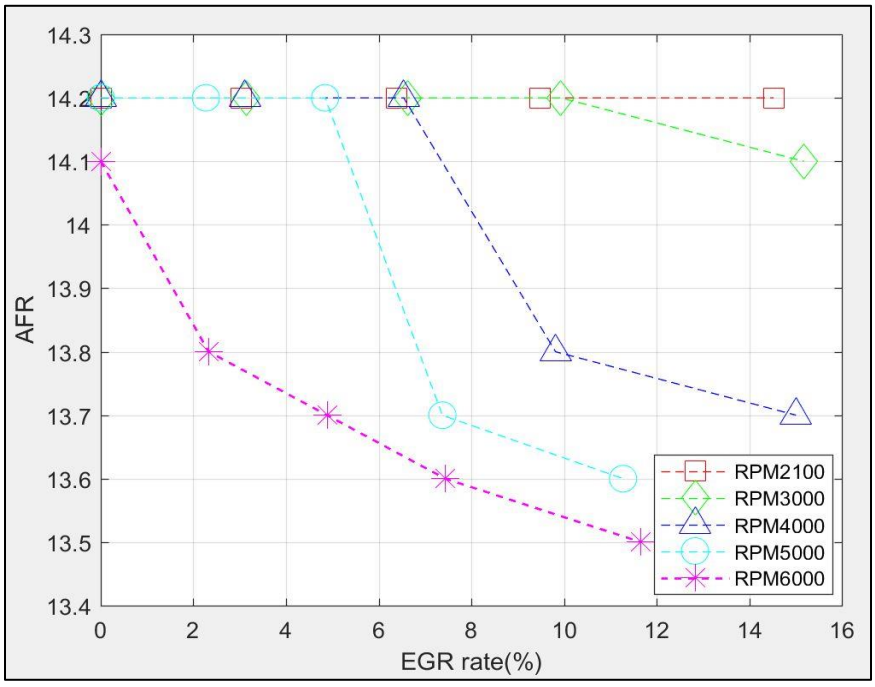


*Figure 31. AFR vs EGR rate(%)*

In this EGR research, AFR decreased as the EGR opening valve and EGR rate increased. This AFR reduction is not unexpected and has been described in the literature [6]. The combustion AFR and throttle AFR were related as:

$$AFR_{Combustion} = AFR_{Throttle} + \Delta AFR_{EGR} \tag{4.4}$$

$$AFR_{Combustion} = \frac{Air + Inert\ gases}{fuel} \tag{4.5}$$

$$AFR_{Throttle} = \frac{Air}{Fuel} \tag{4.6}$$

$$\Delta AFR_{EGR} = \frac{Mass_{Air}}{Mass_{Fuel}} (1+\xi) \frac{O_2}{CO+CO_2+3(C_3H_{3y})} \frac{EGR/100}{1-EGR/100} \tag{4.7}$$

(Where $\xi$: nitrogen/oxygen ratio of air)

Combustion of the stoichiometric AFR uses all the oxygen, leaving theoretically exhaust oxygen-free ($O_2 \simeq 0$). Thus, the $\Delta AFR_{EGR} = 0$ makes $AFR_{Combustion} = AFR_{Throttle}$. But, as applying the EGR system to the engine for real combustion, leaving exhaust oxygen from the default condition of no EGR, was lowered more from AFR14.2 as the EGR valve opening and EGR rate increased. In addition, CO, $CO_2$, and HC increased more and the $\Delta AFR_{EGR}$ made

$AFR_{Combustion} < AFR_{Throttle}$. Thus, the $AFR_{Combustion}$ gradually decreased with the reduction of the oxygen generated by implementing the EGR system.

At high RPM (RPM4000 - RPM6000), the AFR drop was dramatic (See the Figure 30 and Figure 31). Generally, the aspirated intake air of spark ignition gasoline engines produces the highest reliability of torque and power. Thus, the ECU controlled the AFR optimized for the optimal performances on the range of slightly richer mixture at AFR 14.2 in the case of without EGR, as the default condition, compared to the stoichiometric AFR 14.7. As the air/fuel mixture got richer, the temperature of the burned gases decreased with the diminution of the probability of knock. Thus, the richer mixture for the 49cc single cylinder was inevitable to run at optimally high speed and at a full load. Moreover, richer AFR (AFR14.2 - AFR13.5) resulted in lower peak in-cylinder temperature and then the reduction of exhaust gas temperature and $NO_x$ gas emission compared to the cases of the stoichiometric and lean AFR conditions.

**Relationship amongst Exhaust Temperature, $O_2$, and $NO_x$**

It was found that there was a relationship among exhaust gas temperature, $O_2$, and $NO_x$ at each RPM condition. As shown in the Figure 32 - Figure 36, exhaust gas temperature and the amount of $NO_x$ were inversely proportional to the intake manifold $O_2$ concentration. Giving an account for the relationship, the $O_2$ concentration decreased when the EGR opening valve and the EGR rate increased affiliated with the reduction of exhaust gas temperature and $NO_x$. In addition, when the higher RPM conditions of the engine with the EGR conditions were controlled, the more dramatic was the diminution of the $O_2$ concentration.

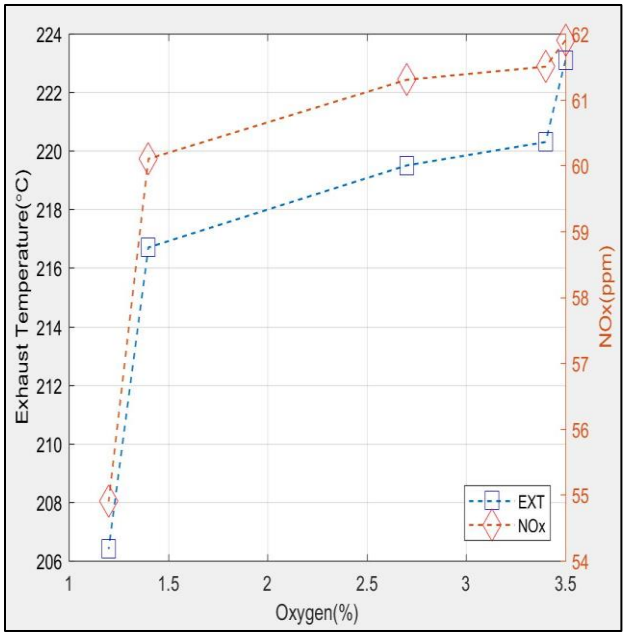


*Figure 32. EXT(℃) vs $O_2$(%) vs $NO_x$(ppm) at RPM2100*

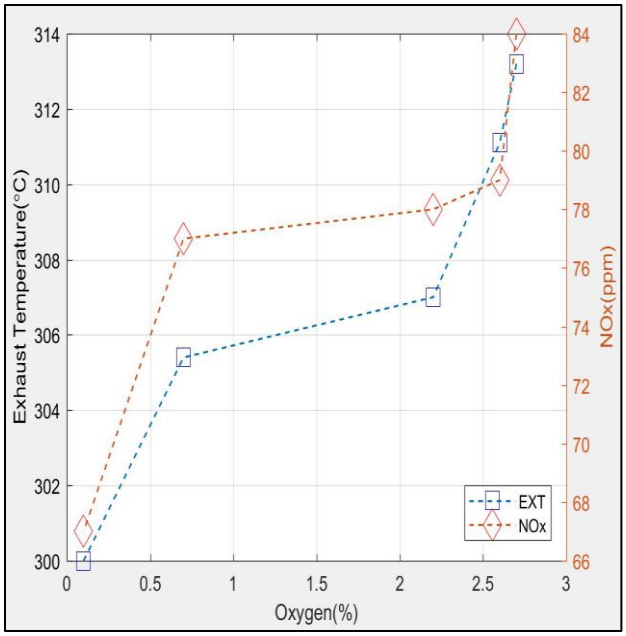


*Figure 33.EXT(℃) vs $O_2$(%) vs $NO_x$(ppm) at RPM3000*

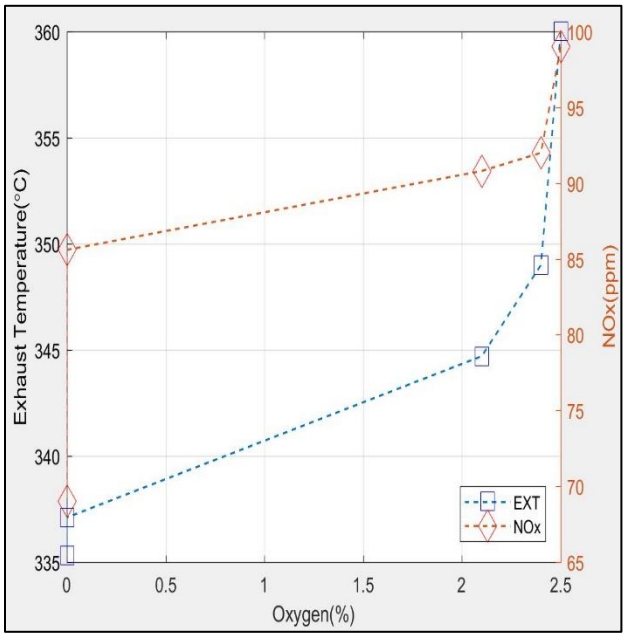


*Figure 34. EXT(℃) vs $O_2$(%) vs $NO_x$(ppm) at RPM4000*

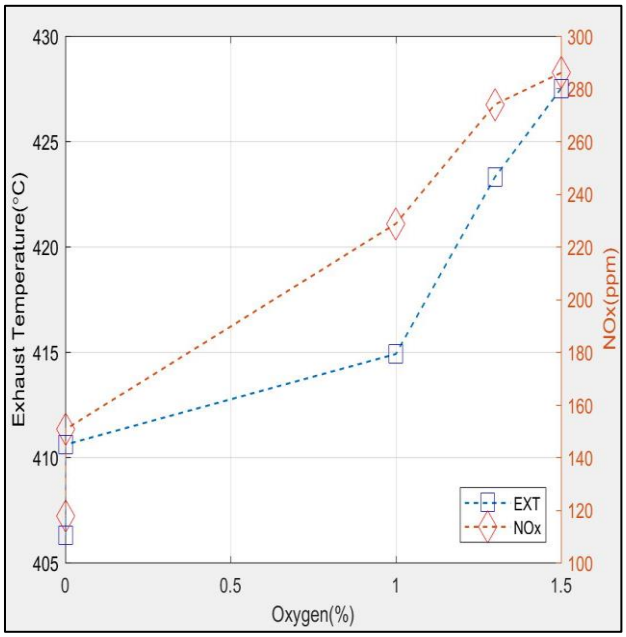


*Figure 35. EXT(℃) vs $O_2$(%) vs $NO_x$(ppm) at RPM5000*

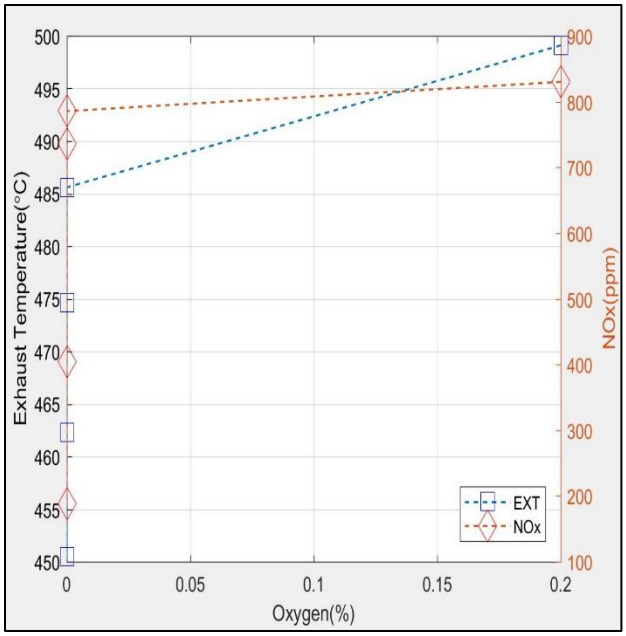


*Figure 36. EXT(℃) vs $O_2$(%) vs $NO_x$(ppm) at RPM6000*

**Engine Coolant Temperature**

The engine works by burning the unleaded gasoline fuel for generating its power for running the scooter. The combustion process increases the temperature of the cylinder wall of the engine. Around 35% of reaction heat is used for useful work, 30% is lost in the exhaust gases, and the remaining 35% is lost at the cylinder wall [17]. The heat transfer via the cylinder wall to the surroundings is accomplished by the engine coolant as either water or oil, or a mixture of them [25]. The engine coolant recirculates and takes away the heat as conduction, convection, and radiation heat transfer modes released from the cylinder wall and again releases the absorbed heat to the atmosphere of the coolant as convection and radiation heat transfer modes. Moderate or heavy loads require a high temperature of the coolant since there is more required power to do the work of the engine, resulting in more fuel combustion per unit time and more heat to reject, as compared to the cases of light loads.

As might be expected, the cooling of the in-cylinder combustion temperature meant that the engine coolant temperature decreased as the EGR opening valve and EGR rate increased (See the Figure 37 and Figure 38).

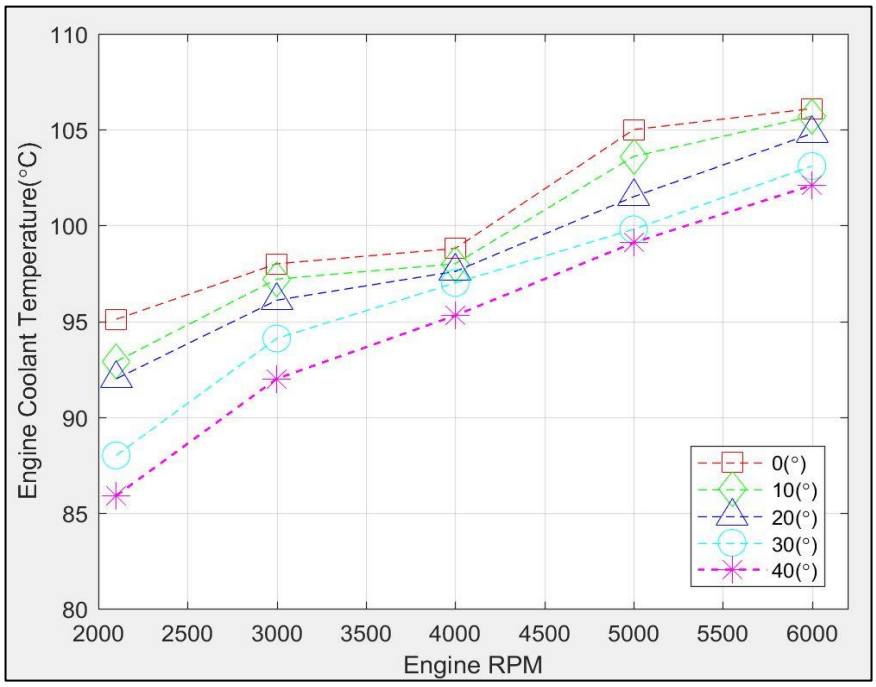


*Figure 37. Engine Coolant Temperature(℃) vs EGR opening valve(°)*

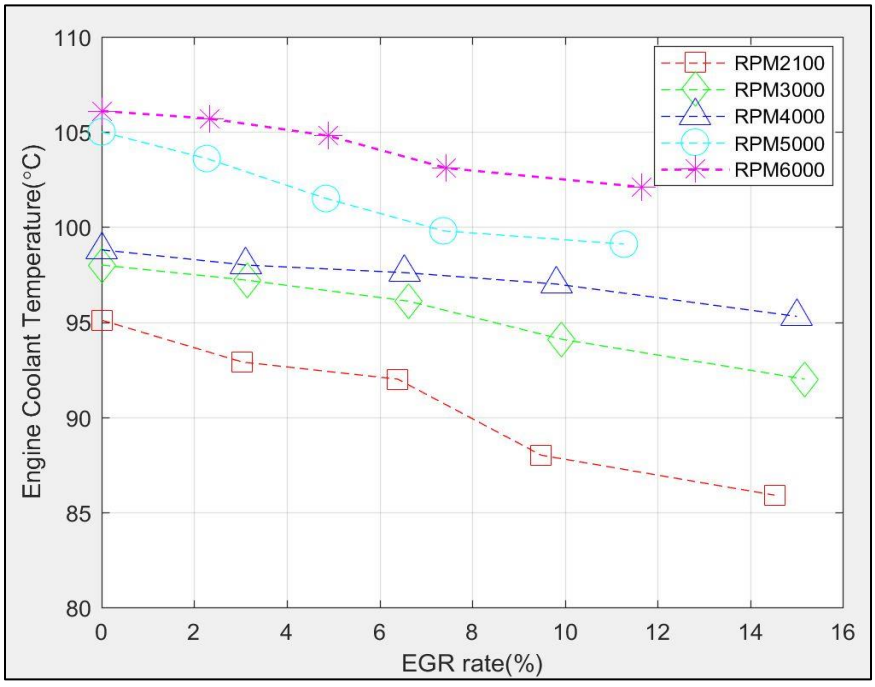


*Figure 38. Engine Coolant Temperature(℃) vs EGR rate(%)*

By analyzing the tendency of the engine coolant temperature, it seems clear that the EGR system had its intended effect on decreasing the peak flame temperature during the combustion process. Obviously, the range of the EGR rate, 7.5% - 12%, had the more dramatic temperature drop at each RPM condition.

**Ratio of Exhaust Gas Temperature and Engine Coolant Temperature (E/C Temperature Ratio)**

The increased temperature of the coolant was also correlated to an increase in the temperature of the exhaust gas temperature. This correlation indicated how the heat transfer as convection and radiation modes from the cylinder wall to the surroundings of the coolant effectively worked. Based on the literature review [26], the ratio of the exhaust gas temperature and engine coolant temperature is a function of various engine parts and the specific design of the engine. It is sufficient, therefore, to analyze the effectiveness of the coolant and a safe working load for any fuel. The E/C ratio assumed that the amount of heat transferred to the cylinder wall was equal to the amount of heat dissipated to the surroundings by the coolant. And also, as the RPM conditions (loads) increase, the ratio increases, which indicates an increasingly inefficient coolant to transfer heat from the cylinder wall to its surroundings. The ratio of more than 1 means that the coolant is not able to keep up with the increasing performance needed to take away all the released heat from the cylinder. Thus, the larger the ratio made, the larger the effectiveness of the coolant. Hence, this ratio is a measure that could predict the effectiveness of the coolant and even the efficiency (life) of the engine. The results showed that with the EGR system

applied to the 49cc spark ignition small scale engine at each RPM condition (load), the E/C ratio was the significant criteria in analyzing the effectiveness of the EGR system.

Based on the results of the EGR test, overall, as the RPM conditions (loads) increased, the E/C ratio remarkably increased as expected. This was due to more heat being generated per unit time for the loads and then increased the rate of heat transfer from the cylinder wall to its surroundings by the coolant. On the other hand, looking into the details for the effect of EGR, there were some variations of the E/C ratio distinguished at high RPM (RPM4000 - RPM6000). Particularly, at RPM4000 and RPM6000 with gradually increasing the EGR rate 0% to around 15%, the steady reductions of the E/C ratio were made by -0.13 (at RPM4000) and -0.29 (at RPM6000) on the difference between the rate of 0% to about 15% compared to the moderate variations of the ratio at other RPM conditions (loads). The lower ratios were analyzed and reflected higher effectiveness cooling of the cylinder wall and therefore suggested improved life of the engine. Furthermore, by investigating on the moderate fluctuation of the ratios at the other RPM conditions, it also gave an idea of that the EGR system was still promising without losing the effectiveness of the coolant and life of the engine. Thus, the EGR rate 7.5%-12% were encouraged to be utilized with high RPM (RPM4000 - RPM6000) (see the Figure 39 and Figure 40).

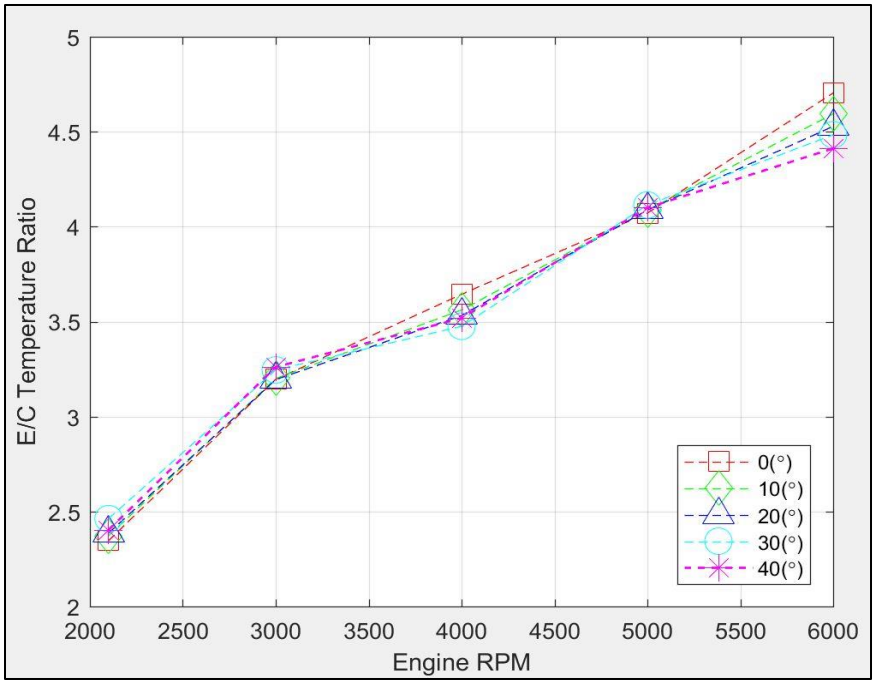


*Figure 39. E/C Temperature Ratio vs EGR opening valve(°)*

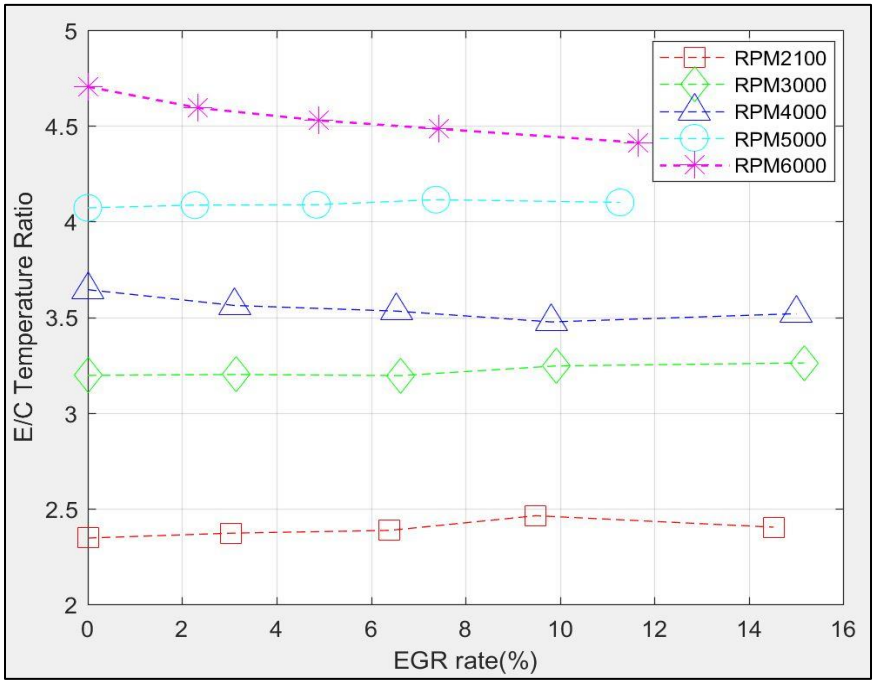


*Figure 40. E/C Temperature Ratio vs EGR rate(%)*

**Intake Air Temperature**

In terms of the intake air temperature, there was also correlation among the intake air temperature, and the EGR opening valve and EGR rate on the engine. The EGR system was classified as a hot EGR system, and thus, the exhaust gases were recirculated without being cooled down. This resulted in an increased intake air temperature. In addition, the intake air temperature had a proportional relation to the RPM of the engine (See the Figure 41 and Figure 42).

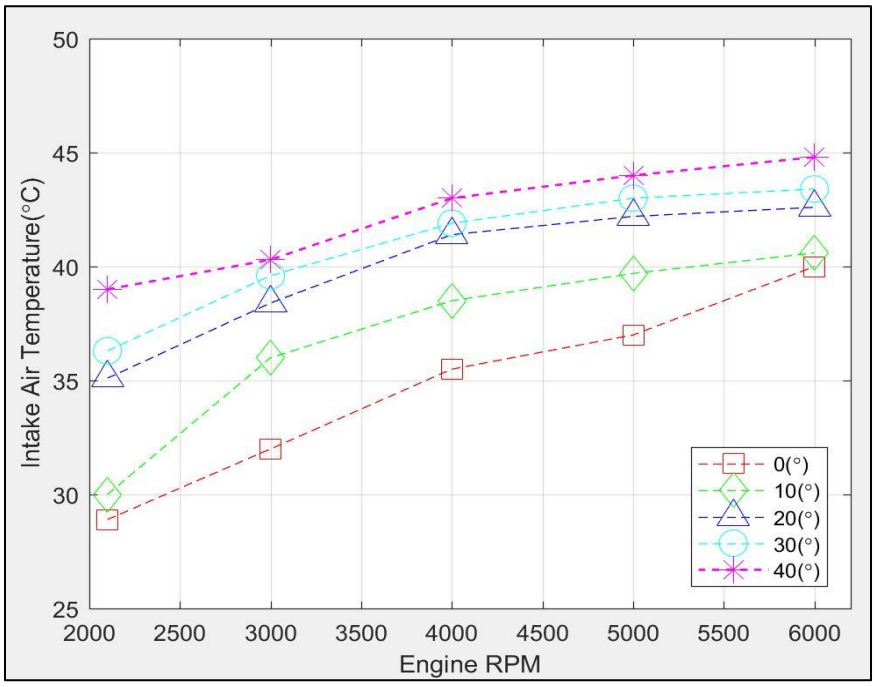


*Figure 41. Intake Air Temperature(℃) vs EGR opening valve(°)*

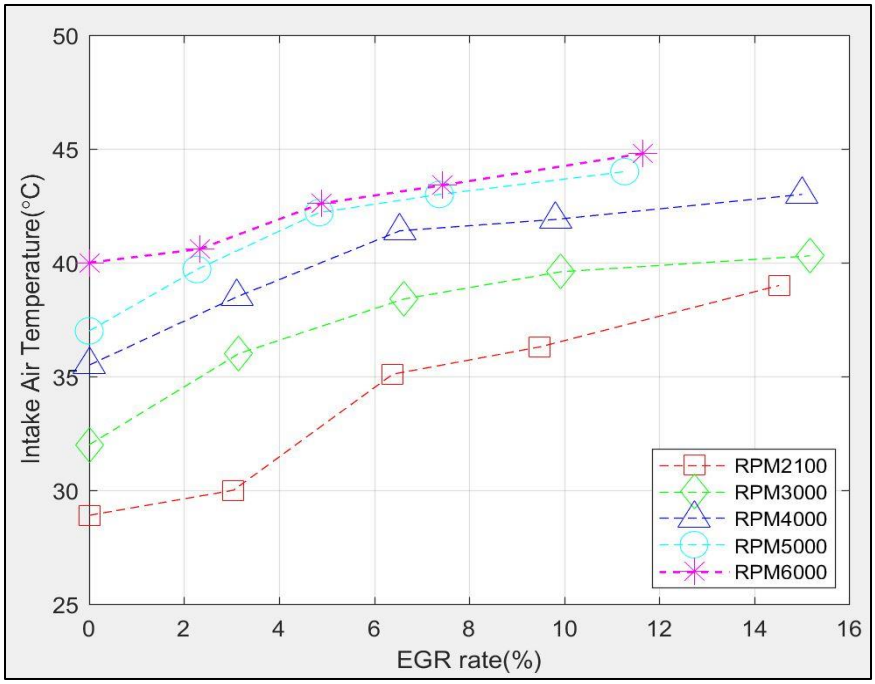


*Figure 42. Intake Air Temperature(°C) vs EGR rate(%)*

**Fuel Consumption**

Based on reviewing the literature [13], specific fuel consumption was based on the torque delivered by the engine with respect to the fuel mass flow delivered to the engine. Measuring all parasitic engine losses provides the brake specific fuel consumption (*BSFC*) (4.8) and measuring specific fuel consumption based on the in-cylinder pressures provides the indicated specific fuel consumption (*ISFC*) (4.9). The gravimetric net indicated specific fuel consumption ($ISFC_{Net}$) provides an insight to analyze the trends of the fuel consumption but it requires an in-cylinder pressure measurement that is currently unavailable in the experiment. The $ISFC_{Net}$ was using a mass flow rate of the intake air, $\dot{m}_{Air}$, the lambda value, $\boldsymbol{\lambda}$, the indicated power, $P_i$, and the stoichiometric air/fuel ratio, $AFR_{Stoichiometry}$, using the theoretical equation for the fuel consumption. The indicated

fuel consumption is included here for the future work when the indicated power will be measured with an in-cylinder pressure transducer.

$$BSFC = \frac{\dot{m}_f}{\dot{w}_b} \tag{4.8}$$

$$ISFC = \frac{\dot{m}_f}{\dot{w}_i} = \frac{\dot{m}_{Air} \times AFR_{Stoichimetric} \times \lambda}{P_i} \tag{4.9}$$

$\dot{m}_f$ = Fuel consumption, grams per minute

$\dot{w}_i$ = Indicated power $\dot{w}_b$ = Brake power

$\frac{d(W_n)}{dt} = \dot{w}_n$ = Power, kilowatts

As shown in the Figure 43 and Figure 44, higher engine speeds (higher RPM conditions and loads) produced higher *BSFC* since more fuel consumption was required for the same torque and power of the engine, mostly because of increasing friction losses within the engine. Higher friction losses gave rise to reducing the brake torque, $\frac{d(W_n)}{dt}$, resulting in an increased *BSFC*. Lower engine speeds (lower RPM conditions and loads) produced higher *BSFC* due to lower frictional loss and increased time for the heat transfer

from the working fluid to the cylinder walls. This point also decreased the brake torque, $\frac{d(W_n)}{dt}$, resulting in an increasing *BSFC*.

Fuel consumption slightly increased as EGR opening valve and EGR rate increased. But, it turned out that the penalties were not high. The penalties were +2.6mg/s (+9.8%) between the EGR rate 0% and +14.5% at the idle condition of RPM2100, +3.6mg/s (+9.1%) between the EGR rate 0% and 15.2% at RPM3000, +4.8mg/s (+9.1%) between the EGR rate 0% and 15.0% at RPM4000, +5.6mg/s (+9.0%) between the EGR rate 0% and 11.3% at RPM5000, and +8.6mg/s (+8.7%) between the EGR rate 0% and 11.7% at RPM6000 (See the Figure 43 and Figure 44). As the amount of intake manifold $O_2$ decreased with the EGR opening valve and the EGR rate increased, the energy produced by the combustion decreased. As applying the EGR effect, in order to reach the RPM conditions that were the same as the cases of the EGR opening valve (0°) and EGR rate (0%) at each constant RPM condition, the butterfly valve of the scooter was required to open wider to have the air enter more into the displacement. But, at the same time, being controlled by the ECU affiliated with the butterfly valve, more fuel was required through the fuel injector so that the air/fuel mixture entering the combustion chamber was higher in order to reach the RPM conditions. In addition, the dilution effect of EGR in the main stream entering the engine cylinder led to richer AFR and more fuel consumption rather than the case of the EGR opening valve (0°) and EGR rate (0%) (See the Figure 29, Figure 30, Figure 43, and Figure 44) (A.3).

As another perspective for the reduction of the fuel consumption, the delayed ignition timing controlled by the ECU for optimal torque and power of the engine was

considered [9]. The higher EGR rate led to the higher dilution effect, which then benefited from a delayed ignition timing in order for the cylinder to allow more air/fuel mixtures during every expansion stroke to burn and optimally generate the corresponding torque and power of the engine.

Moreover, the penalties of the fuel consumption with the EGR system were also expected to result from complicated effects such as combustion phasing, pumping losses, and higher knock from the rich air/fuel mixture. The effects are reserved for investigation in future research.

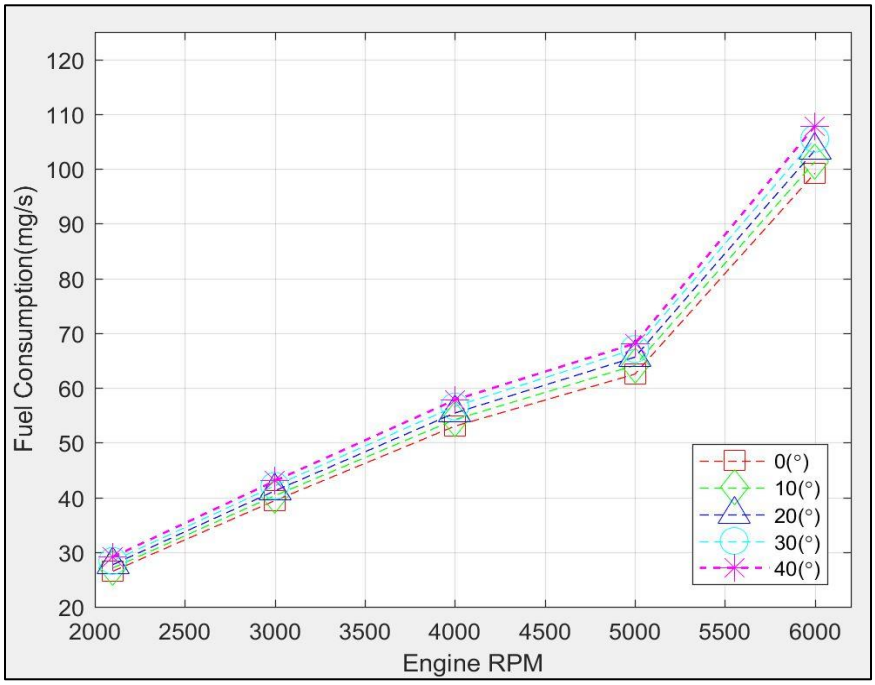


*Figure 43. Fuel Consumption(mg/s) vs EGR opening valve(°)*

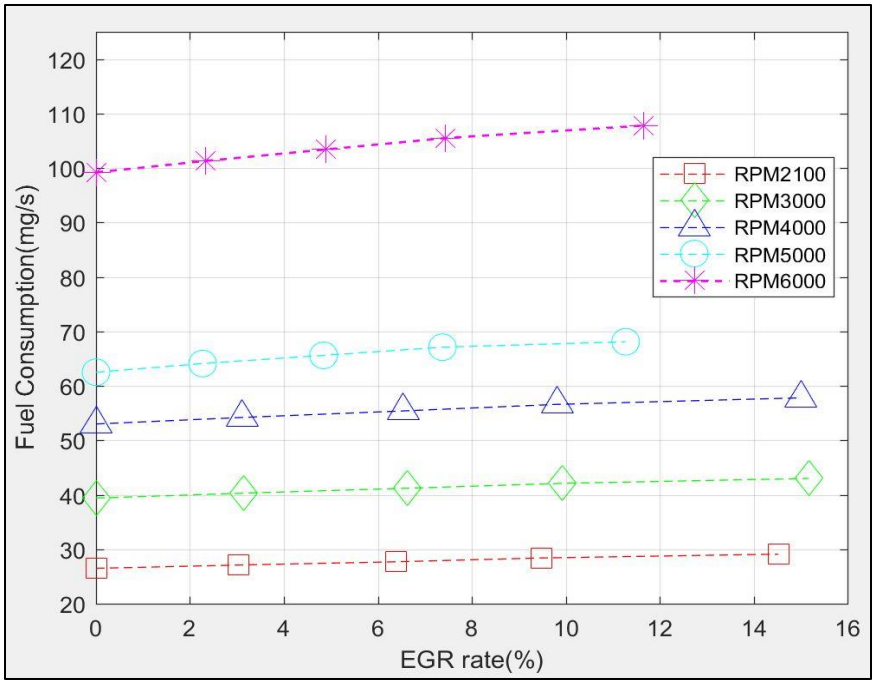


*Figure 44. Fuel Consumption(mg/s) vs EGR rate(%)*

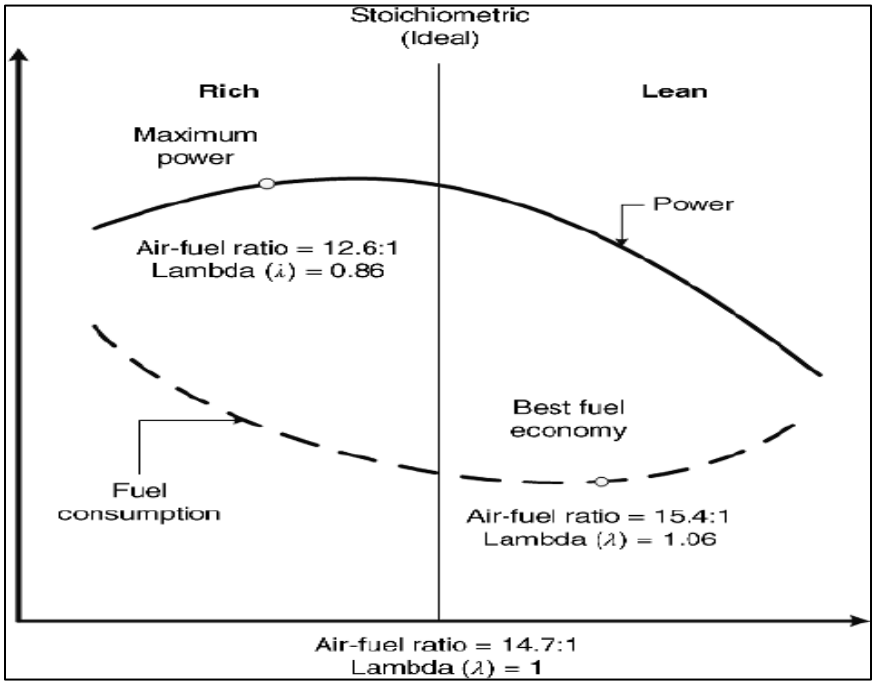


*Figure 45. Effects of air/fuel ratio on fuel consumption of an internal gasoline engine [68]*

As described in the Figure 45, decreased AFR influences the fuel consumption of the engine in the rich regions of AFR.

**Carbon Monoxide (CO) and Hydrocarbons (HC)**

The other shortcomings of the EGR system were the increase of CO and HC concentration in the exhaust. There was more CO produced as the EGR opening valve and the EGR rate increased. Recall the combustion of the governing EGR equation (2.2).

$$CH_yO_z + n(O_2 + \xi N_2) + \frac{EGR}{100}(aCO_2 + bH_2O + cC_3H_{3y} + dNO + eH_2 + fO_2 + gCO + hN_2)$$

$$\rightarrow aCO_2 + bH_2O + cC_3H_{3y} + dNO + eH_2 + fO_2 + gCO + hN_2$$

As shown in the equation (2.2), without regard to $n$ and $\xi$ moles of the fresh intake oxygen and nitrogen, the EGR value increasing means that $cC_3H_{3y}$ and $gCO$ are increased.

The trends of CO showed not a good descriptor of trend without regard to the EGR opening valve and the EGR rate. CO particles were produced at a lower RPM (RPM2100 - RPM4000) than higher RPM (RPM4500 - RPM6000). It is a characteristic since the fuel mixture was relatively leaner in the richer AFR conditions around AFR 14.2 at high RPM rather than at low RPM. Thus, complete combustion occurred less than at low RPM (RPM2100 - RPM4000) and there should be less unburned gas than at higher RPM (RPM4500 - RPM6000) (See the Figure 46 and Figure 47). In the case of HC, the trends of HC showed the curved shapes regardless of the EGR opening valve and the EGR rate (See the Figure 48 and Figure 49). This was due to the fact that the HC was also affected by relative variation from a richer state to a leaner state of air/fuel mixture as the RPM conditions increased. Importantly, in the perspective of the effect of EGR, CO and HC increased as EGR opening valve and EGR rate increased. This was due to the fact that the

reduced oxygen availability preferentially drove the reaction toward incomplete oxidative state. Also, the HC levels were high, and some of this can be due to partial flame quenching and misfire from the insufficient $O_2$ concentration and wall quenching from the low flame temperature in the combustion chamber when the EGR is employed.

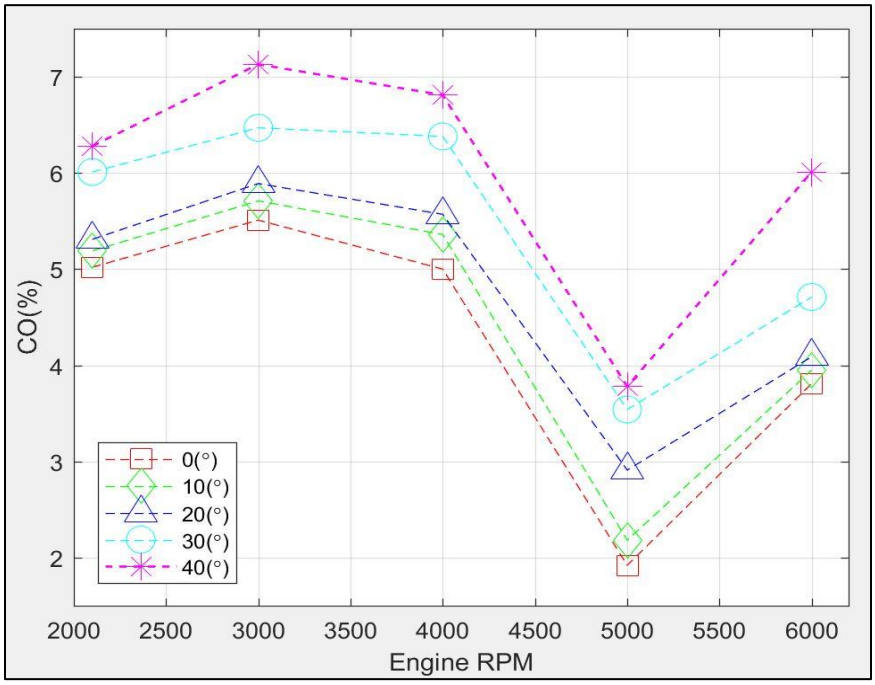


*Figure 46. CO(%) vs EGR opening valve(°)*

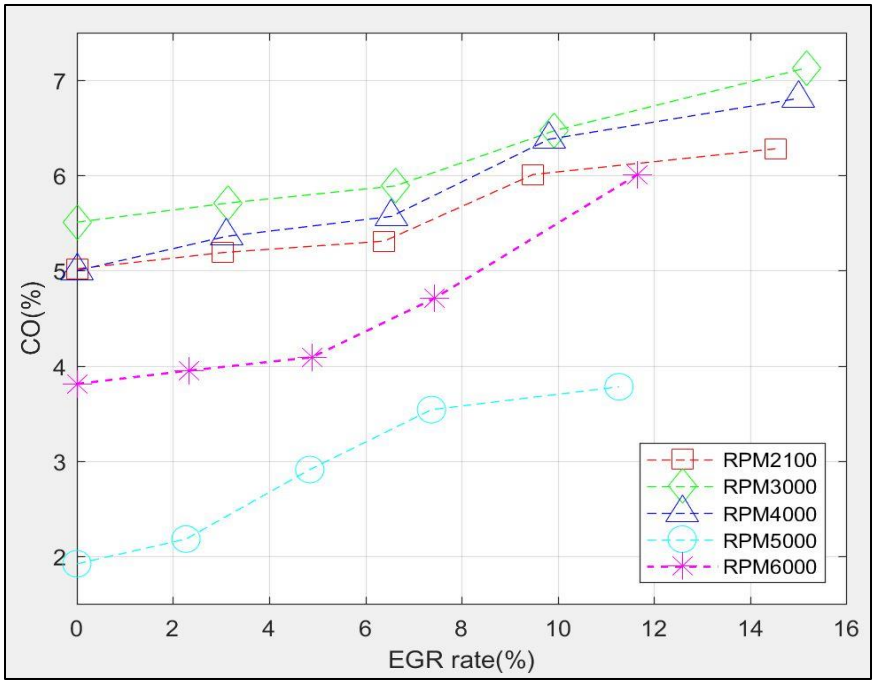


*Figure 47. CO(%) vs EGR rate(%)*

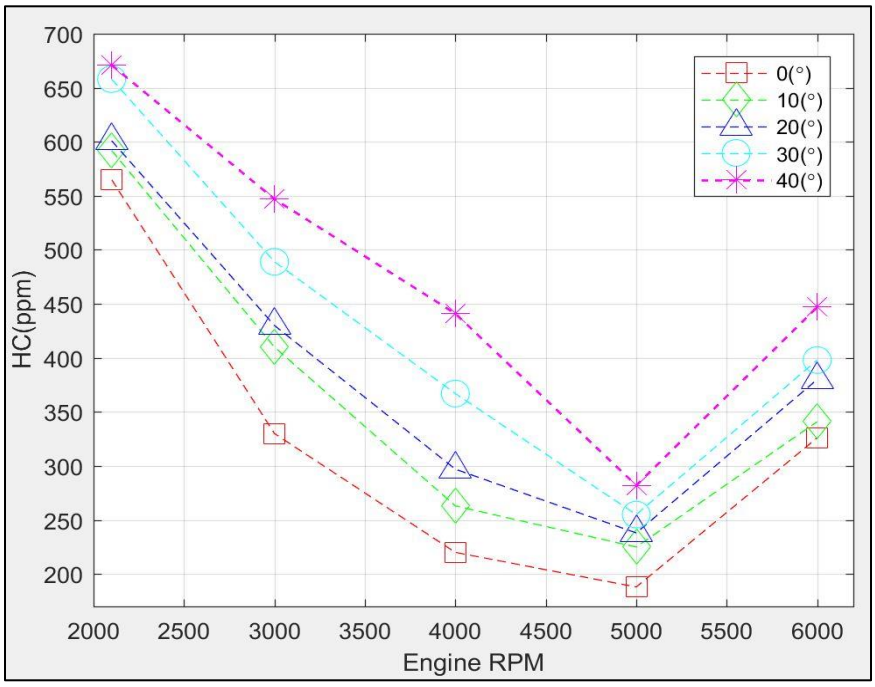


*Figure 48. HC(ppm) vs EGR opening valve(°)*

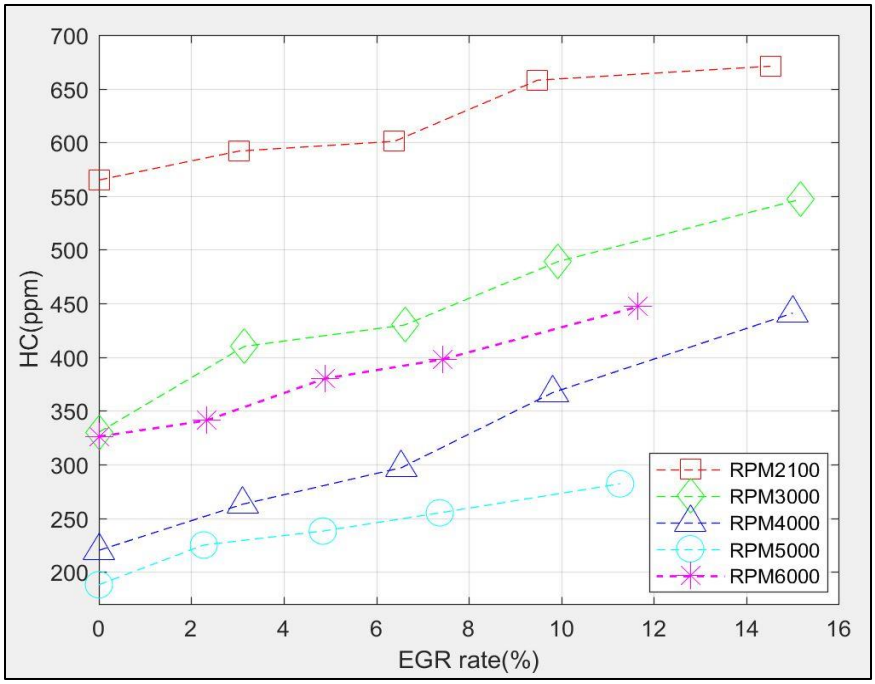


*Figure 49. HC(ppm) vs EGR rate(%)*

The trends of CO and HC were influenced by factors such as AFR, intake manifold $O_2$ concentration, and $CO_2$ (See the Figure 50) [68]. They were correlated to each other within their mechanisms.

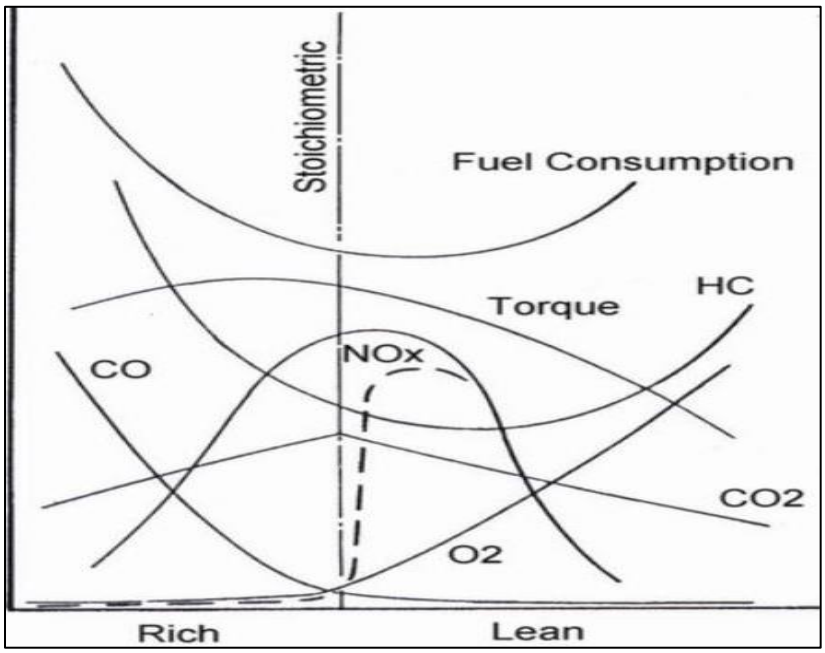


*Figure 50. Relationship of gas emission, fuel consumption, and torque with regard to AFR [68]*

Concerning CO and HC gas emission, they were relatively higher at richer AFR. However, at the AFR, the amount of $NO_x$ was lowered. It had an inverse relationship with CO and HC to optimize the all three emissions at the same time, there is a promising range for EGR applications to be considered. The optimistic and optimal EGR applications were expected to utilize the range of high RPM (RPM4000 - RPM6000) affiliated with EGR rate (7.5% - 12%).

In addition, being different from the intake air temperature, 28.9℃ - 44.8℃, of the test results, excessively low intake air temperature can lead to incomplete combustion in the chamber since it can indicate poor air/fuel mixture, giving rise to partial misfire.

**Correlation of HC, $NO_x$, and EGR rate**

There was a correlation of HC, NOx, and EGR rate between each other as described in Figure 50 - Figure 54. Looking into the details, over the 7.5% of the EGR rate at each RPM condition, the reduction of NOx was remarkably reduced but HC increased. There was for each case a point of intersection between HC and NOx with respect to the EGR rate. Thus, above each EGR rate corresponding to these cross-over points, the small scale engine was expected to be able to use effectively the EGR system to improve emissions.

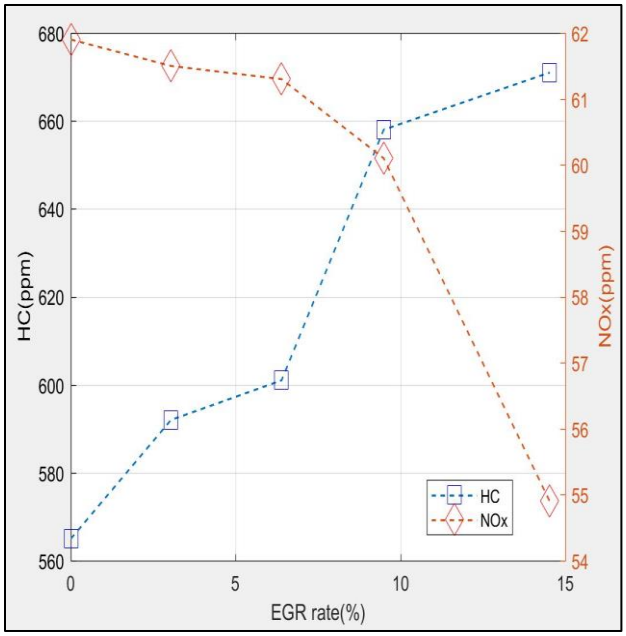


*Figure 51. HC(ppm) vs $NO_x$(ppm) vs EGR rate(%) at RPM2100*

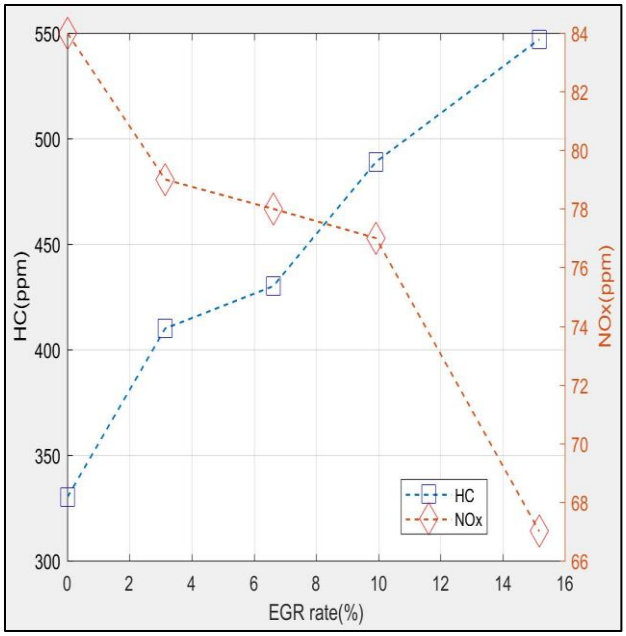


*Figure 52. HC(ppm) vs $NO_x$(ppm) vs EGR rate(%) at RPM3000*

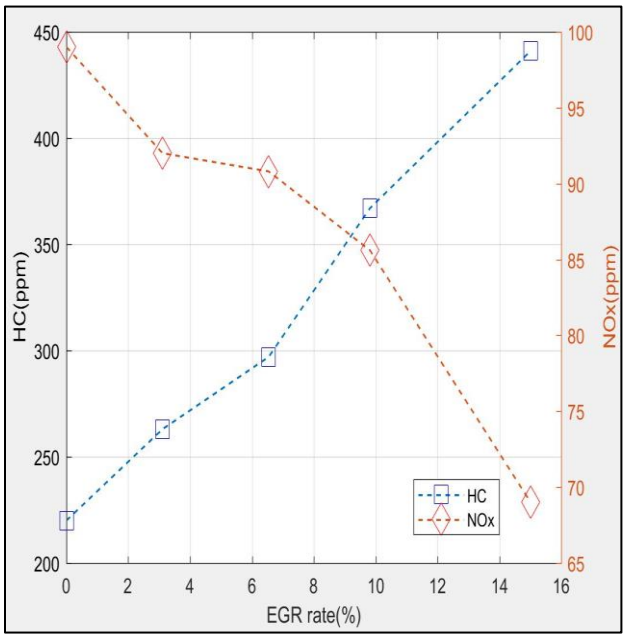


*Figure 53. HC(ppm) vs $NO_x$(ppm) vs EGR rate(%) at RPM4000*

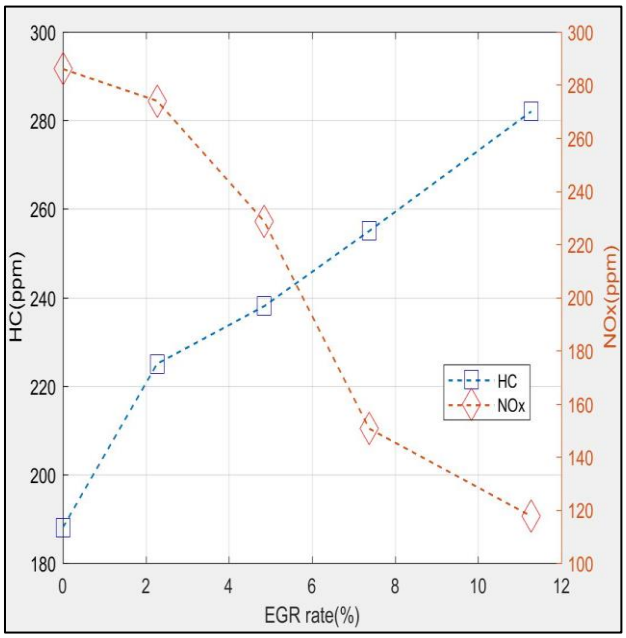


*Figure 54. HC(ppm) vs $NO_x$(ppm) vs EGR rate(%) at RPM5000*

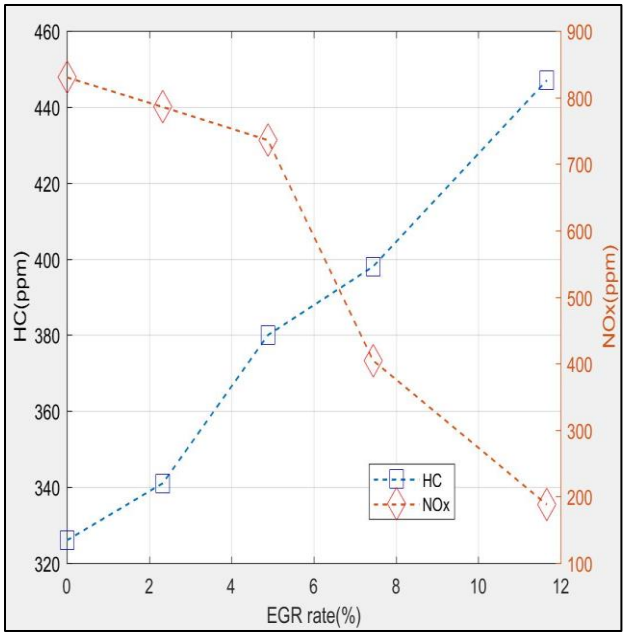


*Figure 55. HC(ppm) vs $NO_x$(ppm) vs EGR rate(%) at RPM6000*

**Correlation of CO, $NO_x$, and EGR rate**

Similarly, CO, NOx, and EGR rate were correlated. Each point of the intersections between CO and NOx with respect to the EGR rate is shown in Figure 55 - Figure 59. The points at each RPM condition were approximately corresponding to the intersection points on the correlation of HC and NOx. Thus, over the 7.5% of the EGR rate, the EGR system can be utilized with overall improvement to the engine operation.

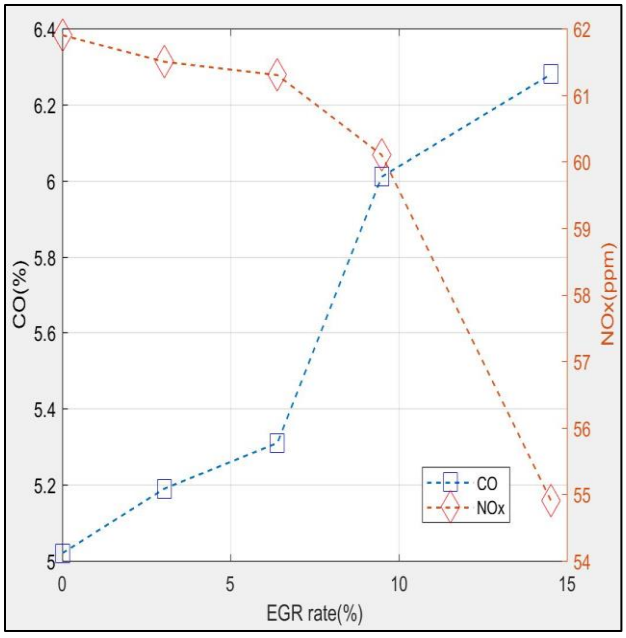


*Figure 56. CO(%) vs $NO_x$(ppm) vs EGR rate(%) at RPM2100*

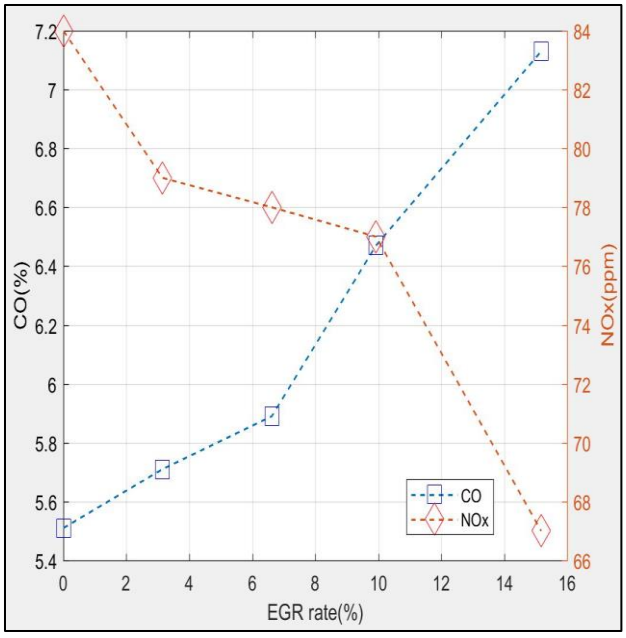


*Figure 57. CO(%) vs $NO_x$(ppm) vs EGR rate(%) at RPM3000*

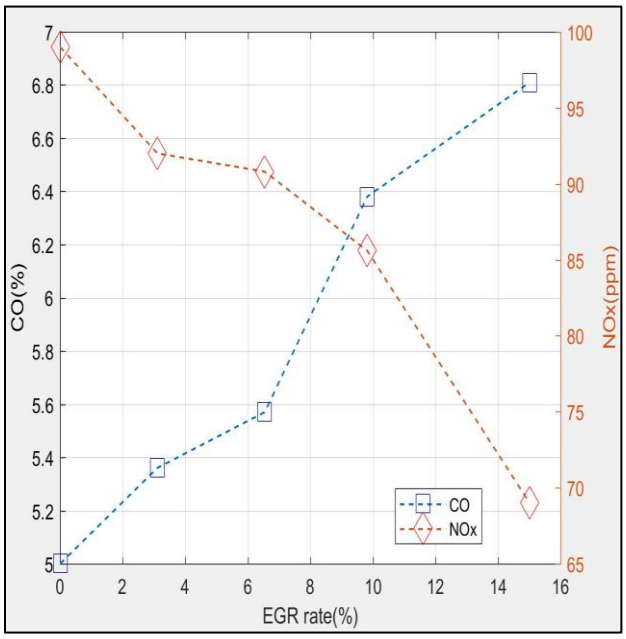


*Figure 58. CO(%) vs $NO_x$(ppm) vs EGR rate(%) at RPM4000*

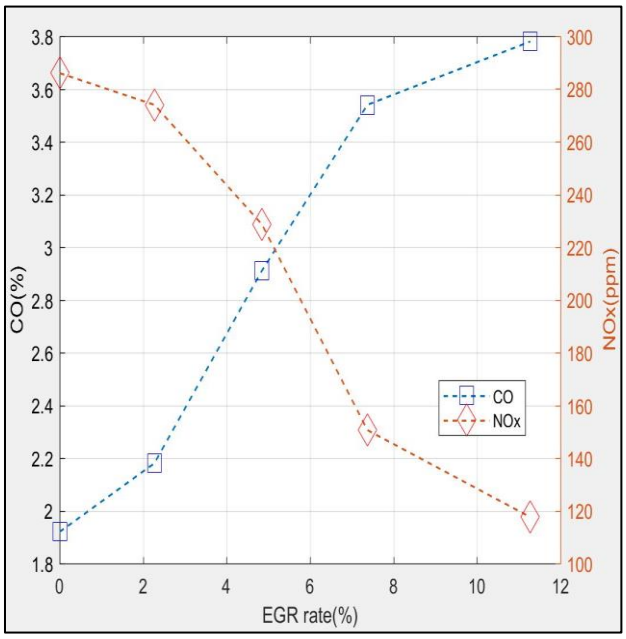


*Figure 59. CO(%) vs $NO_x$(ppm) vs EGR rate(%) at RPM5000*

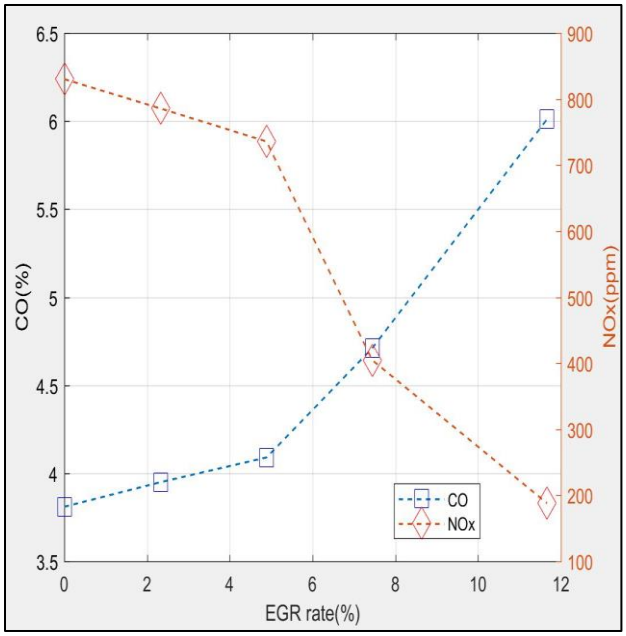


*Figure 60. CO(%) vs $NO_x$(ppm) vs EGR rate(%) at RPM6000*

As described in Figure 51 - Figure 60, as a compromise for the CO, HC, NOx, and EGR rate, the optimal EGR rate was considered 7.5% - 12% at each RPM condition. For more correlations among them, the Appendix shows the details.

**Carbon Dioxides ($CO_2$)**

The amount of $CO_2$ produced by the combustion process with the EGR system increased compared to the case of no EGR. The unburned gases were recirculated to the intake port and main stream to the displacement and had a chemical reaction with the intake manifold $O_2$ in the combustion chamber, yielding more $CO_2$ during the combustion process. Consequently, the more increased the EGR opening valve and the EGR rate were, the more $CO_2$ was yielded (See Figure 61 and Figure 62).

The trends and variation of $CO_2$ affiliated with the EGR effect were correlated to the variation of CO, HC, $O_2$, and AFR.

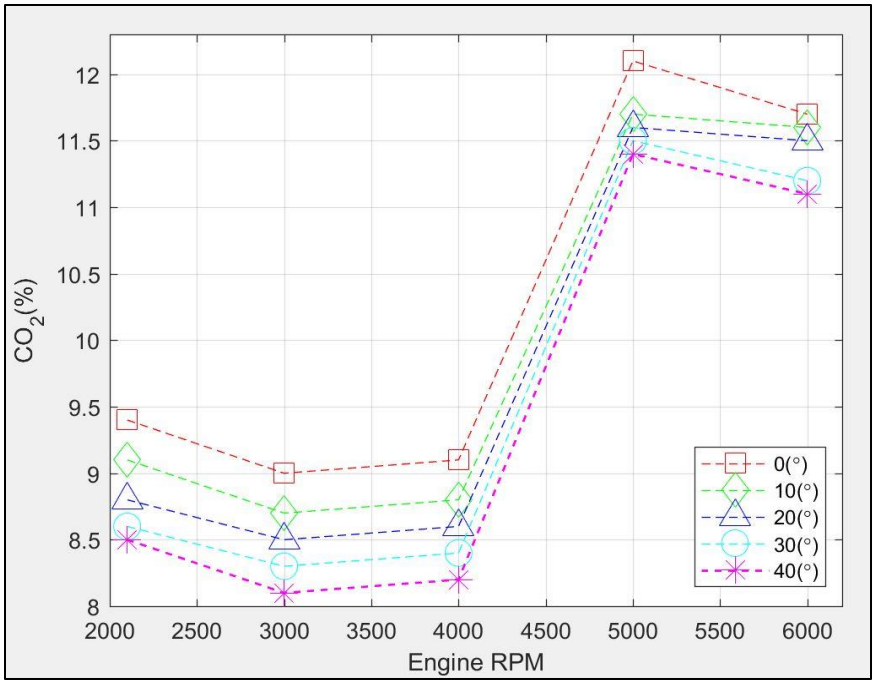


*Figure 61. $CO_2$(%) vs EGR opening valve(°)*

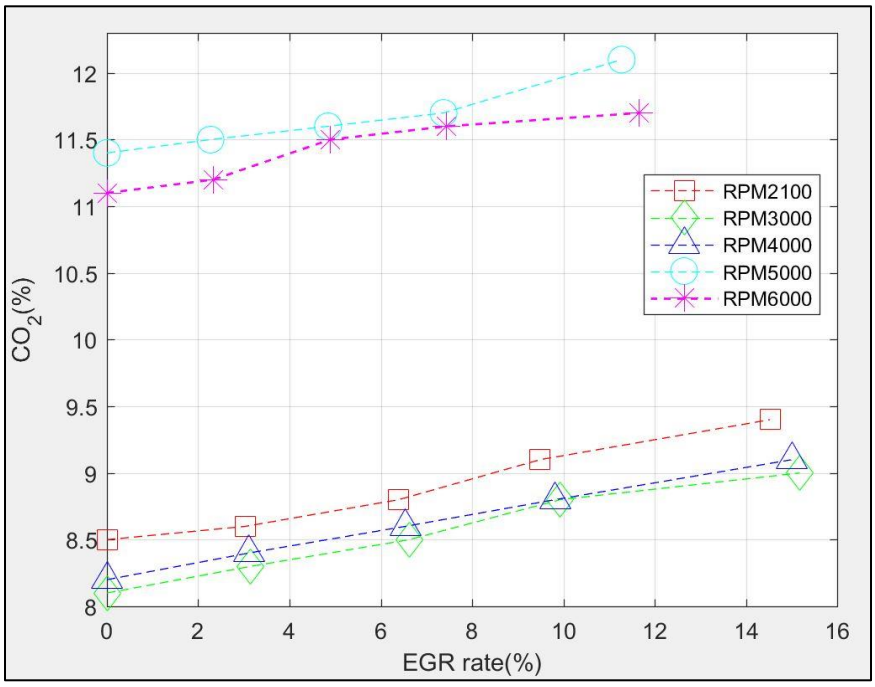


*Figure 62. $CO_2$(%) vs EGR rate(%)*

**Chassis Shaft Roll Torque**

The torque of the chassis was measured by the Mustang dynamometer. Even though it was not directly indicated; the torque of the 49cc engine was a critical measurement, so deriving the torque of the engine was based on the following equation (4.10).

$$Engine\ torque = \frac{Dynamometer\ shaft\ torque \times Dynamometer\ shaft\ RPM}{Engine\ RPM} \quad (4.10)$$

The Mustang dynamometer chassis shaft roll initiated the rotation to be measured from RPM4000. The torque of the chassis shaft roll decreased as the EGR opening valve and EGR rate increased (See the Figure 63 and Figure 64). However, the amount of the penalty was not significant. It turned out that RPM4000, RPM5000, and RPM6000 corresponded to -4N·m, -5N·m, and -6N·m change of the chassis torque.

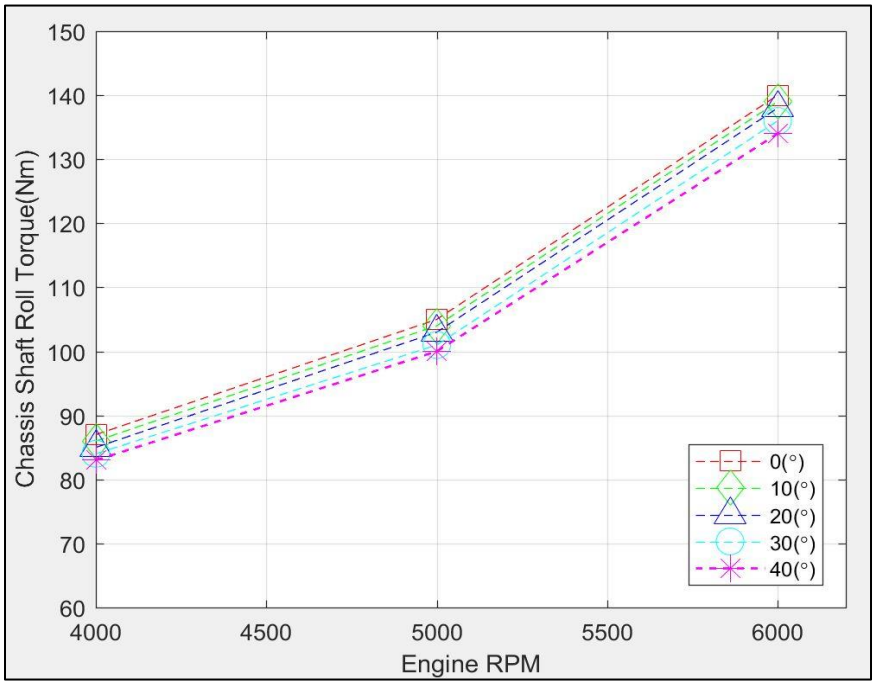


*Figure 63. Chassis Shaft Roll Torque(Nm) vs EGR opening valve(°)*

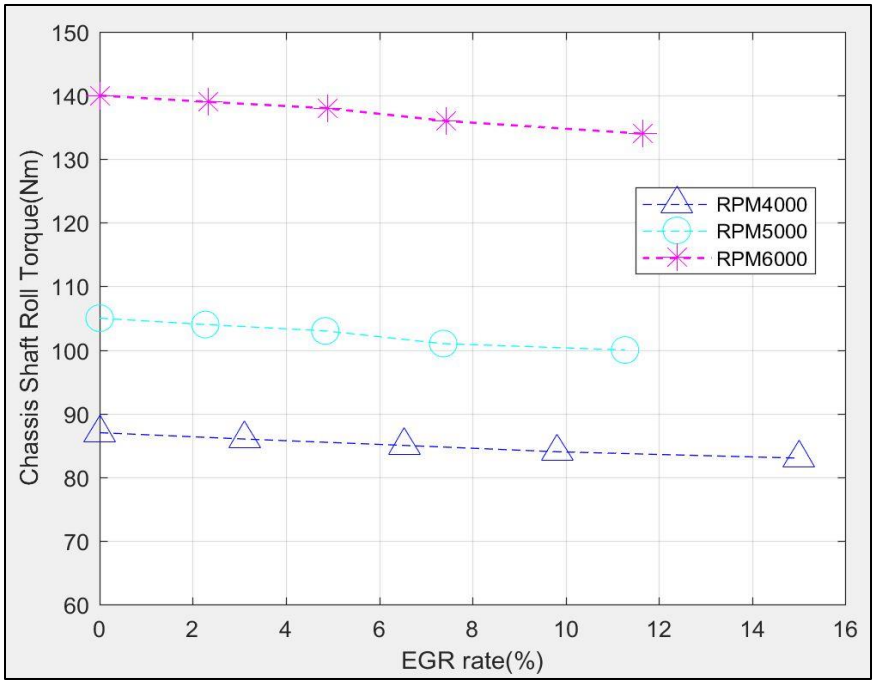


*Figure 64. Chassis Shaft Roll Torque(Nm) vs EGR rate(%)*

**Engine Torque**

BMEP is the brake mean effective pressure in the cylinder and is derived from the torque, RPM, and the displacement of engines.

$$BMEP = \frac{2\pi \times T \times N}{V_d} \tag{4.11}$$

$$\dot{w} = T(2\pi \times N) \tag{4.12}$$

$$BSFC = \frac{\dot{m}_f}{\dot{w}_b} \tag{4.13}$$

$N$ = Engine speed, revolutions/minute

$T$ = Torque, N·m

$V_d$ = Displacement, liters

At each constant RPM condition (load), the brake mean effective cylinder pressure had a correlation to the torque of the engine.

The torque of the engine was derived from the dyno shaft roll torque, dyno shaft roll RPM, and the engine RPM based on the Mustang Dynamometer operator manual (See (4.10)). In the equation, there was an assumption that there was not any loss within transmissions of the engine of the scooter during the combustion process. Engine torque decreased as the EGR opening valve and EGR rate increased (See Figure 65 and Figure 66). However, the amount of the penalty was not that significant. It turned out that RPM4000, RPM5000, and RPM6000 corresponded to -0.14N·m, -0.31N·m, and -0.59N·m of the engine's torque. Thus, it is still promising to apply the EGR system to the 49cc spark ignition engine at high RPM.

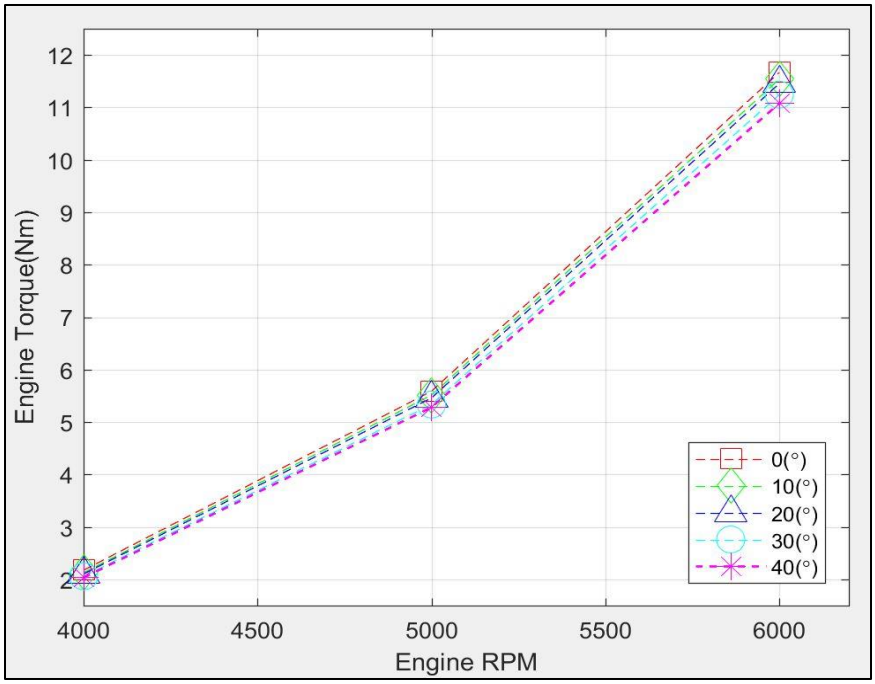


*Figure 65. Engine Torque(Nm) vs EGR opening valve(°)*

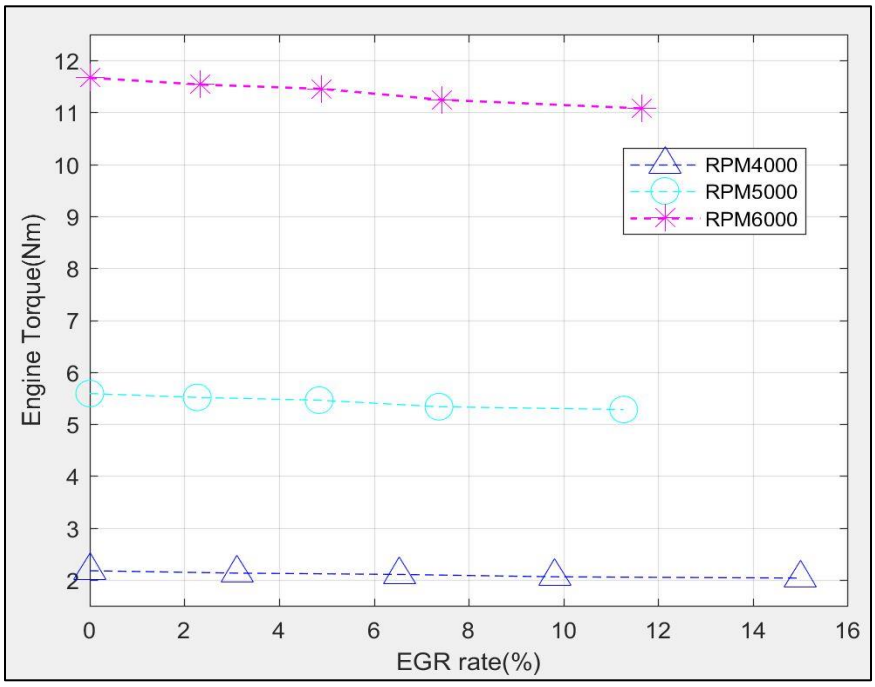


*Figure 66. Engine Torque(Nm) vs EGR rate(%)*

**Engine Power and Delayed Ignition Timing**

Engine power was derived from the engine torque and engine RPM as in equation (4.14).

$$Engine\ power = \frac{Engine\ torque \times Engine\ RPM}{9565} \tag{4.14}$$

Power is the rate of doing work. Thus, the engine power is interpreted as the following:

$$Engine\ power = \frac{Engine\ work}{Engine\ running\ time} \tag{4.15}$$

The engine work is derived from

$$W_{Brake} = W_{Gross} - W_{Pump} - W_{Friction} \tag{4.16}$$

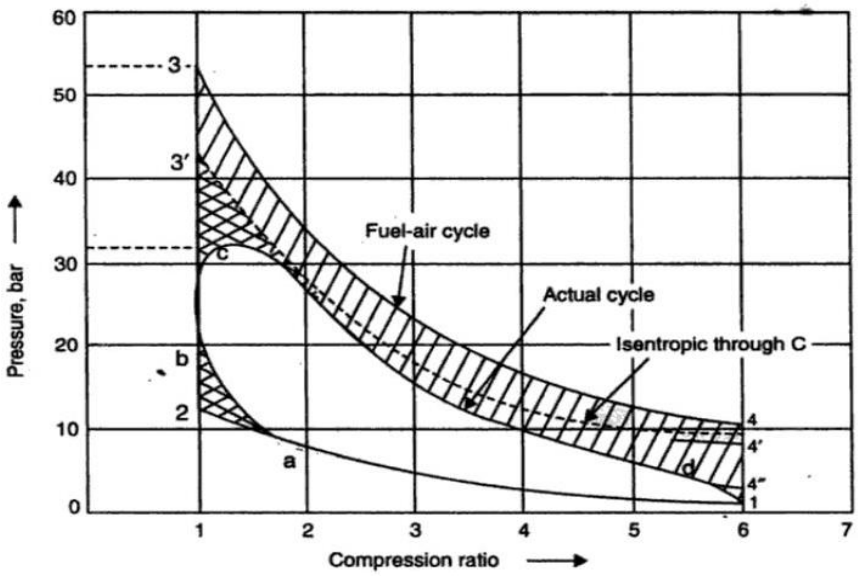


*Figure 67. The difference of the works between the ideal Otto cycle and the actual Otto cycle [64]*

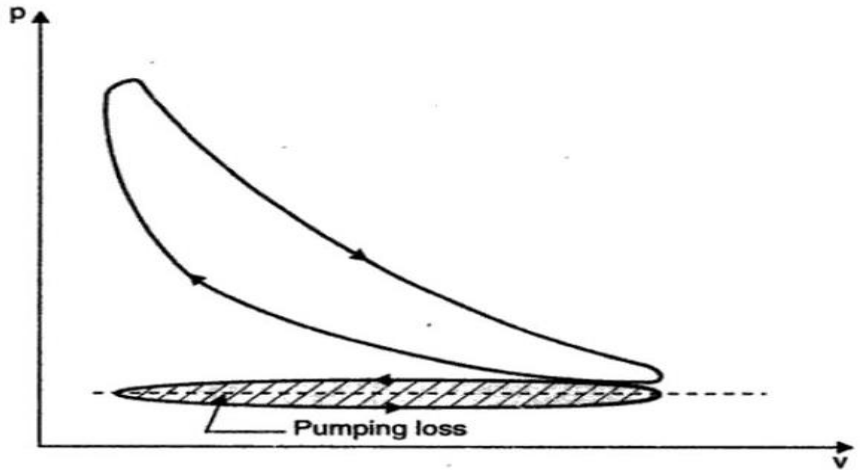


*Figure 68. Effect of the engine oil temperature on the friction loss of the work [65]*

$W_{Gross}$ is creating positive work from running the engine, particularly compression and expansion stroke processes [64], including heat transfer, during the Otto cycle; refer to the equation of the thermal efficiency, $\eta_{Thermal} = 1 - \frac{1}{r_c^{(\gamma-1)}}$, of the engine described earlier. $W_{Pump}$ is the thermodynamic work of moving air into and out of the cylinder [65]. Generally, $W_{Pump}$ increases when RPM conditions (loads) decrease in spark ignition engines since throttling of the intake air increases the pumping work relative to the other work aspects.

Based on reviewing the literature [21] and [65] in terms of simulation of the $W_{Pump}$, the higher dilution levels at the intake manifold part had positive effects on reducing the $W_{Pump}$ (A.3). As the dilution effects of the $CO_2$ and $H_2O$ of the EGR effect was larger in the condition of increasing the EGR rate from 0% to 15%, the higher intake manifold pressure naturally lowered the $W_{Pump}$ (A.3). But, while the $W_{Pump}$ was reduced, the $W_{Gross}$ also decreased due to the reduced peak in-cylinder pressure, which resulted from the

recirculated compositions with higher heat capacity and the in-cylinder temperature lowering with the EGR system. These losses of $W_{Gross}$ and $W_{Pump}$ together decreased the $W_{Brake}$ which led to the loss of the torque and power of the engine as the EGR rate increased from 0% to 12% at high RPM conditions in the experimental investigation. Based on reviewing the literature [13], these results also supported the idea that as the EGR rate increased, there were always delayed ignition timings with decreasing the in-cylinder pressure by failing to achieve the standard and maximum pressure. The delayed spark ignition timing due to the EGR effect also played a significant role in decreasing the $W_{Gross}$. Thus, one of the reasons for the loss of the performance was due to the more delayed ignition timing based on the default ignition timing (B.T.D.C), 5.0° / 2100 r/min. Future work will include adjusting the ECU during EGR to make up for this behavior. In the literature [40] and [41] in terms of internal spark ignition combustion engines, there were derived functional forms of the ignition delay expression with an EGR rate. It was as following:

$$\tau(p, T, \lambda, EGR) = a\left(\frac{p}{T}\right)^{-b} e^{c/T} f(\lambda, EGR) \quad (4.17)$$

The ($p/T$) term in the pre-exponential indicated the density of $\tau$. The factor accounted for $\lambda$ and EGR rate dependence from the $p$-$T$ dependence.

$$\tau(ms) = 2.71\times10^{-5} \left(\frac{p(bar)}{T(K)}\right)^{-1.73} e^{5190/T(K)} (1-w_d)^{-0.618} \quad (4.18)$$

$W_d = EGR + x_r$ (air/fuel mixture is stoichiometric) (4.19)

$W_d = EGR + x_r + k_L + \delta$ (air/fuel mixture is lean) (4.20)

$$\delta = \frac{m_a - m_{a,stoi}}{m_a - m_f} = \frac{\lambda - 1}{\lambda + \left(\frac{F}{A}\right)_{stoi}}$$ (air/fuel mixture is lean) (4.21)

$W_d = EGR + x_r + k_R[(-\delta)\ (F/A)_{stoi}]$ (air/fuel mixture is rich) (4.22)

$$\frac{m_a - m_{a,stoi}}{m_a - m_f} = (-\delta)\ (F/A)_{stoi}$$ (air/fuel mixture is rich) (4.23)

$x_r$ = Residual gas fraction = $\frac{m_r}{m_a + m_f}$ (4.24)

$\delta$ = The excess air mass fraction

$k_L$ = The difference between the dilution effect of excess air and burned gas

$k_R$ = The difference between the dilution effect of excess fuel and burned gas

As described in the equation (4.18), the ignition delayed timing had a correlation with in-cylinder pressure, in-cylinder temperature, dilution work, EGR rate, and gas fraction. With considering the equations of (4.18), (4.22), and (4.23) for the engine of the scooter, which had generally run in the rich regions of air/fuel mixture with the EGR system, the in-cylinder temperature was the main component to influence the delaying of

the ignition timing. Thus, in the experimental investigation, as the EGR rate gradually increased, the lowered in-cylinder temperature led to more delayed ignition timing.

Theoretically, in internal combustion engines, advanced ignition timings give rise to higher peak in-cylinder pressure, and their corresponding crank angles are close to top dead center (T.D.C). From reviewing additional literature [9], the patterns of in-cylinder pressure with the EGR rate from 0% to 25% had an evident correlation with the ignition timing. Compared to the condition of no EGR, the peak in-cylinder pressure was gradually reduced and the corresponding ignition timing was delayed substantially as the EGR rate increased. Using higher EGR rate lowered in-cylinder temperature and pressure during the expansion stroke because of its higher heat capacity, dilution, thermal, and chemical effects.

Looking into the details, engine power decreased as the EGR opening valve and EGR rate increased (See Figure 69 and Figure 70). However, the amount of the power penalty was also not that critical. It was found that RPM4000, RPM5000, and RPM6000 corresponded to -0.06 HP, -0.16 HP, and -0.37 HP loss. In the same manner of the torque of the engine, these results confirm that it is promising to apply the EGR system to the 49cc spark ignition engine at high RPM.

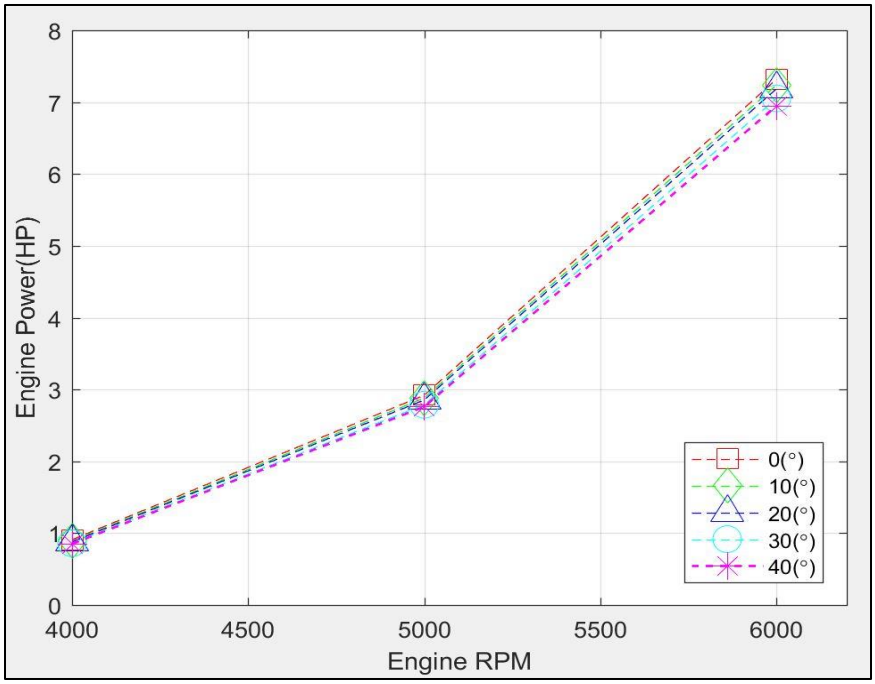


*Figure 69. Engine Power(HP) vs EGR opening valve(°)*

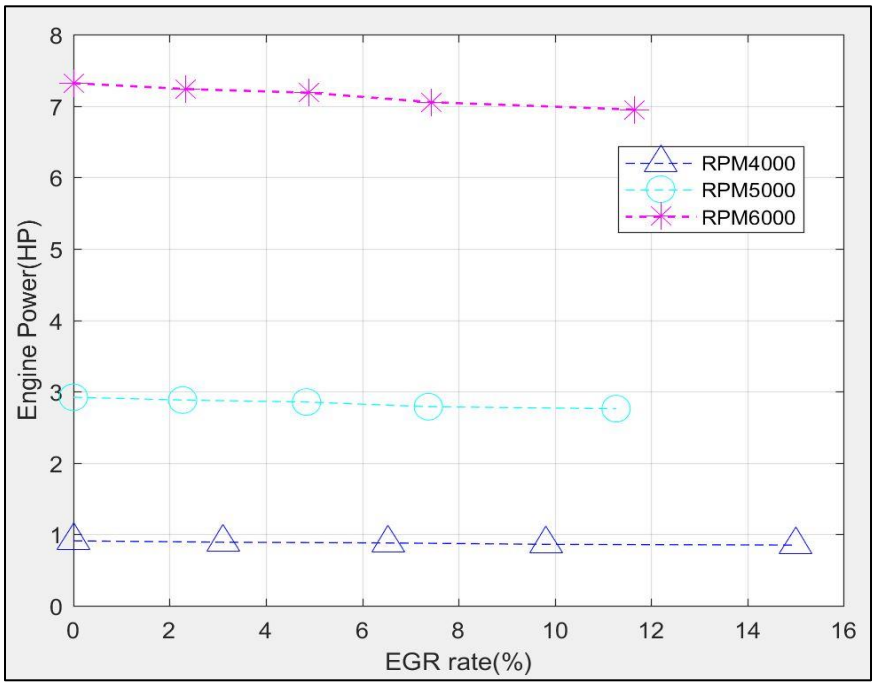


*Figure 70. Engine Power(HP) vs EGR rate(%)*

**Thermal Efficiency**

Recall, the thermal efficiency of an Otto cycle was described in equation (2.6):

$$\eta_{Thermal} = 1 - \frac{1}{r_c^{(\gamma-1)}}$$

Considering the thermal efficiency of the ideal Otto cycle, it is an indication of fuel conversion efficiency as the ratio between the work produced per cycle to the amount of fuel energy supplied per cycle during the combustion process, the equation (4.25) derived from the definition (4.26).

$$\eta = \frac{W}{Q_H} \tag{4.25}$$

$$\eta = 1 - \frac{T_C}{T_H} \tag{4.26}$$

$\eta$ = Thermal efficiency

$W$ = Net work

$Q_H$ = Heat flow in

$T_H$ = Hot sink temperature

$T_C$ = Cold sink temperature

As applying the EGR system to the 49cc engine, the thermal efficiency was expected to increase due to the increase of $\gamma$ of the (2.6) with the recirculated composition. And then EGR reduced knock propensity in the cylinder since the increased dilution effect decreased the in-cylinder temperature, which was the $T_H$ of the (4.26) during combustion (A.3). Thus, it was estimated that the reduced knock propensity had little influence on increasing the thermal efficiency of the engine through lowering the in-cylinder temperature.

**Rate of Heat Release**

The rate of heat release is the amount of heat energy released from air/fuel mixture during burning in high pressure and temperature in a cylinder in a unit time. It was a reliable approach that the rate of heat release was a standard to consider how the EGR system had affected generating heat energy in the cylinder. In reviewing the literature [42] and [43], the rate of heat release equation was introduced with the first law of thermodynamics, that is, the energy conservation in the cylinder, between the inlet valve closed and the exhaust valve closed.

$$\text{Rate of heat release} = \frac{d(mc_vT)}{d\theta} + p\frac{dV}{d\theta} + \frac{dQ_{ht}}{d\theta} \tag{4.27}$$

$m$ = Mass of air/fuel mixture

$T$ = Mean gases temperature

$p$ = In-cylinder pressure

$\theta$ = Crank angle

$C_v$ = Specific heat capacity under constant volume

$V$ = Instantaneous volume

$Q_{ht}$ = heat transfer to the cylinder wall

Assuming that the gases were ideal,

$$pV = mRT \tag{4.28}$$

$R$ = characteristic gas constant of the cylinder gases

Variation of gas state equation with crank angle was the following:

$$p\frac{dV}{d\theta} + V\frac{dp}{d\theta} = mR\frac{dT}{d\theta} \tag{4.29}$$

The rate of heat release was the following:

$$\text{Rate of heat release} = \frac{\gamma}{\gamma-1} p\frac{dV}{d\theta} + \frac{1}{\gamma-1} V\frac{dp}{d\theta} - \frac{pV}{(\gamma-1)^2}\frac{d\gamma}{d\theta} + \frac{dQ_{ht}}{d\theta} \tag{4.30}$$

(Where $\gamma$ = Specific heat ratio)

$$\frac{dQ_{ht}}{d\theta} = hA(T-T_w)\frac{N\pi}{30} = hA\left(\frac{pV}{mR} - T_w\right)\frac{N\pi}{30} \tag{4.31}$$

$h$ = Heat transfer coefficient

$A$ = Area in contact with the gases

$N$ = Engine RPM

$T_w$ = Temperature of the in-cylinder

As described in the equations of the (4.30), and (4.31), the rate of heat release was mainly dependent on $p$ (in-cylinder pressure) with the small contribution of $\gamma$ (specific heat ratio) (note: specific heat ratio, $\gamma$, had a reverse proportion to the rate of heat release [42]). It has been discussed that the use of the EGR system decreased the in-cylinder pressure, $p$, due to the lowered in-cylinder temperature, delayed ignition timing, and reduced oxygen, and then it was considered that it reduced the rate of heat release in the cylinder with the correlation based on the above equations. Therefore, the combustion pressure and heat release with same trends were inversely proportional to the EGR rate. Hence, the rate of heat release is clearly decreasing as the EGR opening valve and EGR rate increases from 0% to 15% at each RPM condition.

# CHAPTER 5: Summary and Conclusion

Although full-scale vehicle IC engines have been studied in different sizes and configurations for improvements, small scale IC engines, which have many opportunities for a wide range of applications, have not been as thoroughly studied. Furthermore, improvements in small engines have not been attempted at the same scale as those for larger engines. The challenges of applying exhaust gas recirculation (EGR) to a small scale HCCI engine, which is a promising small scale engine from previous research, included the critical drawbacks of a decrease of the torque and power of the engine and an increase of HC and CO, even though it had some merits. So then, a 4-stroke spark ignition small scale engine may represent a promising candidate for other emission control methodologies, most specifically EGR. That is, to overcome the important challenge of the excessive gas emissions from small scale SI engines, an EGR system was devised and applied to such a small scale engine as the 49 cc spark ignition engine used in this study.

Until recently, there have been few uncovered types of research of EGR systems applied to the 49cc spark ignition small scale engine. Thus, the EGR technique for the 49cc small scale SI engine was a meaningful approach, including the detailed study of how the EGR system affected the operation of the engine. No prior study on this technique at this scale has been reported. Recirculated exhaust in the inlet charge resulted in absorbing heat in the combustion chamber, lowering the flame temperature during the combustion process, and then reducing exhaust gas temperature. Ultimately, $NO_x$ decreased as a result of the drop of the temperatures. This was due to the lowering of the intake $O_2$ concentration as it was diluted by the recirculated gases from the combustion process (the dilution effect) with small contributions of the higher specific heat capacity of $CO_2$ and $H_2O$

of the gases over that of $O_2$ and $N_2$ in the combustion chamber (the thermal effect) and the dissociation of $CO_2$ (the chemical effect) for the reduction of $NO_x$. After investigating by applying the EGR copper pipe customized to the engine, the EGR system was found to affect exhaust gas emission and the torque and power of the engine through the EGR opening valve and EGR rate at each RPM condition. Results show that EGR was very effective and applicable to reduce $NO_x$ emissions and sometimes reduce other pollutant emissions (e.g., CO, HC), particularly at high RPM of the single cylinder where the system requires moderate to heavy load and typically operated in the rich regions of air/fuel mixtures. There were slight penalties of increased fuel consumption and loss of torque and power of the engine when subjected to EGR but these were acceptably small. Thus, after analyzing the trends of the gas emissions of $NO_x$, HC, CO, and $CO_2$ and the torque and power of the engine based on the results, it was determined that a range of EGR rate between 7.5% - 12% could be promising at high RPM (RPM4000 - RPM6000) for the optimized balance between all exhaust emissions and the engine performance. Based on the ratio of the exhaust gas temperature and engine coolant temperature [26], as an approach, the EGR system at high RPM (RPM4000 - RPM6000) had a positive effect on reducing the ratio, which means easing the burdens of the heavy loads for the life of the engine. This important measure also showed that the optimal EGR rate was 7.5% - 12%, and that it was promising for high RPM conditions (loads) of the engine.

# CHAPTER 6: Future Research

The main objective of the research for thermal effects of exhaust gas recirculation on combustion of the spark ignition 49cc small scale engine was to set up a simple scooter with small scale SI engine associated with the various sensors and experimental equipment in order to measure reliable data and analyze the relationship among them. For further research, using an in-cylinder pressure transducer mounted into the spark plug is promising to analyze the relationship more deeply in details and find the indicated power and fuel consumption and to identify the reasons for the variation of gas emission and loss of engine performance in the similar approaches of [49] and [50]. Another future study would be varying the fuel from the regular unleaded gasoline (Octane 87) to bioethanol as an environmental-friendly fuel to see if this would be a better combination with the EGR system [58]. At no EGR condition as a default, the combustion processes are the following:

Gasoline: $C_7H_{13.3} + 10.33(O_2 + 3.785N_2) \rightarrow 7CO_2 + 6.66H_2O + 39.1N_2 + 4.19MJ$ (6.1)

Ethanol: $3.44C_2H_2OH + 10.33(O_2 + 3.785N_2) \rightarrow 6.88CO_2 + 10.32H_20 + 39.1N_2 + 4.24MJ$ (6.2)

As shown in the equation (6.1) and (6.2), ethanol has around 30% more triatomic molecules in the combustion products compared to the gasoline combustion process. This indicates that the products from the ethanol combustion process have the greater heat capacity rather than that of the gasoline. This eventually results in the compressed gas temperature decreasing by high latent heat, with an assumption that the cooling heat loss

in the combustion chamber decreases with ethanol [58]. In conjunction with the EGR system, ethanol applied to the small scale 49cc SI engine is a further promising research.

In order to utilize the method with bioethanol, the fuel circuits are required to be adapted to the new fuel source since ethanol is more corrosive than the regular unleaded gasoline. Not only that, the amount of the bioethanol required at each engine cycle also is different. This method could be a future work after replacing the original ECU with an aftermarket ECU to control and change a variety of parameters of the engine. It would allow reading data and controlling specific variables such as crank angle, air/fuel mixtures, and fuel injection timing which would give solutions for the fluctuation of the gas emission and the loss of the power by the EGR system for the new optimizations. Thus, this requires the utilization of an aftermarket ECU that is connected to all the sensors of the original ECU. The research with the high end EGR control was conducted as a hot EGR system without any cooler system. The more dropped in-cylinder temperature and exhaust temperature would be expected by the EGR system with a cooler system customized for further research as a partly cooled EGR or fully cooled EGR system. It could have effects on more remarkably decreasing the amount of $NO_x$ compared to the EGR system with no cooler system [59]. Based on reviewing the literature related to the sizes and configurations of an EGR system [60], changing the sizes and configurations for the flow of the recirculated exhaust gases in the EGR system could influence on the turbulent flows of the fresh intake manifold air and the recirculated exhaust gases and moreover substituting the original copper material of the pipe with a better thermal conductive material pipe for more heat drop or loss of the recirculated exhaust gases through the pipe.

The suggested ideas for the further research could be the effective synergies by the collaboration of them in either an experiment or simulation.

The further types of research are the following:

Further future research is the following:

(1) Installing in-cylinder pressure transducer affiliated with the spark plug and then measuring in-cylinder pressure, analyzing the effects of EGR related to the test results and trends, finding the reasons among them [49] and [50].

(2) With the EGR system, as a synergy, test on mixed ethanol with the regular unleaded gasoline (e.g. E0 - E80) for analyzing exhaust gases emissions and the performance of the engine [58].

(3) Applying an aftermarket ECU for controlling the specific variables (e.g. crank angle, air/fuel mixtures, and fuel injection timing), reading all data and analyzing them at once.

(4) Customizing EGR cooler to apply to the EGR copper pipe for more heat drop [59].

(5) Based on the current EGR copper pipe, compared to the results of the experimental test, simulation and analysis related to the flow of the exhaust gas emission through the EGR copper pipe and changing the model for improvement. For example, changing the interior, the exterior, the thickness, the length in the sizes or configurations of the EGR copper pipe or substituting the EGR copper pipe material with pipes of different thermal conductivity for varying heat drop [60].

# References


[1] Avinash Kumar Agrawal, Shrawan Kumar Singh, Shailendra Sinha, and Kumar Shukla, "Effect of EGR on the Exhaust Gas Temperature and Exhaust Opacity in Compression Ignition Engines", *Sadhana*, Vol.29, Part 3, pp 275 - 284, June, 2004.

[2] Zuhdi Salhab, "Effect of Exhaust Gas Recirculation on the Emission and Performance of Hydrogen Fueled Spark-Ignition Engine", *Global Journal on Researches in Engineering Automotive Engineering*, Vol.12, Issue 2, Version 1.0, 2012.

[3] Hussain. J, Palaniradja. K, Alagumurthi. N, and Marnimaran. R, "Effect of Exhaust Gas Recirculation (EGR) on Performance and Emission of a Compression Ignition Engine with Staged Combustion (Insertion of Unburned Hydrocarbon)", *International Journal of Energy Engineering*, 2012.

[4] Martin Muller, "General Air Fuel Ratio and EGR definitions and their Calculation from Emissions", *SAE International*, SAE paper, Delphi Corp, 2010-01-1285, 2010.

[5] N. Ladommatos, S. M. Abdelhalim, and H. Zhao, "The Effects of Exhaust Gas Recirculation on Diesel Combustion and Emissions", *International Journal of Engine Research*, Vol.1, No.1, 2000.

[6] "General Motors Automotive Engine Test Code, For Spark Ignition Engines", Seventh Edition, The Engine Test Code Committee, 1994.

[7] Mozafari A, "Exhaust Gas Recirculation in Spark-Ignition Engine, Adv Heat Trans" *ASME*, PD64(1):197-202, 1994.

[8] Eran Sher, "Hand Book of Air Pollution from Internal Combustion Engines-Pollutant Formation and Control", Library of Congress Cataloging, McGraw-Hill Inc, 1998.

[9] Fang Xi Xie, Qing Nian Wang, Xiao Ping Li, Yan Su, and Wei Hong, "Influence of Ignition Timings and EGR on Performance and Emissions of a Spark-Ignition Methanol Engine with high Compression Ratio", *Advanced Materials Research*, Vol.953-954, pp.825-829, June, 2014.

[10] Nitu B, Singth I, Zhong L, Badreshany K, Henien NA, and Bryzik WW, "Effect of EGR on Autoignition, Combustion, Regulated Emissions, and Aldehdes in DI diesel Engines", *SAE International*, SAE Paper No.2002-01-1153, Society of Automotive Engineers Inc, 2002.

[11] Lapuerta M, Hernandes JJ, and Gimenez F, "Evaluation of Exhaust Gas Recirculation as a Technique for Reducing Diesel Engine Emissions", *SAGE Journals*, Automotive Engineering, 213:85-93, 2000.

[12] Heywood JB, “Internal Combustion Engines Fundamentals”, International Edition. New-York, Mc-Graw Hill, 1988.

[13] Tomas Lattimore, “Combustion and Emissions of a Direct Injection Gasoline Engine Using EGR”, *the university of Birmingham*, Doctoral Thesis, December, 2015

[14] R.S.G Baert, D.E. Beckman, and A. Veen, “Efficient EGR Technology for Future HD Diesel Engine Emission Targets”, Society of Automotive Engineers, *SAE International*, SAE Paper No.1999-01-0837, 1999.

[15] Abd-Alla GH, “Using Exhaust Gas Recirculation in Internal Combustion Engines: a Review”, *Energy Convers Manage*, 43:1027-42, 2002.

[16] P. Naresh, V. Madhava, and A. V. Hari Babu, “Exhaust Gas Recirculation System”, Science Q, Journal of Bioprocessing and Chemical Engineering, Vol.3, Issue 3, ISSN:2348-3768.

[17] Willard W. Pulkrabek, “Engineering Fundamentals of the Internal Combustion Engine”, pp.59-60, 2004.

[18] DAS LM, Mathur R. “Exhaust Gas Recirculation for $NO_x$ Control in a Multi Cylinder Hydrogen Supplemented S.I. Engine”, *International Journal Hydrogen Energy*, 18(12):1013-8, 1993.

[19] Wade R W. “Light Duty $NO_x$-HC Particulate Trade-Off”, *SAE International*, SAE Paper No.800335, 1980.

[20] Ladommatos N, Balian R, Horrocks R, and Cooper L, “The Effect of Exhaust Gas Recirculation on Combustion and $NO_x$ Emissions in a High-Speed Direct Injection Diesel Engine”, *SAE International*, SAE Paper No.96840, 1996.

[21] R. Cosgarea, M. Aleonte, and C. Cofaru, “The Influence of the Internal Exhaust Gas Recirculation (EGR) on the Pumping Losses”, *Engineering Sciences*, Bulletin of the Transilvania University of Brasov, Vol.4(53), No.1-2011, 2011.

[22] Engell R. “The Influence of EGR on Heat Release Rate and NO formation in a DI Diesel Engine”, *SAE International*, SAE Paper No.2000-01-1807, Society of Automotive Engineers Inc, 2000.

[23] Salhab Z. “Thermodynamic and Emission Parameters of Spark-Ignition Engines Powered by Gaseous Fuels”, Doctoral Work, 2001.

[24] Zeldovich Y. B., “The Oxidation of Nitrogen in Combustion and Explosions”, *Acta Physicochimica*, USSR, Vol.21, pp 577-628, 1946.

[25] Willard W. Pulkrabek, “Engineering Fundamentals of the Internal Combustion Engine”, pp.334-340, 2004.

[26] Pawan Kumar, “Significance of the Ratio of Exhaust Temperature to Coolant Temperature and Its Effect on Various Engine Working Parameters”, *World Congress on Engineering*, Vol.II, July 1-3, 2009.

[27] Berggren, G., “Exhaust Gas Recirculation System for Gasoline Engines”, United Patent Application Publication, US 2008/0066725 A1, 2008.

[28] Antonio Gomez, “Development and Verification of an Instrumented Small Engine Testbed”, Master Project, University of California, Irvine, 2015.

[29] Instructional Manual, Integrated Emissions System Model 700, Enerac Inc, 2014.

[30] Service Manual, Yamaha Vino 50 Classic 2013, Yamaha Inc, 2013.

[31] Model IMS Instruction Manual, The Apollo Intelligent Meter Series.

[32] Instructional Manual, A Quick Guide to National Instruments USB-6009, National Instruments.

[33] Highway Motorcycles: Exhaust Emission Standards, Office of Transportation and Air Quality of EPA emission standards, EPA-420-B-16-016, March, 2016.

[34] Toyota Motor Sales, Emission Sub Systems, Exhaust Gas Recirculation, USA, Pages 1-9, 2006.

[35] Kyoung Doug Min, “Rapidly Changing Environment: Current Status and Outlook of Automobile technology - Automobile Power, Where to Go”, The Korean Society of Automotive Engineers Seminar, 2018.

[36] Marklines, Automotive Industry Portal.

[37] Ulf Lundqvist, Gudmund Smedler, Per Stalhammar, “A Comparison Between Different EGR Systems for HD Diesel Engines and Their Effects on Performance, Fuel Consumption and Emissions”, Society of Automotive, Engineers, 2000.

[38] Susumu Kohketsu, Kazutoshi Mori, Kenji Sakai, Takazoh Hakozaki, “EGR Technologies for a Turbocharged and Inter-Cooled Heavy-Duty Diesel Engine”, Society of Automotive Engineers, 1997.

[39] D. A. Pierpont, D. T. Montgomery, and R. D. Reitz, “Reducing Particulate and NOx Using Multiple Injections and EGR in a D.I. Diesel”, *SAE International*, SAE Paper No.95017, February, 1995.

[40] McKenzie, Jacob, and Wai K. Cheng, "Ignition Delay Correlation for Engine Operating with Lean and with Rich Fuel-Air Mixtures", *SAE International*, SAE Paper No.2016-01-0699, 2016.

[41] Woschni, G. "A Universally Applicable Equation for the Instantaneous Heat Transfer Coefficient in the Internal Combustion Engine", *SAE International*, SAE Paper No.670931, 1967.

[42] R. Ebrahimi, "Effect of Specific Heat Ratio on Heat Release Analysis in a Spark Ignition Engine", *Scientia Iranica*, Sharif university of Technology, September, 2011.

[43] Toshio Shudo and Hiroyuki Suzuki, "Applicability of Heat Transfer Equations to Hydrogen Combustion", JSAE Review, Vol.23, Issue 3, pp.303-308, July, 2002.

[44] Department Of Energy, "Report on the First Quadrennial Technology Review", U.S, 2011.

[45] Korea Institute of Machinery and Materials.

[46] 2017 Shanghai Auto Show, Daimler AG and Future Automobile Power System Committee.

[47] H. T. Aichlmayr, D. B. Kittelson, andM. R. Zachariah. Miniature free-piston homogeneous charge compression ignition engine-compressor concept–part i: performance estimation and design considerations unique to small dimensions. *Chemical Engineering Science*, 57(19):4161–4171, October 2002.

[48] Department Of Energy, "Basic Research Needs for Clean and Efficient Combustion of 21st Century Transportation Fuels", Workshop of Basic Energy Sciences Arlington, VA, U.S, 2007.

[49] Therkelsen, Peter Lynn. "SI to HCCI Operation of a Small Macro-Scale 4-Stroke Engine", Ph.D Dissertation, University of California, Irvine, 2009.

[50] Jae Hyung Lim, "Performance Mapping of a Small-Scale Water-Cooled 4-Strok IC Engine: Potential for HCCI Operation", M.S Thesis, University of California, Irvine, 2010.

[51] R. K. Rajput, "Internal Combustion Engines", pp.69-76, 2005.

[52] R. K. Rajput, "Internal Combustion Engines", pp.496-510, 2005.

[53] R. K. Rajput, "Internal Combustion Engines", pp.216-218 2005.

[54] Fuquan Zhao, Thomas W. Asmus, Dennis N. Assanis, John E. Dec, James A. Eng,

and PaulM. Najt, editors, “Homogeneous Charge Compression Ignition (HCCI) Engines, Key Research and Development Issues”. Number PT-94. *SAE International*, 400 Commonwealth Drive,Warrendale, PA 15096, USA, 2003.

[55] KrzysztofMotyl and Tadeusz J. Rychter, “HCCI Engine - a Preliminary Analysis”, *Journal of KONES Internal Combustion Engines*, 10:3–4, 2003.

[56] Kathi Epping, Salvador Aceves, Richard Bechtold, and John Dec, “The Potential of HCCI Combustion for High Rfficiency and Low Rmissions”, *SAE International*, Paper No.2002-01-1923, 2002.

[57] Joel Martinez-Frias, Salvador M. Aceves, Daniel L. Flowers, J. Ray Smith, and Robert Dibble, “Thermal Charge Conditioning for Optimal HCCI Engine Operation”, *ASME*, Vol.24, pp.67-75, March, 2002.

[58] Koichi Nakata, Shintaro Utsumi, Aatsuharu Ota, Katsunori Kawatake, Takashi Kawai and Takashi Tsunooka, “The Effect of Ethanol Fuel on a Spark Ignition Engine”, *SAE International*, SAE Paper.2006-01-3380, Toyota Motor Corporation, October, 2006.

[59] Radu Florea, Dinu Taraza, Naeim A. Henein, and Walter Bryzik, “Transient Fluid Flow and Heat Transfer in the EGR Cooler”, *SAE International*, SAE Paper.2008-01-0956, April, 2008.

[60] Pavlos Dimiriou, Richard Burke, Colin Copeland, Sam Akehurst, “Study on the Effects of EGR Supply Configuration on Cylinder-to-Cylinder Dispersion and Engine Performance Using 1D-3D Co-Simulation”, *SAE International*, *JSAE Review*, SAE Paper.2015-32-0816, JSAE Paper.20159816, November, 2015.

[61] Engine and Emission Technology Online, DieselNet.

[62] Alain Maiboom, Xavier Tauzia, and Jean-Francois Hetet, “Influence of EGR Unequal Distribution from Cylinder to Cylinder on NOx-PM Trade-Off of a HSDI automotive Diesel Engine”, *Applied Thermal Engineering*, Elsevier, 29(10), pp.2043, 2009.

[63] R. K. Rajput, “Internal Combustion Engines”, pp.248-281, 2005.

[64] R. K. Rajput, “Internal Combustion Engines”, pp.162-200, 2005.

[65] R. K. Rajput, “Internal Combustion Engines”, pp.461-481, 2005.

[66] Stephen K. Hall, Joana Chakraborty, and Randall J. Ruch, “Chemical Exposure and Toxic Responses”, pp.106-107, 1996.

[67] Michael Rößler, Thomas Koch, Corina Janzer, and Matthias Olzmann, “Mechanisms of the $NO_2$ Formation in Diesel Engines”, *MTZ worldwide*, Vol.78, Issue.7-8, pp.70-75, July, 2017.

[68] Roger Bywater, “Engine Technology for the Modern World”, AJ6 Engineering, ch.4, 2014.

[69] Zheng, Yun; Wang, Jianchen; Yu, Bo; Zhang, Wenqiang; Chen, Jing; Qiao, Jinli; Zhang, Jiujun, "A review of high temperature co-electrolysis of H O and CO to produce sustainable fuels using solid oxide electrolysis cells (SOECs): advanced materials and technology", Chem. Soc, Rev. 46 (5): 1427–1463, doi:10.1039/C6CS00403B, 2017.

[70] Spencer L. Seager and Michael R. Slabaugh, “Chemistry for Today, General, Organic, and Biochemistry”, Cengage Learning, pp.365, 2010.

[71] N. Ladommatos, S. M. Abdelhalim, H. Zhao, and Z.Hu, “The Dilution, chemical, and Thermal Effects of Exhaust Gas Recirculation on Diesel Engine Emissions - Part 2: Effect of Carbon Dioxide”, *SAE International*, SAE Paper.961167, ISSN 0148-7191, May, 1996.

[72] N. Ladommatos, S. M. Abdelhalim, H. Zhao, and Z.Hu, “The Dilution, chemical, and Thermal Effects of Exhaust Gas Recirculation on Diesel Engine Emissions - Part 3: Effects of Water Vapour”, *SAE International*, SAE Paper.971659, ISSN 0148-7191, May, 1997.

# Appendices

## Correlation of HC, CO, and $NO_x$

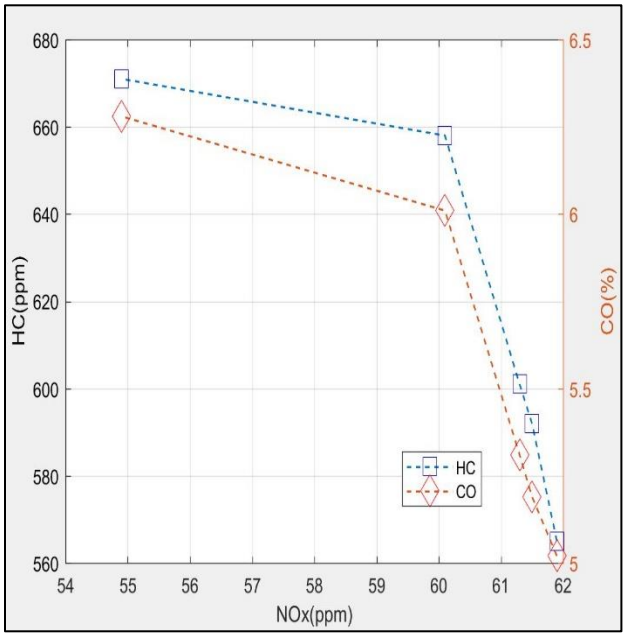


*HC(ppm) vs CO(%) vs $NO_x$(pm) at RPM2100*

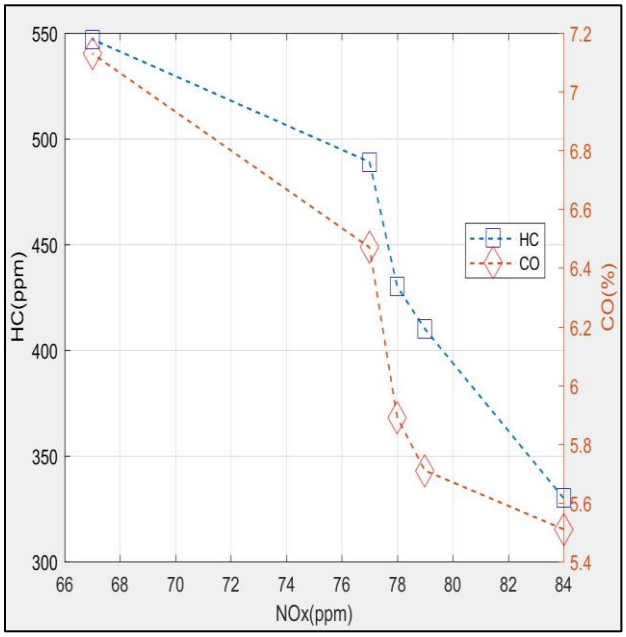


*HC(ppm) vs CO(%) vs $NO_x$(pm) at RPM3000*

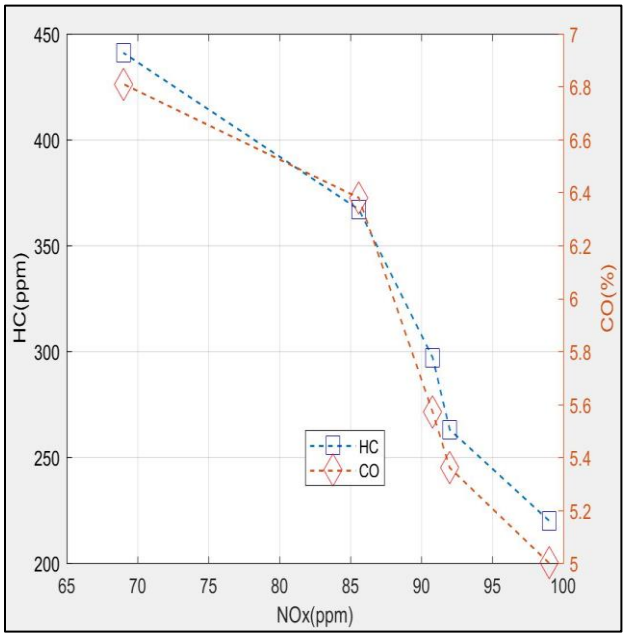


*HC(ppm) vs CO(%) vs $NO_x$(pm) at RPM4000*

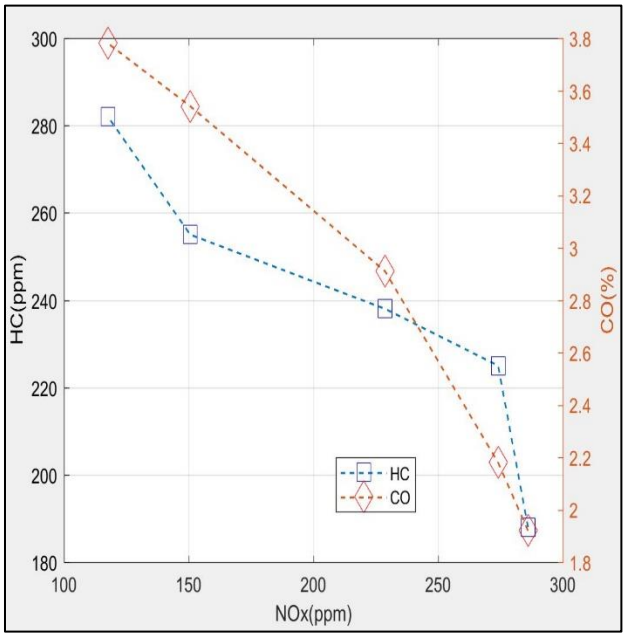


*HC(ppm) vs CO(%) vs $NO_x$(pm) at RPM5000*

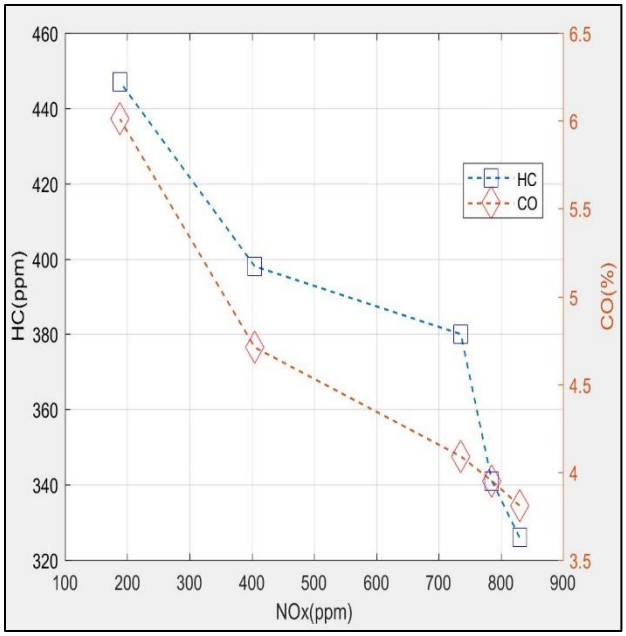


*HC(ppm) vs CO(%) vs $NO_x$(pm) at RPM6000*

## Correlation of HC, $O_2$, and EGR rate

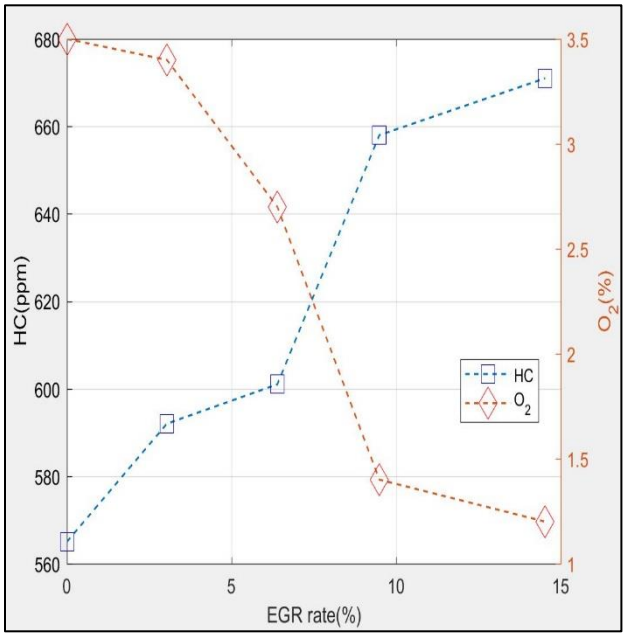


*HC(ppm) vs $O_2$(%) vs EGR rate(%) at RPM2100*

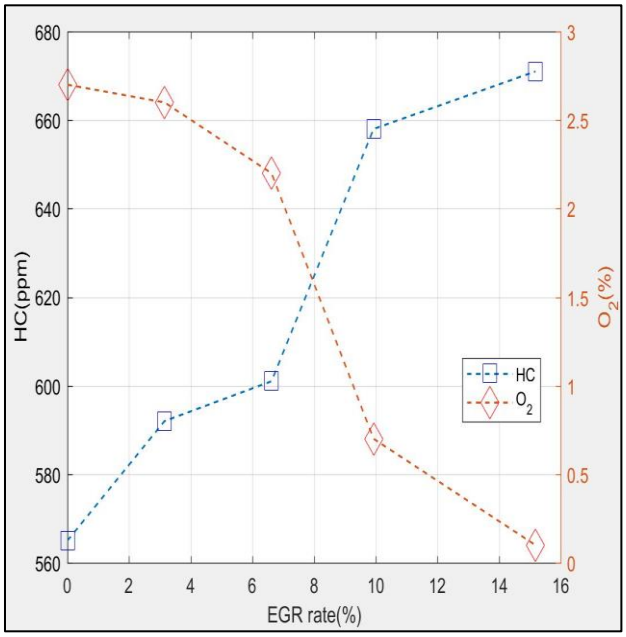


*HC(ppm) vs $O_2$(%) vs EGR rate(%) at RPM3000*

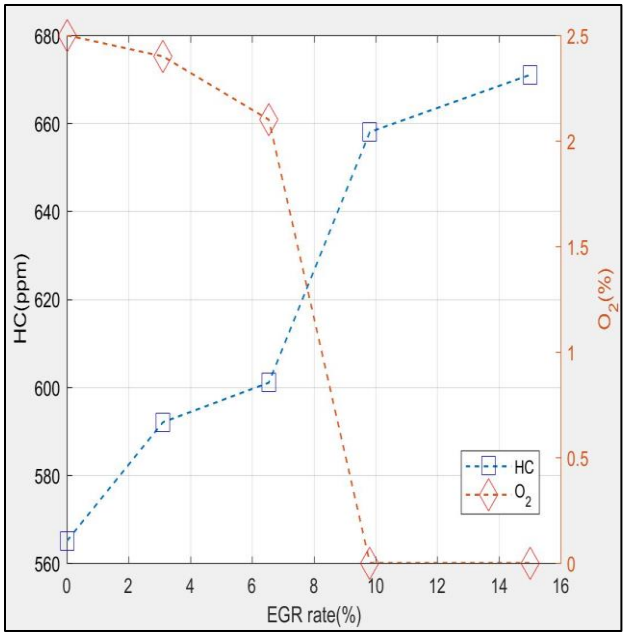


*HC(ppm) vs $O_2$(%) vs EGR rate(%) at RPM4000*

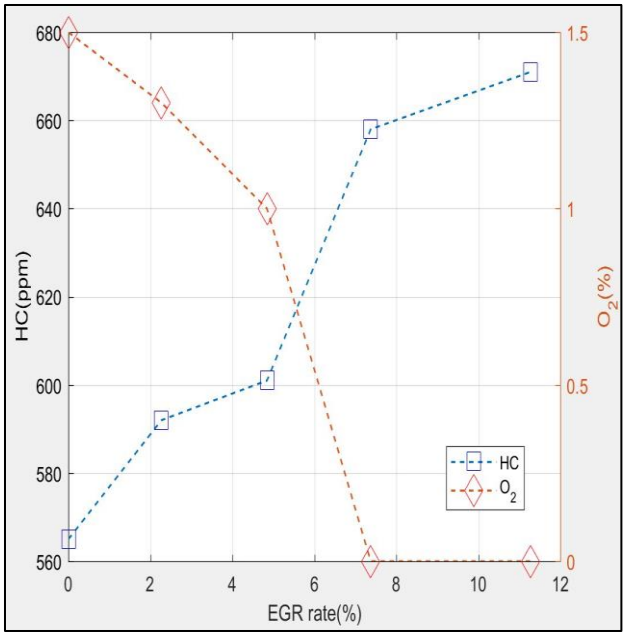


*HC(ppm) vs $O_2$(%) vs EGR rate(%) at RPM5000*

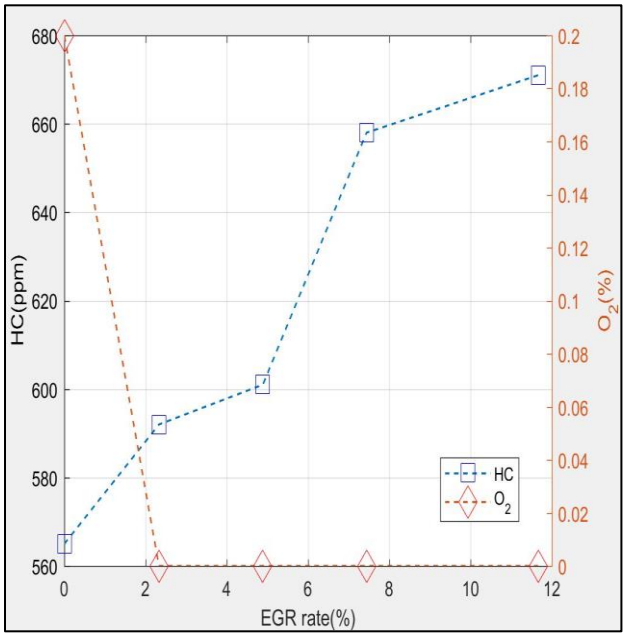


*HC(ppm) vs $O_2$(%) vs EGR rate(%) at RPM6000*

## Correlation of CO, $O_2$, and EGR rate

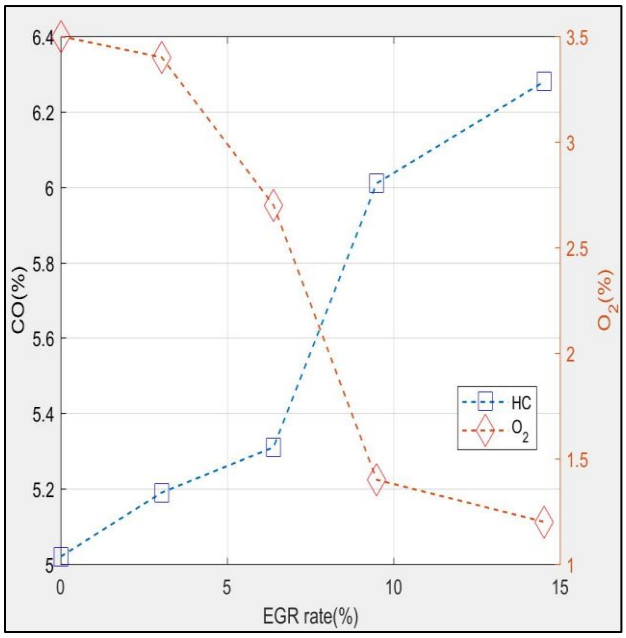


*CO(%) vs $O_2$(%) vs EGR rate(%) at RPM2100*

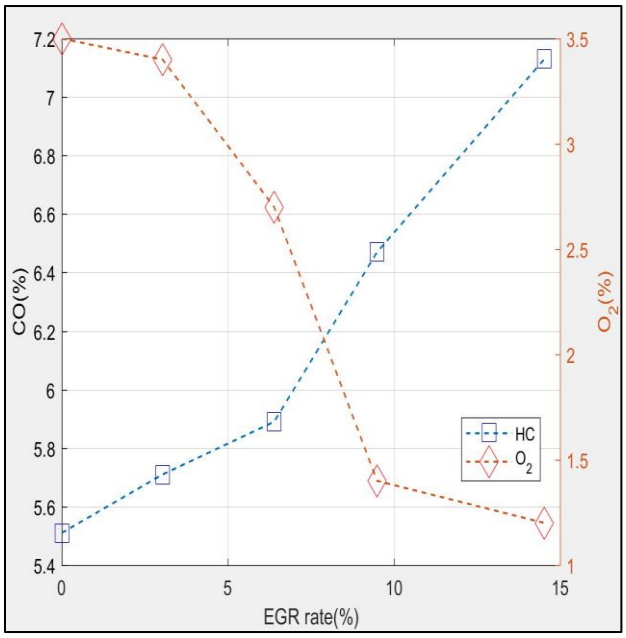


*CO(%) vs $O_2$(%) vs EGR rate(%) at RPM3000*

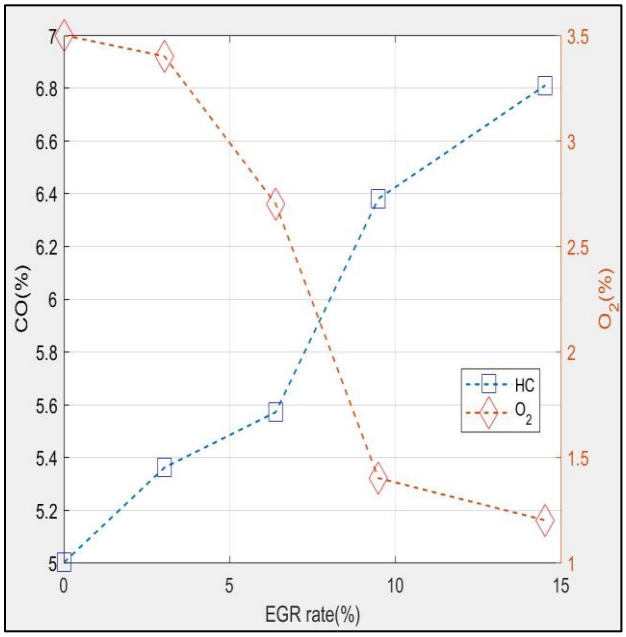


*CO(%) vs $O_2$(%) vs EGR rate(%) at RPM4000*

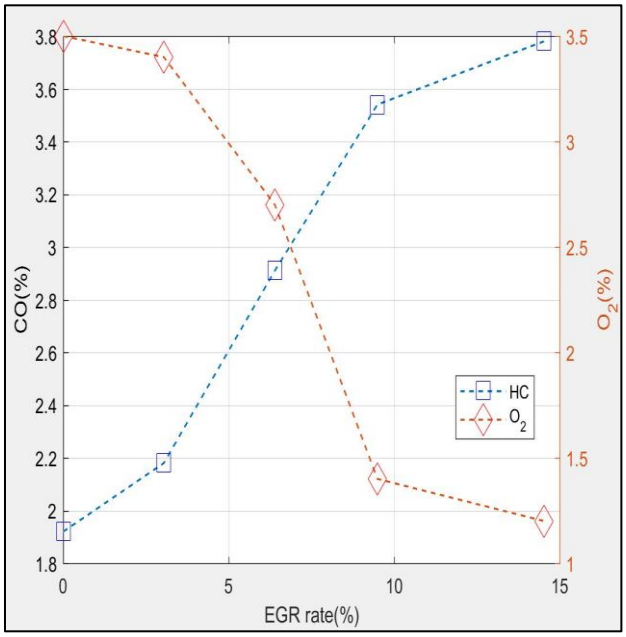


*CO(%) vs $O_2$(%) vs EGR rate(%) at RPM5000*

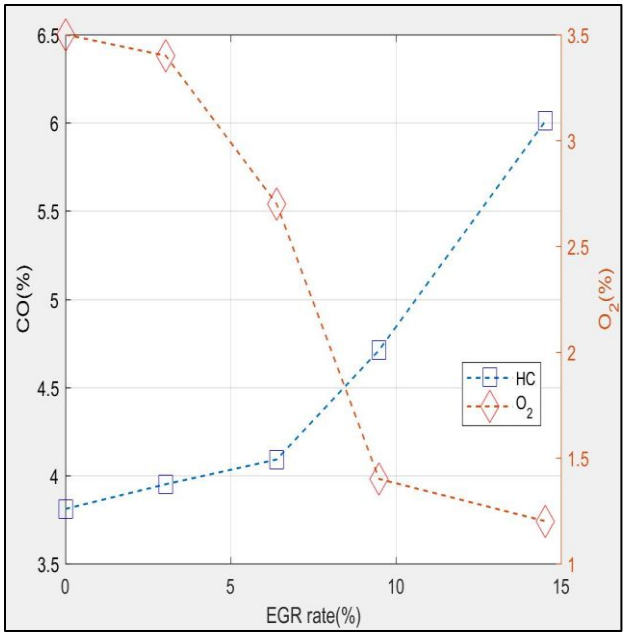


*CO(%) vs $O_2$(%) vs EGR rate(%) at RPM6000*

**Basic Equations of EGR [62]**

In general cases, the EGR rate of cylinder j is defined as the follow:

$$X_{EGR,\,j}\,(\%) = \frac{[CO_2]_{Intake,j} - [CO_2]_{Ambient}}{[CO_2]_{Exhaust} - [CO_2]_{Ambient}} \times 100 \qquad \text{(A.1)}$$

$[CO_2]_{Intake,\,j}$ = The $CO_2$ concentration at the inlet manifold port of cylinder j

$[CO_2]_{Exhaust,\,j}$ = The $CO_2$ concentration at the exhaust manifold port of cylinder

The mean EGR rate is the following:

$$X_{EGR}\,(\%) = \frac{1}{i} \times \sum_{j=1}^{i} X_{EGR,j}\,(\%) \qquad \text{(A.2)}$$

The EGR mass flow is the following:

$$\dot{m}_{EGR} = \dot{m}_{Air} \times \frac{\rho_{EGR}}{\rho_{Air}} \times \frac{[CO_2]_{Mix}}{[CO_2]_{Exhaust} - [CO_2]_{Mix}} \qquad \text{(A.3)}$$

Mix = The mixture of the fresh intake manifold air and the recirculated exhaust gases

It is deduced from

$$\dot{m}_{Mix} = \dot{m}_{EGR} + \dot{m}_{Air} \qquad \text{(A.4)}$$

applying the thermodynamic first principle to the flow through Air-EGR connection for the enthalpy, $h_{Enthalpy,\ Mix}$ of the Air-EGR gases:

$$h_{Enthalpy,\ Mix} = \frac{\dot{m}_{Air} \times h_{Air} + \dot{m}_{EGR} \times h_{EGR}}{\dot{m}_{Air} + \dot{m}_{EGR}} \tag{A.5}$$

with the $CO_2$ conservation:

$$\frac{dn(CO_2)_{EGR}}{dt} + \frac{dn(CO_2)_{EGR}}{dt} = \frac{dn(CO_2)_{Mix}}{dt} \tag{A.6}$$

With $CO_2$ concentration and volume flows:

$$D_{Volume\ flow,\ EGR} \times [CO_2]_{Exhaust} = (D_{Volume\ flow,\ Air} + D_{Volume\ flow,\ EGR}) \times [CO_2]_{Mix} \tag{A.7}$$

$D_{Volume\ flow,\ EGR}$ = Volume flow of the recirculated exhaust gases ($m^3/s$)

$D_{Volume\ flow,\ Air}$ = Volume flow of the fresh intake manifold air ($m^3/s$)

$$\frac{\dot{m}_{EGR}}{\rho_{EGR}} \times [CO_2]_{Exhaust} = (\frac{\dot{m}_{Air}}{\rho_{Air}} + \frac{\dot{m}_{EGR}}{\rho_{EGR}}) \times [CO_2]_{Mix} \tag{A.8}$$

Hence, the EGR mass flow is derived from the fresh intake manifold air flow and $CO_2$ concentration for further research related to the mass flows of the fresh intake manifold air flow and $CO_2$ with an EGR system.